Review | Received 1 June 2026; Revised 19 July 2026; Accepted 20 July 2026; Published 31 July 2026
https://doi.org/10.55092/la20260005

Targets and strategies for cancer diagnosis and imaging

Peng Gao[1], Wei Pan[1], Na Li[1,*] and Bo Tang[1,2]

[1] College of Chemistry, Chemical Engineering and Materials Science, Key Laboratory of Molecular and Nano Probes, Ministry of Education, Collaborative Innovation Center of Functionalized Probes for Chemical Imaging in Universities of Shandong, Institute of Molecular and Nano Science, Shandong Normal University, Jinan 250014, China
[2] Laoshan Laboratory, Qingdao 266237, China

* Correspondence author; E-mail: lina@sdnu.edu.cn.

Highlights:

- Targets and strategies for cancer diagnosis and imaging are reviewed.
- The targets are systematically classified into extracellular, membrane, and intracellular targets.
- The advancements, challenges and future directions of related strategies are pointed out.

Abstract: Cancer diagnostic imaging is undergoing a fundamental transition from conventional anatomical visualization to molecular-targeted and functionally driven profiling of tumor biology. Next-generation imaging no longer merely detects morphological lesions, but decodes the dynamic biological states underlying tumor initiation, progression, immune remodeling, metabolic reprogramming, and therapeutic response. Imaging targets with high specificity, biological accessibility, and functional relevance are primary drivers of this technological transition. Current cancer imaging targets can be categorized into three spatial layers: extracellular biomarkers, membrane-associated targets, and intracellular biomarkers. Progress in nanotechnology, molecular engineering, bioorthogonal chemistry, and artificial intelligence (AI) has greatly facilitated the construction of multimodal, multi-target, and intelligent imaging systems. Nevertheless, clinical translation still faces prominent obstacles, including tumor heterogeneity, temporal biomarker fluctuation, limited tissue penetration, nonspecific background signals from off-target activation, and translational gaps. This review systematically classifies imaging targets based on their spatial distribution and biological function, summarizes the latest advances in cancer diagnosis and imaging, and discusses emerging research directions and future prospects for next-generation precision oncology.

Keywords: cancer biomarkers; cancer diagnosis; cancer imaging; multimodal probes; bioactive species

1. Introduction

Cancer remains a leading cause of mortality worldwide, imposing substantial burdens on healthcare systems and society [1–3]. Clinical outcomes are heavily stage-dependent, making early detection and precise therapeutic monitoring central objectives of modern oncology [4–6]. Conventional imaging

modalities, including computed tomography (CT), magnetic resonance imaging (MRI), ultrasound, and positron emission tomography (PET), have significantly advanced cancer diagnosis and disease management [7–10]. However, these approaches primarily detect anatomical abnormalities or nonspecific metabolic alterations and often suffer from insufficient sensitivity and specificity, particularly for early-stage tumors, minimal residual disease, and highly heterogeneous malignancies [11–14]. These limitations have spurred the rapid development of molecular imaging strategies capable of visualizing tumor-associated biological processes at cellular and subcellular resolution [15–19].

Unlike conventional anatomical imaging, molecular imaging integrates imaging modalities with biological targeting elements, including antibodies, peptides, aptamers, small molecules, activatable probes, and engineered nanomaterials, to selectively visualize tumor-associated molecular events *in vivo* [20–23]. Critically, the performance of a molecular imaging system is fundamentally determined by the nature of its target. An ideal imaging target should exhibit high tumor specificity, sufficient abundance, favorable accessibility, biological stability, clear disease relevance, and compatibility with imaging probes and signal amplification strategies [24–28]. Consequently, the evolution of cancer imaging has increasingly become a process of discovering and engineering biologically informative imaging targets.

Current cancer imaging targets can be broadly categorized by their spatial localization and biological functionality. Extracellular targets, including circulating proteins, extracellular vesicles, circulating tumor DNA (ctDNA), cytokines, and metabolites, offer minimally invasive opportunities for systemic tumor monitoring through liquid biopsy [29–31]. These targets reflect tumor burden, metastatic progression, stromal remodeling, and therapeutic response. Advances in exosome profiling, ctDNA amplification, and ultrasensitive biosensing have substantially expanded the scope of extracellular molecular diagnostics [29,31–33].

Membrane-associated biomarkers represent the most clinically mature class, owing to their direct accessibility to imaging probes and targeting ligands [34]. Numerous membrane proteins, such as epidermal growth factor receptor (EGFR), human epidermal growth factor receptor 2 (HER2), programmed death-ligand 1 (PD-L1), integrins, prostate-specific membrane antigen (PSMA), and epithelial cell adhesion molecule (EpCAM), are aberrantly overexpressed in diverse malignancies and have become major targets for PET, fluorescence-guided surgery, radionuclide imaging, and targeted nanomedicine [35–38]. Beyond merely enabling tumor localization, these biomarkers are intimately linked to angiogenesis, metastasis, immune regulation, and therapeutic responsiveness, allowing imaging systems to convey functional biological information alongside anatomical visualization [35–37,39].

Intracellular targets represent a rapidly growing frontier in next-generation cancer imaging [40–42]. Unlike extracellular and membrane-associated biomarkers, which primarily reflect accessible tumor phenotypes, intracellular targets provide direct insights into the dynamic molecular states that drive tumor progression and therapeutic adaptation [43–46]. These targets encompass oncogenic nucleic acids, signaling proteins, metabolic enzymes, reactive oxygen species (ROS), glutathione (GSH), metal ions, hypoxia-associated factors, and organelle-specific biomarkers [47–49]. They participate in tumor metabolic reprogramming, oxidative stress regulation, ferroptosis, cuproptosis, apoptosis, autophagy, and drug resistance [50–54]. Consequently, intracellular imaging is shifting from static biomarker visualization toward dynamic functional-state imaging capable of monitoring real-time tumor physiology and cell-fate transitions.

More broadly, the evolution of cancer imaging targets mirrors a paradigm shift in oncology: early strategies focused on detecting structural abnormalities and overexpressed receptors, whereas emerging

systems increasingly aim to visualize dynamic biological processes, including immunometabolic remodeling, redox fluctuations, therapy-induced stress responses, and regulated cell death pathways [25,55,56]. This transition from static molecular recognition to dynamic functional imaging is redefining the conceptual framework of precision oncology.

Concurrently, advances in materials science, nanotechnology, molecular engineering, and computational imaging have greatly accelerated the development of multifunctional imaging systems [57,58]. Multimodal platforms that integrate PET, MRI, fluorescence imaging, photoacoustic imaging, and biosensing technologies synergistically improve sensitivity, spatial resolution, and diagnostic accuracy [59–63]. Furthermore, activatable and microenvironment-responsive probes that react to enzymes, pH, ROS, hypoxia, or metal ions enable highly selective "off–on" imaging strategies with markedly reduced background interference [64–67]. The integration of multi-omics profiling and artificial intelligence (AI)-assisted image analysis is further transforming cancer imaging from qualitative observation into intelligent, quantitative, and predictive diagnostics [68].

In this review, we systematically categorize cancer imaging targets according to their spatial localization and biological functionality—extracellular, membrane-associated, and intracellular—and comprehensively discuss representative biomarkers, imaging modalities, probe engineering strategies, and translational applications (Figure 1). It should be noted that the spatial localization of tumor markers is not static, their expression and distribution fluctuate dynamically with the progression of cancer. Moreover, positional overlap frequently exists among different markers. In this review, we categorize their localization into three compartments, which is aims to break through the limitations of conventional research frameworks and offer a novel systematic perspective for readers to comprehend the complex landscape of tumor markers. At the end of this review, we also highlight emerging directions, including dynamic biomarker imaging, activatable and logic-gated probes, ferroptosis- and cuproptosis-associated imaging, multimodal integration, and AI-assisted precision imaging. Finally, we examine current limitations and future opportunities toward intelligent, real-time, and systems-level cancer visualization for next-generation precision oncology.

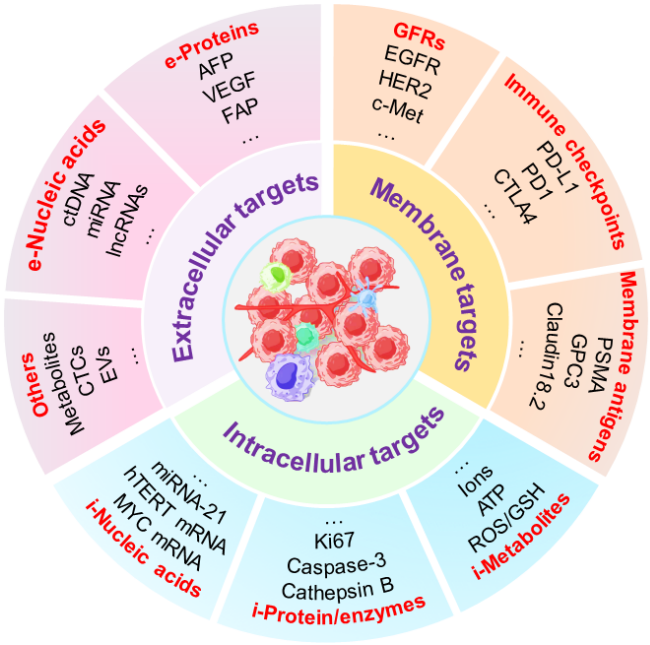

Figure 1. A schematic overview of targets for cancer diagnostic imaging, categorized as extracellular targets, membrane targets and intracellular targets according to their spatial localization.

2. Extracellular targets for cancer imaging

2.1. Overview of extracellular targets

As one of the most clinically translatable biomarker subtypes, extracellular imaging targets are naturally accessible in body fluids and the tumor microenvironment (TME) without crossing cell membranes [69,70]. Compared with intracellular targets that require efficient membrane penetration and endosomal escape, extracellular biomarkers are more suitable for non-invasive or minimally invasive imaging and have become core supports for liquid biopsy and longitudinal tumor monitoring [71–74].

Extracellular molecular signals not only indicate tumor existence but also reflect dynamic crosstalk between tumor cells and the TME. Tumor-derived extracellular molecules change continuously during malignant progression and carry rich information about tumor burden, angiogenesis, stromal remodeling, immune escape, metastasis and therapeutic response [73,75]. Different from membrane targets that mainly provide spatial localization and intracellular targets that reflect intrinsic cellular signaling, extracellular biomarkers occupy an intermediate position: they balance easy systemic detection and effective reflection of tumor evolutionary characteristics.

Advances in ultrasensitive biosensing, activatable probe design, PET tracers, fluorescence imaging and nanotechnology have greatly expanded the connotation of extracellular targets, which are no longer limited to classic serum markers but include dynamic stromal, immune and metabolic characteristics [76–80]. Current extracellular imaging targets are divided into protein biomarkers, extracellular nucleic acids and extracellular vesicles, which differ significantly in accessibility, specificity, stability and functional information, jointly constructing a multi-dimensional molecular imaging system for cancer diagnosis and treatment monitoring.

2.2. Protein targets

Extracellular protein biomarkers are the most mature and widely used subtype in clinical practice. These proteins participate in tumor proliferation, angiogenesis, immune remodeling, invasion and stromal activation, enabling protein-based imaging to simultaneously achieve tumor detection and functional evaluation of TME activity [81,82]. Derived from tumor cells, stromal fibroblasts, endothelial cells and infiltrating immune cells, extracellular proteins can reflect tumor-stroma interaction beyond simple lesion identification [83–85]. Meanwhile, their high abundance, mature detection technology and good compatibility with antibody/peptide/activatable probe endow them with prominent translational advantages.

2.2.1. Classical tumor-associated antigens

(1) Alpha-Fetoprotein

Alpha-fetoprotein (AFP) is a classic serum biomarker clinically applied for hepatocellular carcinoma (HCC) screening [86]. Its abnormal expression is closely correlated with vascular invasion, malignant phenotype and poor prognosis, and dynamic AFP monitoring can effectively warn of HCC postoperative recurrence [87]. Nevertheless, conventional AFP detection is vulnerable

to non-specific biomolecule interference in complex serum, resulting in compromised sensitivity and anti-interference ability.

To solve this problem, Ding *et al.* constructed a metal-organic framework (MOF)-based electrochemiluminescence (ECL) biosensor with an "On−Off−On" dual-mode strategy for trace AFP detection (Figure 2A) [88]. The Zn/Ru-MOF bimetallic framework enhances ECL emission via coordination-induced luminescence enhancement; complementary aptamer chains trigger resonance energy transfer to quench signals, while target AFP competitively dissociates quenching probes and recovers ECL signals. Modified zwitterion further forms an antifouling interface to suppress non-specific adsorption. The sensor achieves an ultra-low detection limit of 4.7 fg/mL and stable performance in real serum, providing a high-performance tool for clinical trace AFP monitoring and HCC recurrence evaluation.

(2) Prostate-Specific Antigen

Prostate-specific antigen (PSA) serves as the standard biomarker for prostate cancer screening and dynamic monitoring [89]. Traditional lateral flow detection suffers from low sensitivity and geometric mismatch with laser spots [90]. To address these defects, a syringe-based wettability-enhanced photothermal vertical flow biosensor (SW-PVFB) was developed for non-invasive PSA detection (Figure 2B) [91]. The platform relies on sandwich immunoassay combined with photothermal conversion: patterned nitrocellulose (NC) membranes enrich immune complexes and reduce signal loss, while $TaTe_2$ nanosheets act as high-efficiency photothermal probes. Under 808 nm laser irradiation, temperature variation is positively correlated with PSA concentration. The platform supports dual colorimetric/photothermal readout with a detection limit of 0.028 ng/mL, and can be integrated with smartphones to realize portable point-of-care prostate cancer detection.

(3) CA19-9 and CA125

CA19-9 and CA125 are typical soluble glycoprotein biomarkers widely used in pancreatic and ovarian cancer diagnosis respectively [92]. Released into extracellular fluid and peripheral circulation, they dynamically reflect tumor burden, stromal remodeling and disease progression. Their easy accessibility in body fluids makes them indispensable components of minimally invasive cancer diagnosis.

As a core biomarker for pancreatic ductal adenocarcinoma (PDAC), circulating CA19-9 level is closely related to tumor progression, metastasis and therapeutic response. Li *et al.* developed an exogenous-label-free colorimetric/Surface-Enhanced Raman Scattering (SERS) dual-mode immunosensing platform based on Au NCs@Pt nanozyme (Figure 2C) [93]. Coral-like Au NCs provide electromagnetic hotspots, while Pt clusters exhibit peroxidase-like activity to catalyze 3,3',5,5'-Tetramethylbenzidine (TMB) oxidation. The generated oxidized TMB (oxTMB) acts as both colorimetric substrate and SERS reporter, avoiding dependence on exogenous Raman tags. Magnetic bead-based sandwich immunoassay realizes specific CA19-9 capture and dual signal amplification. The assay completes detection within 15 min with a linear range of 1–200 IU/mL and a detection limit of 0.16 IU/mL, achieving 100% diagnostic accuracy in 60 clinical serum samples.

CA125 is the routine biomarker for ovarian cancer surveillance and therapeutic evaluation, with elevated level closely associated with peritoneal dissemination and advanced malignancy. To improve the stability and antifouling ability of traditional peptide-based sensors, Jin *et al.* designed an aptasensor based on cyclic peptide nanotubes (CPNTs) and Rh−$Ti_3C_2T_x$ dual-enzyme nanozyme (Figure 2D) [94]. CPNTs form a dense hydration layer to resist serum non-specific adsorption; Rh-$Ti_3C_2T_x$ possesses

glucose oxidase and peroxidase activity to realize *in situ* H_2O_2 generation and electrochemical signal amplification. Specific binding of CA125 hinders interfacial electron transfer and reduces current signal in a concentration-dependent manner. The aptasensor exhibits wide linear range and an ultra-low detection limit of 0.005 $U \cdot mL^{-1}$, maintaining stable performance in undiluted human serum for clinical ovarian cancer sample detection.

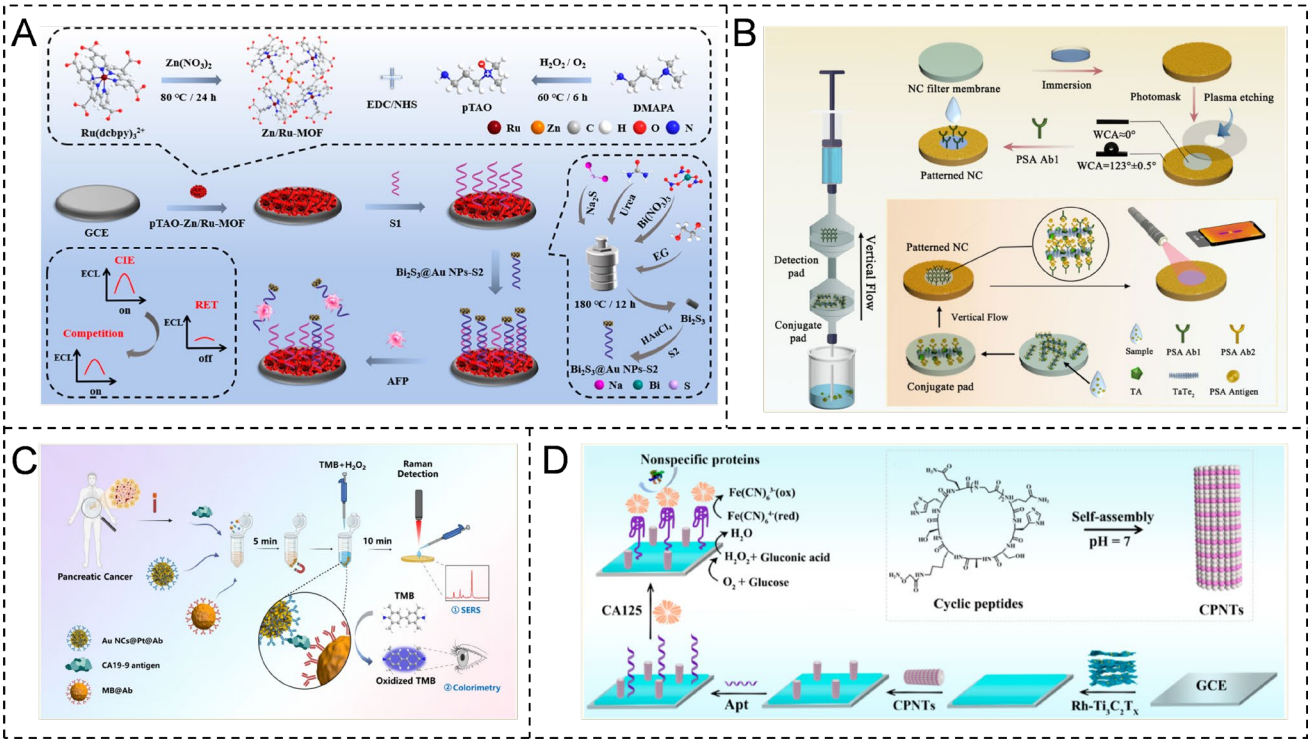

Figure 2. Strategies for sensing extracellular tumor-associated antigens. **(A)** The "On−Off−On" ECL biosensor based on Zn/Ru-MOF for AFP detection. Reprinted with permission [88]. Copyright 2025 American Chemical Society; **(B)** The SW-PVFB for PSA detection. Reprinted with permission [91]. Copyright 2026 American Chemical Society; **(C)** The Au NCs@Pt nanozyme-based colorimetric/SERS dual-mode immunosensor for pancreatic cancer biomarker CA19-9 detection. Reprinted with permission [93]. Copyright 2026 American Chemical Society; **(D)** The CPNT-based aptasensor with Rh-$Ti_3C_2T_x$ dual-enzyme nanozyme for CA125 detection. Reprinted with permission [94]. Copyright 2025 American Chemical Society.

2.2.2. Growth factors and cytokines

Different from classic tumor antigens that mainly reflect tumor burden, extracellular growth factors and cytokines can directly characterize angiogenesis, inflammatory response, immune remodeling and therapeutic resistance, playing an increasingly important role in functional tumor imaging and treatment monitoring [95].

(1) Vascular Endothelial Growth Factor

Vascular endothelial growth factor (VEGF) is the key regulator of tumor angiogenesis, controlling neovascular remodeling, vascular permeability and tumor metastasis [96]. VEGF-targeted imaging can evaluate angiogenic activity and dynamically monitor the efficacy of anti-angiogenic therapy [97].

Different from conventional imaging focusing only on tumor cells, VEGF imaging expands the target scope to stromal and vascular components of the TME [98,99].

Yuan *et al.* constructed a "signal on-off-super on" sandwich aptasensor for ultrasensitive VEGF detection. Gold nanoparticles (AuNPs)@$Ti_3C_2T_x$ composite provides large specific surface area and high conductivity for aptamer immobilization and signal amplification [100]. Methylene blue labeled at the aptamer inner base generates initial signal-on state after VEGF-induced conformational change; activated clustered regularly interspaced short palindromic repeats/Cas12a (clustered regularly interspaced short palindromic repeats (CRISPR)/Cas12a) triggers non-specific probe cleavage to attenuate current (signal-off); positive voltage enrichment gathers redox fragments near electrodes and further amplifies signals to achieve super-on state. This triple amplification strategy endows the sensor with wide linear range and excellent stability for VEGF biological analysis.

(2) Interleukin-6

Interleukin-6 (IL-6) is a pleiotropic pro-inflammatory cytokine closely correlated with tumor progression, cancer cachexia, immune remodeling and drug resistance, with abnormal upregulation observed in multiple malignancies. Imaging targeting IL-6 enables sensitive visualization of inflammatory TME and reflects immune activation and systemic inflammation, representing the integration of cancer imaging and immunometabolic profiling [101].

In clinical practice, inflammatory cytokines such as IL-6, IL-12 and C-reactive protein (CRP) show concentration differences across multiple orders of magnitude, bringing challenges for simultaneous detection. Shi *et al.* developed an all-in-one diagnostic kit based on DNA-encoded nanocatalyst assembly (Figure 3A) [102]. By regulating antibody quantity on Pt@AuNPs via single-stranded DNA competitive binding, the detection range can be flexibly adjusted. Three nanoplatforms with different valence states and DNA dendritic structures realize gradient detection from high concentration to ultra-trace level, achieving IL-6 quantification down to 4 pg/mL. The platform can simultaneously detect multiple cytokines in breast cancer serum, and dynamic cytokine changes during treatment provide reference for personalized tumor immunotherapy.

(3) Soluble Programmed Death Ligand-1

As a soluble subtype of membrane programmed death-ligand 1 (PD-L1), soluble programmed death ligand-1 (sPD-L1) have become vital extracellular biomarkers for evaluating tumor immune escape and immune checkpoint blockade efficacy. Wu *et al.* proposed an aptamer-coupled droplet CRISPR/Cas12a platform for amplification-free sPD-L1 detection (Figure 3B) [103]. Without sPD-L1, structure-switching aptamer remains closed and cannot activate Cas12a; target binding displaces blocking sequence and triggers Cas12a trans-cleavage activity to turn on fluorescence signal. Picoliter microdroplets concentrate reaction components and suppress background fluorescence, achieving nearly 1000-fold sensitivity enhancement. The platform completes detection within 70 min with a detection limit of 0.5 pM and 100% accuracy in clinical plasma samples, serving as a rapid liquid biopsy tool for tumor immunotherapy monitoring.

Li *et al.* designed a double-photoelectrode photoelectrochemical (PEC) sensing platform with an antenna-like mechanism for sPD-L1 detection (Figure 3C) [104]. p-type MIL-68(In)−NH_2 MOF acts as photocathode and CdSe/$MgIn_2S_4$ heterojunction as photoanode; MOF organic ligands capture photons and accelerate carrier transfer via ligand-to-metal charge transition. Fermi energy difference between two electrodes inhibits carrier recombination and enhances photocurrent response. Specific

PD-L1 binding hinders interfacial electron transfer, resulting in regular photocurrent decline with target concentration, realizing ultra-trace sPD-L1 detection down to 3.26 $\times 10^{-6}$ ng/mL.

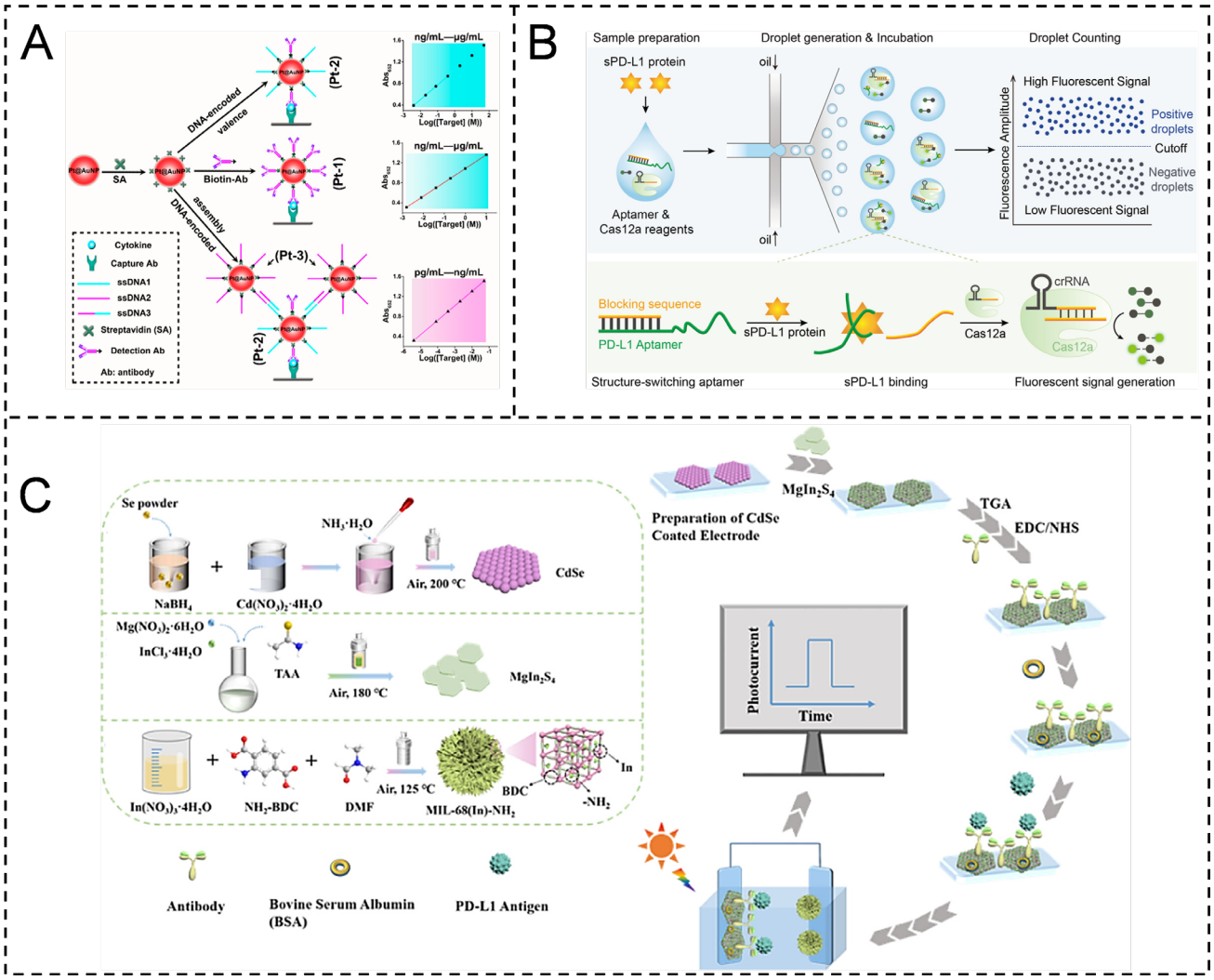

Figure 3. Strategies for sensing extracellular tumor-associated growth factors and cytokines. **(A)** The DNA-encoded nanocatalyst assembly-based all-in-one diagnostic platform for gradient and simultaneous detection of multiple inflammatory cytokines represented by IL-6. Reprinted with permission [102]. Copyright 2024 American Chemical Society; **(B)** The aptamer-coupled droplet CRISPR/Cas12a platform for amplification-free, rapid sPD-L1 detection. In the absence of sPD-L1, the structure-switching aptamer maintains a closed conformation and fails to activate Cas12a. Reprinted with permission [103]. Copyright 2026 American Chemical Society; **(C)** The dual-photoelectrode PEC sensing platform with an antenna-like mechanism for ultra-trace sPD-L1 detection. Reprinted with permission [104]. Copyright 2023 American Chemical Society.

2.2.3. Proteases and stromal proteins

Proteases and stromal proteins are emerging fast-developing extracellular imaging targets [105–107]. Unlike classic tumor antigens that reflect tumor cell abundance, these biomarkers directly characterize extracellular matrix (ECM) remodeling, stromal activation and invasive phenotype, highlighting that TME is an active driver rather than a passive scaffold of tumor progression.

(1) Matrix Metalloproteinases

Matrix metalloproteinases (MMPs) are core extracellular proteases regulating ECM degradation, tumor invasion, angiogenesis and metastasis, with significantly elevated enzymatic activity in aggressive malignancies. Different from always-on imaging probes, MMP-activatable fluorescence probes remain quenched in normal tissues and only activate after specific proteolytic cleavage in tumor lesions, improving imaging specificity and reducing background interference [108,109]. MMP-based imaging can further dynamically evaluate tumor invasiveness and metastatic potential.

Zhong *et al.* developed a low-cost portable MMP-1 detection platform by integrating commercial pregnancy test strips, magnetic separation and peptide cleavage strategy (Figure 4A) [110]. Complementary DNA strands are conjugated with MMP-cleavable peptide and human chorionic gonadotropin (hCG) protein and assembled on magnetic nanoparticles. Without MMP-1, hCG probes are fixed on beads and generate no strip signal; MMP-1 specifically cleaves peptide sequences to release free hCG-DNA complexes, which produce visible red bands on test strips after magnetic separation. This strategy converts MMP detection into hCG signal readout without complex antibody preparation, achieving a visual detection limit of 65.5 pg/mL in saliva and better anti-interference performance than enzyme-linked immunosorbent assay (ELISA), suitable for early oral cancer screening.

(2) Fibroblast Activation Protein

Fibroblast activation protein (FAP) is a landmark stromal biomarker specifically expressed on cancer-associated fibroblasts (CAFs) and highly enriched in desmoplastic stroma of epithelial tumors, showing important diagnostic value for fibrotic tumors such as pancreatic cancer [111,112]. Given that the FAP catalytic pocket is negatively charged, Zhang *et al.* proposed a universal strategy by introducing positive charges into fluorescent fluorophore skeletons to enhance probe affinity and sensing sensitivity (Figure 4B) [113]. The optimized dual positively charged near-infrared probe FQCy7 remains silent under physiological conditions and emits strong fluorescence after specific FAP cleavage, providing a new design idea for high-performance FAP-targeted imaging probes.

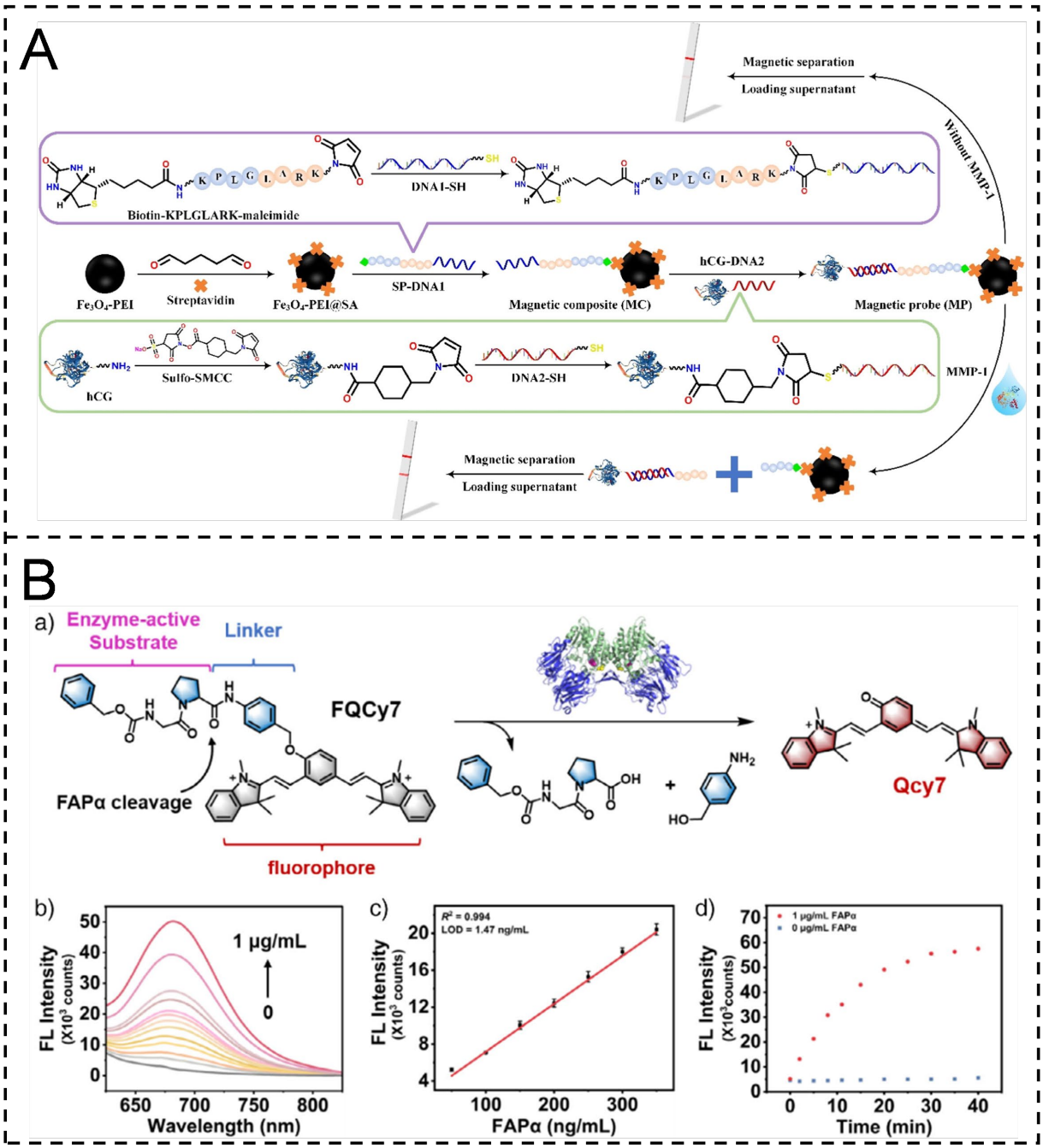

Figure 4. Strategies for sensing tumor-associated proteases and stromal proteins. **(A)** Schematic of the magnetic separation-assisted and hCG signal readout-based strategy for portable detection of MMP-1. Reprinted with permission [110]. Copyright 2022 American Chemical Society; **(B)** Design and characterization of the near-infrared activatable fluorescent probe FQCy7 for FAP. Reprinted with permission [113]. Copyright 2025 Wiley-VCH.

2.3. Extracellular nucleic acid targets

Extracellular nucleic acids are transformative biomarkers for cancer molecular imaging and liquid biopsy. Different from protein biomarkers reflecting downstream phenotypic changes, ctDNA, extracellular microRNAs (miRNAs) and long non-coding RNAs (lncRNAs) carry tumor-specific genetic and epigenetic information including oncogenic mutation, transcriptional dysregulation and clonal evolution, enabling tumor profiling at genomic and transcriptomic levels [72,114,115].

Circulating tumor-derived nucleic acids dynamically change during tumor progression and treatment intervention, which can better reflect intratumoral heterogeneity and adaptive drug resistance than static tissue biopsy [116]. Nevertheless, nucleic acid biomarkers generally have high molecular specificity but low abundance and poor *in vivo* stability, requiring ultrasensitive amplification and signal enhancement strategies for practical imaging application.

2.3.1. Circulating tumor DNA

ctDNA is fragmented tumor-derived DNA released into peripheral blood via apoptosis, necrosis and active secretion, retaining tumor-specific mutation and epigenetic characteristics. ctDNA detection realizes non-invasive real-time evaluation of tumor mutation landscape and captures intratumoral heterogeneity and systemic metastasis evolution that cannot be fully reflected by single-site tissue biopsy [114,115].

(1) KRAS Mutation ctDNA

KRAS proto-oncogene, GTPase (KRAS) mutation is a key genomic biomarker for pancreatic and colorectal cancer, occurring in the early stage of tumorigenesis. Dynamic monitoring of mutant KRAS ctDNA is of great value for early diagnosis, postoperative recurrence surveillance and therapeutic response evaluation [117]. Advances in droplet digital polymerase chain reaction (ddPCR), next-generation sequencing (NGS), catalytic DNA circuits and nanoparticle-assisted fluorescence amplification have greatly improved detection sensitivity, and longitudinal monitoring of mutant allele frequency can identify therapy-induced clonal selection prior to anatomical morphological changes [118].

To overcome the dependence on large instruments and complex operation of traditional ctDNA detection, Tang *et al.* integrated recombinase polymerase amplification (RPA), CRISPR-Cas9 and catalytic hairpin assembly (CHA) into a lateral flow strip platform for simultaneous detection of lung cancer-related KRAS ctDNA and miRNA-223 (Figure 5A) [119]. RPA pre-amplifies target ctDNA; CRISPR-Cas9 specifically recognizes amplicons and captures gold nanoparticle probes to produce visible test line signals; CHA reaction triggers cyclic strand displacement amplification for high-sensitivity miRNA detection on another test line. This dual-index platform realizes one-step visual detection in saliva, reduces false positives of single-biomarker detection, and provides portable point-of-care testing (POCT) tool for non-invasive lung cancer early screening.

(2) EGFR Mutation ctDNA

EGFR mutation detection based on ctDNA has become an indispensable part of non-small cell lung cancer (NSCLC) precision medicine, enabling dynamic monitoring of targeted therapy sensitivity, acquired resistance and temporal tumor evolution [120]. Compared with local tissue biopsy, circulating EGFR ctDNA better reflects spatial heterogeneity among metastatic lesions. Chen *et al.* constructed an ultrasensitive electrochemical biosensor based on Au@MNPs network for direct ctDNA detection in whole blood (Figure 5B) [121]. A dispersible electrode sensing strategy was adopted to solve the bottlenecks of ultra-low ctDNA abundance, slow mass transfer and complex sample pretreatment. Probe-modified Au@MNPs are uniformly dispersed in samples to capture target ctDNA *in situ* and shorten molecular diffusion distance; nanoparticle complexes are enriched on gold electrodes via external magnetic field. Methylene blue and potassium ferricyanide form cyclic redox amplification system to enhance electrochemical response, achieving trace ctDNA detection down to 5 fM within 20 min. The sensor exhibits excellent anti-interference ability in undiluted whole blood, providing a rapid ultrasensitive strategy for non-invasive ctDNA liquid biopsy.

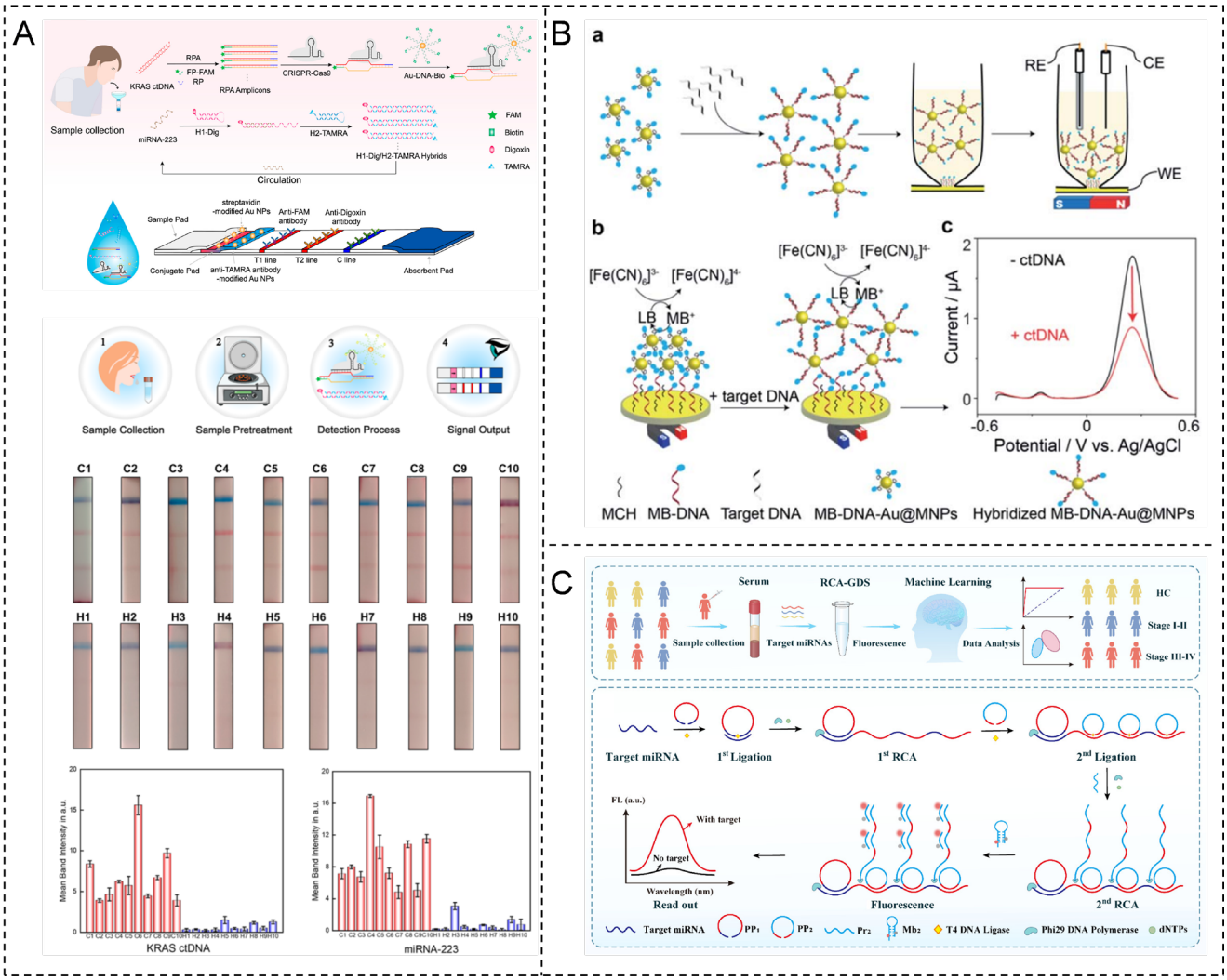

Figure 5. Strategies for sensing tumor-associated extracellular nucleic acids. **(A)** Schematic of the lateral flow strip platform integrating RPA, CRISPR-Cas9, and CHA for simultaneous visual detection of KRAS ctDNA and miRNA-223. Reprinted with permission [119]. Copyright 2025 American Chemical Society; **(B)** The Au@MNPs network-based electrochemical biosensor for ultrasensitive ctDNA detection. Reprinted with permission [121]. Copyright 2021 Royal Society of Chemistry; **(C)** Schematic of the RCA-based dual-step fluorescent platform for circulating miRNA detection. Reprinted with permission [122]. Copyright 2025 American Chemical Society.

2.3.2. Extracellular RNAs

Extracellular miRNAs and lncRNAs participate in oncogenic signaling, metastasis, immune regulation and drug resistance, serving as promising functional imaging biomarkers [123–127]. Unlike genomic DNA mutations reflecting tumor genotype, noncoding RNAs dynamically characterize transcriptional activity and phenotypic plasticity, and are closely associated with epithelial–mesenchymal transition (EMT), stemness maintenance, metabolic reprogramming and immune remodeling [128].

miR-21 is one of the most widely studied oncogenic miRNAs with broad overexpression in solid tumors and hematological malignancies [129–131]. It inhibits multiple tumor suppressor pathways to promote proliferation, metastasis, chemoresistance and immune escape [122]. High circulating stability and definite tumor correlation make miR-21 a representative biomarker for liquid biopsy-assisted

molecular imaging. To improve the low sensitivity of traditional linear rolling circle amplification (RCA) for trace miRNA detection, Tao *et al.* developed an RCA-generated DNA seagrass (RCA-GDS) fluorescent sensing platform (Figure 5C) [122]. Two padlock probes are adopted for cascade amplification: target miR-21 initiates cyclization and primary RCA of the first probe, and generated repetitive sequences activate the second padlock probe to trigger secondary RCA for exponential signal amplification. Abundant amplicons hybridize with molecular beacons to restore fluorescence emission. The platform achieves attomolar detection limit and single-base discrimination ability under isothermal conditions. Combined with The Cancer Genome Atlas (TCGA) bioinformatics analysis and machine learning, miR-21/miR-182/miR-183 signature realizes precise classification of healthy individuals and early/advanced breast cancer patients.

2.4. Extracellular vesicle targets

Extracellular vesicles (EVs, especially exosomes) are next-generation core platforms for cancer molecular imaging [132–135]. Encapsulated by lipid bilayer membranes, EVs protect internal proteins, nucleic acids and metabolites from enzymatic degradation and maintain high stability in circulation. Beyond passive biomarker carriers, tumor-derived exosomes mediate intercellular communication and participate in immune suppression, stromal remodeling, angiogenesis and metastatic niche formation, enabling EV-based imaging to reflect dynamic tumor-TME crosstalk rather than isolated molecular changes [132,134,136].

2.4.1. Exosomal surface proteins

(1) PD-L1-Positive Exosomes

EV membrane-bound PD-L1 is a pivotal biomarker for lung cancer diagnosis and anti-PD-1/PD-L1 immunotherapy efficacy evaluation [137–139]. However, soluble PD-L1 in body fluids severely interferes with specific EV-PD-L1 detection. Song *et al.* established a DNA computation combined with herringbone microfluidic chip strategy (DECLA) (Figure 6A) [140]. Cholesterol-modified DNA probes insert into EV lipid bilayer, and PD-L1-specific aptamers act as dual input elements to construct AND-gate DNA logic circuit. Only EVs with complete membrane structure and surface PD-L1 can trigger connector probe activation, eliminating interference from free soluble PD-L1 and serum lipoproteins. Biotinylated EVs are captured by streptavidin-modified microfluidic chips and quantified via anti-CD63 immunofluorescence. The method achieves high-sensitivity quantitative detection and perfectly distinguishes lung cancer patients from healthy donors with an AUC of 1.

(2) EpCAM-Positive Exosomes

EpCAM is highly enriched on the surface of tumor-derived EVs and serves as an ideal marker for capturing tumor-specific EV subpopulations [141]. Hu *et al.* fabricated EpCAM N-terminal epitope-imprinted polymers (epitope-imprinted molecularly imprinted polymers, MIPs) using EpCAM extracellular signature peptide as template (Figure 6B) [142]. The prepared MIPs exhibit excellent specific recognition ability with an imprinting factor up to 6.02, selectively binding EpCAM-high-expressing tumor cells and hardly adsorbing normal 293T cells. MIPs can specifically enrich EpCAM-positive EVs from pancreatic cancer patient urine, and proteomic analysis of enriched EVs reveals consistent expression changes of tumor-associated proteins with tumor and peritumor tissues. As low-cost artificial

antibody materials, EpCAM-MIPs provide a novel tool for epithelial tumor liquid biopsy and pathological monitoring.

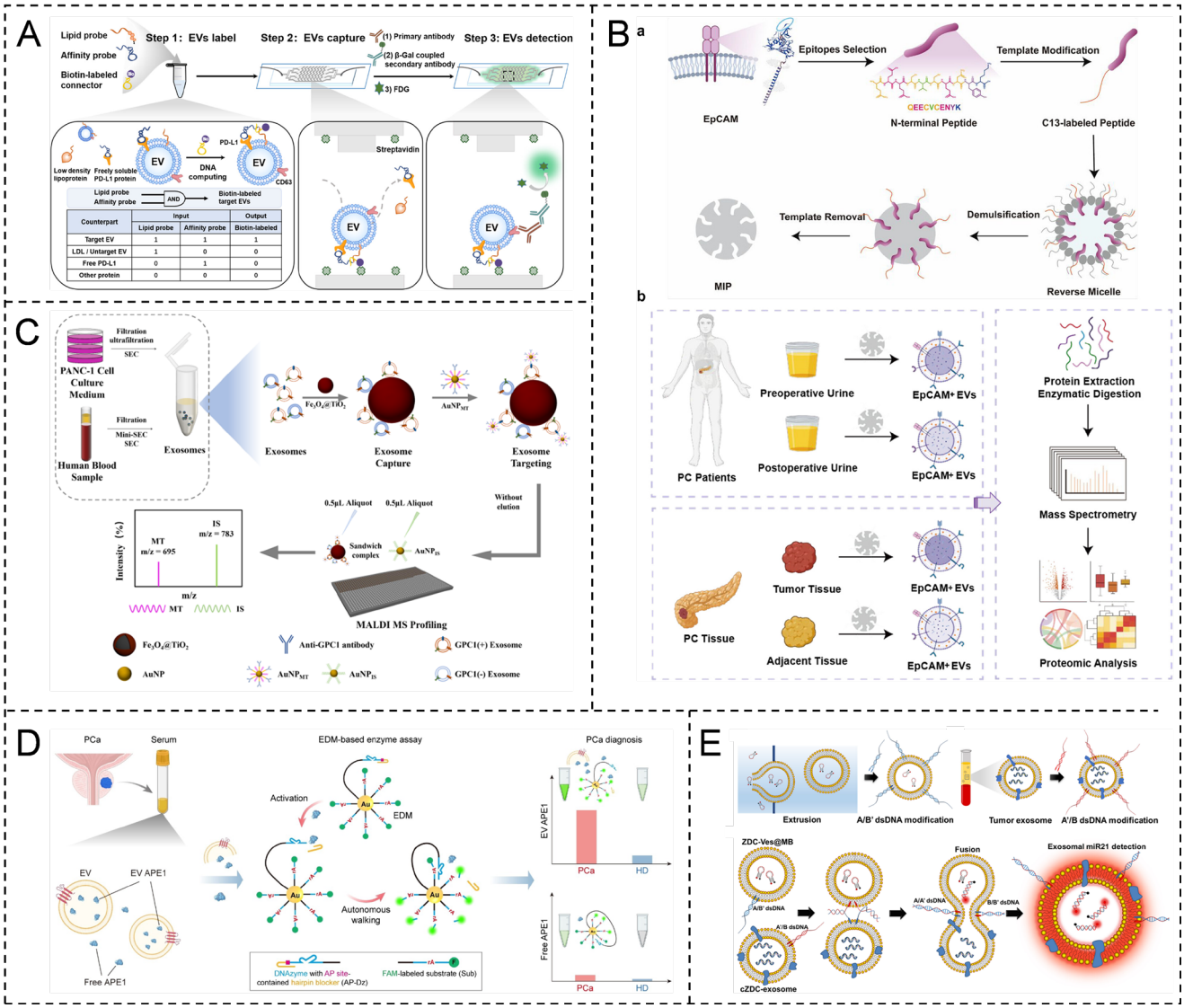

Figure 6. Strategies for sensing and imaging tumor-associated EVs. **(A)** The DECLA for specific detection of PD-L1-positive EVs. Reprinted with permission [140]. Copyright 2023 American Chemical Society; **(B)** EpCAM N-terminal MIPs for enrichment and proteomic analysis of EpCAM-positive exosomes. Reprinted with permission [142]. Copyright 2026 American Chemical Society; **(C)** MALDI-TOF MS-based *in situ* signal amplification strategy for the quantification of GPC1-positive exosomes. Reprinted with permission [143]. Copyright 2023 American Chemical Society; **(D)** The EDM targeting exosomal APE1 for pancreatic cancer (PCa) diagnosis. Reprinted with permission [144]. Copyright 2024, Wiley-VCH; **(E)** Schematic of the DNA-modified exosome fusion strategy for exosomal miRNA detection. Reprinted with permission [145]. Copyright 2022 American Chemical Society.

(3) GPC1-Positive Exosomes

Glypican-1 (GPC1) is specifically enriched on pancreatic cancer-derived exosomes, and GPC1-positive EVs are regarded as promising targets for early pancreatic cancer diagnosis [146]. Gao *et al.* developed a matrix-assisted laser desorption/ionization time-of-flight mass spectrometry (MALDI-TOF MS) *in situ*

signal amplification quantification strategy for GPC1-positive exosomes (Figure 6C) [143]. Size-exclusion chromatography rapidly purifies high-purity exosomes from plasma; Fe_3O_4@TiO_2 magnetic nanoparticles capture exosomes via phospholipid adsorption; anti-GPC1 antibody-modified gold nanoparticles form sandwich recognition system to convert macromolecular protein signals into stable small-molecule mass tag signals for MALDI-TOF MS detection. With internal standard calibration, the method achieves accurate quantification in a wide concentration range and effectively differentiates pancreatic cancer patients from healthy donors for early diagnosis and dynamic progression monitoring.

2.4.2. Exosomal functional enzymes

EV-encapsulated functional enzymes are emerging novel cancer biomarkers [145,147–149]. Traditional ELISA and Western blot can only detect enzyme protein expression rather than real catalytic activity, and low enzyme abundance in EVs brings additional detection challenges. Sun *et al.* developed enzyme-triggered spherical DNA nanomotors (EDM) for ultrasensitive detection of EV-encapsulated apurinic/apyrimidinic endonuclease 1 (APE1) (Figure 6D) [144]. As a key enzyme in DNA base excision repair, APE1 is highly enriched in tumor-derived EVs. EDM is constructed by immobilizing deoxyribozymes (DNAzyme), AP-site hairpin probes and 6-carboxyfluorescein (FAM)-labeled substrates on gold nanoparticles. Active APE1 cleaves AP-site structure to activate DNAzyme and trigger cascaded substrate cleavage for nonlinear fluorescence amplification. The method achieves a detection limit of 177 fM with sensitivity two orders of magnitude higher than ELISA. EV-derived APE1 level is closely correlated with parental tumor stress status, achieving 92% accuracy in distinguishing early prostate cancer patients from healthy donors. The versatile EDM platform can be extended to detect other EV functional enzymes for liquid biopsy and early tumor diagnosis.

2.4.3. Exosomal nucleic acids

Protected by lipid bilayer membranes, exosomal nucleic acids exhibit better stability against enzymatic degradation than free circulating nucleic acids [150,151]. Exosomal miR-21 is markedly overexpressed in tumor-derived EVs and serves as a classic tumor biomarker [152,153]. Traditional detection relies on cumbersome exosome isolation, RNA extraction and quantitative reverse transcription polymerase chain reaction (qRT-PCR), which is time-consuming and may cause miRNA degradation.

A DNA zipper-mediated membrane fusion strategy was established for rapid *in situ* exosomal miR-21 detection (Figure 6E) [145]. Lipid vesicle probes encapsulated with miR-21-targeting molecular beacons are modified with zipper DNA constructs (ZDCs), while isolated exosomes are functionalized with complementary catalytic zinc-dependent DNAzymes (cZDCs). Specific hybridization between ZDC and cZDC triggers spontaneous membrane fusion, enabling molecular beacons to recognize exosomal miR-21 and generate fluorescence signals. The assay completes detection within 30 min without RNA extraction and qRT-PCR, and can effectively distinguish tumor-derived EVs from normal EVs combined with flow cytometry, providing a convenient tool for tumor liquid biopsy.

2.5. Advantages and limitations of extracellular targets

Extracellular targets including proteins, nucleic acids and exosomal vesicles are core biomarkers supporting non-invasive cancer molecular imaging and liquid biopsy. Their universal advantage lies in

easy accessibility in body fluids and TME without membrane crossing, enabling minimally invasive sampling, longitudinal monitoring and postoperative recurrence surveillance, with good compatibility with antibodies, aptamers, nanozymes and multiple imaging modalities.

Each subtype possesses unique strengths: extracellular proteins feature high abundance and mature detection technology, dynamically reflecting tumor angiogenesis, immune remodeling and ECM invasion; extracellular nucleic acids carry tumor-specific genetic and epigenetic signatures with high molecular specificity, capable of tracing clonal evolution and intratumoral heterogeneity beyond tissue biopsy; exosomal vesicles protect internal cargos from enzymatic degradation, mediate intercellular tumor-stroma communication and faithfully recapitulate parental tumor molecular profiles for tumor subtyping and immunotherapy response evaluation.

Nevertheless, extracellular targets still face universal and subtype-specific bottlenecks restricting diagnostic accuracy and clinical translation. Most extracellular biomarkers lack absolute tumor specificity, with abnormal elevation also observed in inflammation, fibrosis and hyperplasia, easily causing false-positive signals. Spatiotemporal heterogeneity and dynamic expression fluctuation during tumor progression further reduce quantitative imaging reliability, and single target detection cannot balance sensitivity and specificity well. Specifically, classic protein markers are vulnerable to serum matrix interference and benign disease influence; extracellular nucleic acids suffer from ultra-low abundance, nuclease degradation and lack of unified isolation and quantification standards; exosomal targets are limited by heterogeneous size/origin, non-standard isolation protocols, soluble biomolecule interference and time-consuming detection procedures.

In the future, multi-marker combined imaging, microenvironment-activatable probe design, cascade signal amplification and AI-assisted quantitative analysis are expected to alleviate above limitations. Establishing unified isolation and analytical standards will further accelerate the clinical application of extracellular target-based intelligent imaging in precision oncology.

3. Membrane targets for cancer imaging

3.1. Overview of membrane targets

Membrane-located biomarkers represent the most clinically mature and translationally advanced category of cancer imaging targets. Unlike intracellular biomarkers that require complex transmembrane delivery and endosomal escape, membrane proteins are directly exposed on the cell surface, enabling straightforward recognition by imaging ligands, antibodies and aptamers [154–156]. Meanwhile, different from freely diffusing extracellular biomarkers diluted in body fluids, membrane targets retain precise spatial localization at tissue and cellular levels, supporting *in situ* tumor delineation and anatomical positioning [18,157,158].

Oncogenic transformation induces extensive remodeling of cell membrane components, including abnormal expression of receptor tyrosine kinases (RTKs), immune checkpoint molecules, cell adhesion proteins and lineage-specific antigens [159–161]. Beyond serving as passive biomarkers, these membrane molecules actively regulate tumor proliferation, angiogenesis, epithelial-mesenchymal transition, immune escape and metastatic progression [162,163]. Therefore, membrane-targeted imaging can simultaneously provide anatomical localization and functional information regarding tumor aggressiveness and treatment response. Benefiting from surface accessibility and stable expression

characteristics, membrane biomarkers are highly compatible with mainstream imaging technologies such as PET, fluorescence-guided surgery, photoacoustic imaging and integrated theranostic platforms. Targets with high membrane density, favorable ligand internalization efficiency and low normal tissue background expression exhibit superior imaging performance, among which EGFR, HER2, PD-L1 and PSMA have become representative benchmarks for precision oncology imaging. According to biological functions and translational characteristics, membrane imaging targets are classified into five subgroups: growth factor receptors, immune checkpoint molecules, adhesion and metastasis-related proteins, tumor-specific membrane antigens, and circulating tumor cell (CTC) surface markers.

3.2. Growth factor receptors

RTKs are the earliest validated and most widely applied membrane imaging targets [164–167]. Their advantages lie in high surface accessibility, close oncogenic relevance and perfect compatibility with targeted therapy. RTKs regulate core malignant phenotypes via phosphoinositide 3-kinase/protein kinase B (PI3K/AKT), mitogen-activated protein kinase (MAPK) and Janus kinase/signal transducer and activator of transcription (JAK/STAT) signaling pathways, controlling cell proliferation, angiogenesis, invasion and metabolic adaptation.

RTK-targeted imaging establishes an important link between molecular imaging and precision therapy, enabling patient stratification, therapeutic response prediction and longitudinal monitoring of drug resistance evolution [154]. Moreover, high receptor density on cell membranes provides favorable conditions for radionuclide imaging and intraoperative fluorescence navigation. Notably, tumor evolution, hypoxic microenvironment and drug intervention continuously reshape RTK expression and activation status. Current research is gradually shifting from static protein quantification to dynamic imaging of receptor phosphorylation, signaling adaptation and drug resistance progression.

3.2.1. Epidermal growth factor receptor

EGFR is a classic prototype membrane target for tumor theranostic imaging, with overexpression and abnormal activation commonly observed in non-small cell lung cancer, glioblastoma, colorectal cancer and head-neck squamous cell carcinoma [168]. It drives malignant proliferation, invasion and anti-apoptotic signaling cascades. Modern EGFR imaging has evolved from traditional immunohistochemical detection to radiolabeled tracers, small-molecule PET probes and near-infrared fluorescence imaging, enabling quantitative mapping of EGFR distribution in primary and metastatic lesions [169–171]. It also supports screening of targeted therapy candidates, early prediction of drug efficacy and precise delineation of tumor margins during fluorescence-guided surgery.

Tan *et al.* designed a circular bivalent aptamer-functionalized afterglow luminescent nanoprobe (cb-Apt-ALNP) (Figure 7A) [172]. The closed-loop circular structure improves nuclease resistance and serum stability. The probe specifically anchors phosphorylated EGFR on cell membranes, and afterglow intensity is dynamically modulated by electron transfer during EGFR phosphorylation. This design realizes *in situ* continuous visualization of EGFR phosphorylation and nuclear translocation at cell, tumor spheroid and *in vivo* levels, effectively distinguishing EGFR activation differences between tumor and normal cells and evaluating the inhibitory effect of targeted drugs.

3.2.2. Human epidermal growth factor receptor 2

HER2 amplification is a validated core biomarker for breast and gastric cancer targeted therapy, closely associated with malignant progression and poor prognosis [173,174]. High membrane abundance and accessibility make HER2 an ideal target for PET and fluorescence imaging, which can compensate for sampling bias of local biopsy and reflect tumor heterogeneity [35,175]. It also assists intraoperative identification of micrometastases and residual tumor foci to optimize surgical resection. Nevertheless, therapeutic intervention often induces HER2 downregulation and internalization, and the widespread existence of HER2-low tumors limits the detection sensitivity of conventional probes. Clinical routine diagnosis relies on immunohistochemistry (IHC) combined with fluorescence *in situ* hybridization (FISH) confirmation, which suffers from subjective judgment deviation, cumbersome operation, high cost and long detection cycle. In addition, traditional aptamer probes are easily degraded in biological fluids, and electrostatic repulsion with negatively charged cell membranes further weakens targeting efficiency [155].

To address these limitations, Xue *et al.* constructed a proximity-driven spatially matched 3D DNA aptasensor (3DDA) for HER2 detection and pathological typing (Figure 7B) [176]. The platform integrates cholesterol-modified tetrahedral nucleic acid frameworks for stable membrane anchoring, HER2-specific aptamers for spatially matched recognition, and CHA circuit for *in situ* signal amplification. The rigid tetrahedral structure enhances serum stability and nuclease resistance. Cellular experiments verify its ability to distinguish HER2-positive and negative cell lines. In clinical breast cancer specimens, the detection results are highly consistent with FISH gold standard, enabling accurate identification of IHC 2+ equivocal cases and providing a low-cost alternative for HER2 molecular subtyping.

3.2.3. c-Met

c-Met, activated by hepatocyte growth factor (HGF) ligand, is a key receptor tyrosine kinase dominating tumor invasion, EMT progression, distant metastasis and drug resistance [177]. Different from EGFR and HER2 focusing on proliferative activity, c-Met imaging mainly reflects aggressive metastatic phenotypes, enabling evaluation of pathway activation status rather than merely protein expression level. Current small-molecule PET and peptide fluorescent probes support c-Met detection in liver, gastric and lung cancers [178]. However, ligand-induced receptor internalization and stromal crosstalk lead to unstable imaging signals and poor quantitative reproducibility.

Traditional pH-responsive nucleic acid probes for c-Met detection rely on rigid i-motif or DNA triplex structures, which are limited by sequence constraints and difficult large-scale synthesis. To break this bottleneck, a novel pH-responsive DNA aptamer (CSL1-II) was designed by introducing unnatural nucleobase with a pKa of 5.9 (Figure 7C) [153]. The aptamer maintains disordered conformation under normal tissue neutral pH with low target binding capacity, while folding into active recognition structure in weakly acidic tumor microenvironment. It can competitively block HGF/c-Met signaling and inhibit tumor migration and invasion without obvious damage to normal cells, providing a versatile design strategy for microenvironment-responsive aptamer construction.

3.2.4. MUC1

Mucin 1 (MUC1) is a transmembrane glycoprotein abnormally overexpressed and aberrantly glycosylated in breast, lung, pancreatic and ovarian epithelial tumors, participating in tumor proliferation, EMT, invasion,

metastasis and immune escape [179,180]. It has become a widely applicable core target for membrane tumor imaging. Current MUC1-targeted imaging mainly adopts aptamer, antibody and nanoplatform-based fluorescent probes for early screening and intraoperative navigation [181–184]. Conventional near-infrared fluorescence probes require repeated washing to reduce background interference, and suffer from poor photostability and weak signal intensity, restricting long-term dynamic *in situ* observation.

Ouyang's group fabricated DNA nanosheet-templated copper nanosheets (DNS/CuNSs) to construct a high-performance Förster resonance energy transfer (FRET)-based MUC1 imaging platform (Figure 7D) [184]. Two-dimensional DNA nanosheets serve as rigid templates for *in situ* growth of copper nanosheets, forming well-defined nanocomposites with optimized optical properties. Combined with Cy5.5 acceptor, the system achieves an ultra-large Stokes shift, effectively reducing autofluorescence and optical scattering interference. This platform realizes wash-free *in situ* imaging, with significantly improved anti-photobleaching stability and signal amplification efficiency, laying a foundation for *in vivo* molecular imaging and targeted theranostic application.

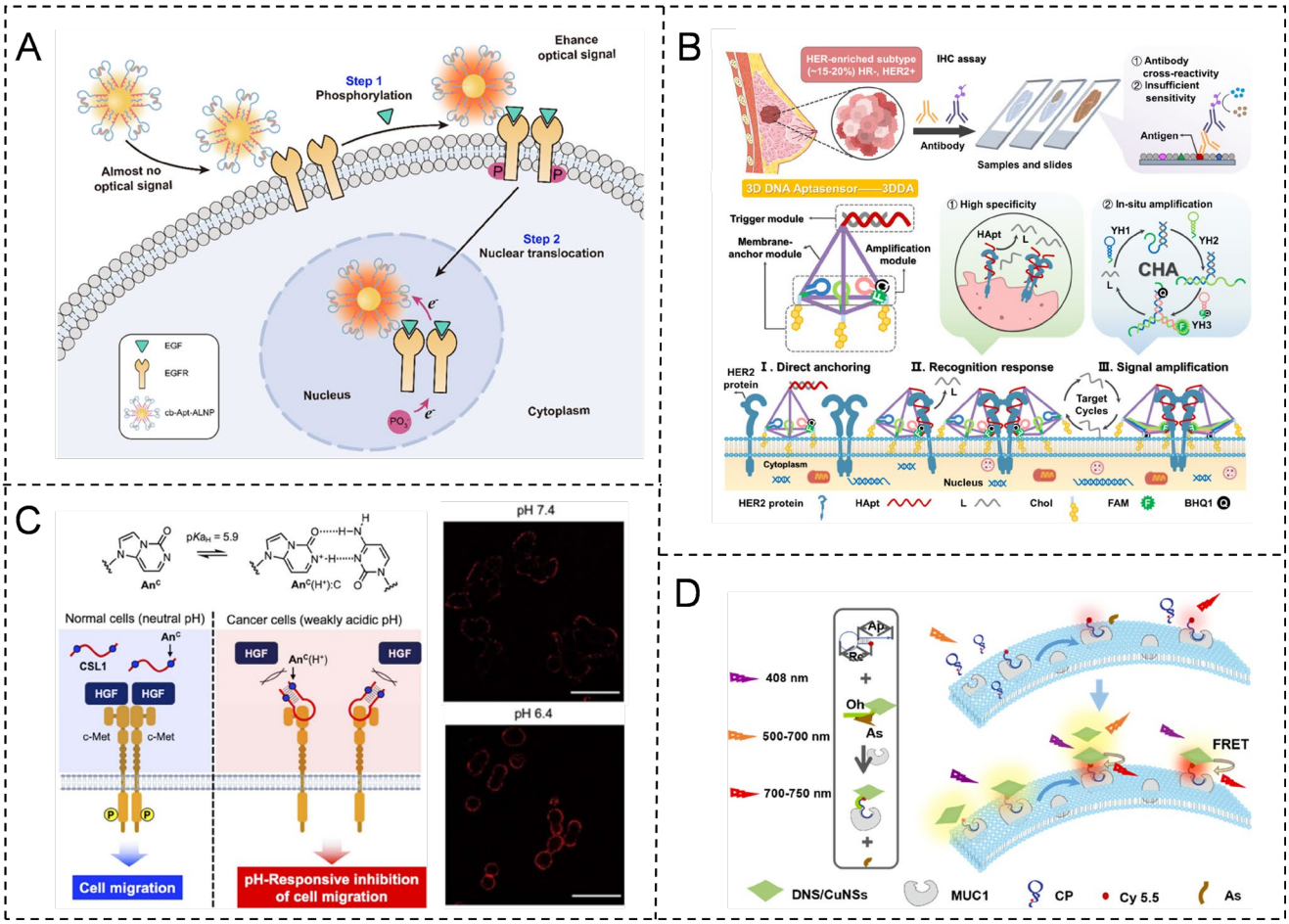

Figure 7. Strategies for imaging tumor-associated growth factor receptors on cell membrane. **(A)** The cb-Apt-ALNP for dynamic visualization of EGFR phosphorylation and nuclear translocation. Reprinted with permission [172]. Copyright 2022 American Chemical Society; **(B)** The proximity-driven spatially matched 3DDA for HER2 detection and pathological subtyping. Reprinted with permission [176]. Copyright 2026 American Chemical Society; **(C)** The CSL1-II for c-Met targeting in weakly acidic tumor microenvironments. Reprinted with permission [153]. Copyright 2024 Royal Society of Chemistry; **(D)** The FRET-based MUC1 imaging platform using DNS/CuNSs. Reprinted with permission [184]. Copyright 2024 American Chemical Society.

3.3. Immune checkpoint targets

Immune checkpoint molecular imaging promotes the development of tumor imaging from simple anatomical lesion localization to functional profiling of tumor immune microenvironment (TIME) [74,185]. Different from conventional membrane biomarkers reflecting tumor proliferation burden, immune checkpoint targets can directly characterize immune activation status, T cell exhaustion degree and immunotherapy response susceptibility [186]. Clinical treatment efficacy is jointly determined by intrinsic tumor biological characteristics and spatiotemporal distribution of TIME, making immune checkpoint profiling an essential prerequisite for precise immunotherapy.

Compared with limited local biopsy of traditional IHC, whole-body molecular imaging enables non-invasive panoramic visualization of immune checkpoint expression in primary and metastatic lesions, supporting patient stratification, early efficacy prediction and longitudinal dynamic monitoring [187,188]. Current research mainly focuses on PD-L1, PD-1 and cytotoxic T-lymphocyte-associated protein 4 (CTLA-4) covering adaptive anti-tumor immunity, while innate immune checkpoint represented by cluster of differentiation 47 (CD47) has gradually expanded the boundary of immune imaging in recent years.

3.3.1. PD-L1

PD-L1 is the most extensively studied immune checkpoint target, expressed on tumor cells, stromal cells and antigen-presenting cells in TME. It binds to PD-1 on activated T cells to inhibit cytotoxic immune response and mediate tumor immune escape. PD-L1 expression is dynamically regulated by inflammatory cytokines, interferon signaling, radiotherapy and chemotherapy, leading to transient pseudo-positive signals irrelevant to long-term anti-tumor immunity [189,190]. In addition, receptor glycosylation and intracellular trafficking alter epitope accessibility, bringing difficulties to quantitative standardization.

PD-L1-targeted ImmunoPET overcomes the sampling bias of IHC and realizes whole-body visualization of heterogeneous checkpoint expression, showing better predictive value for immune checkpoint inhibitor efficacy than local biopsy [191]. Longitudinal imaging can detect immune microenvironment remodeling earlier than anatomical morphological changes [192].

To improve detection specificity, recent studies focus on TME-responsive activatable probes and AI-assisted quantitative analysis. Li *et al.* constructed an orthogonal nucleic acid-peptide amplification circuit integrating matrix metalloproteinase 2 (MMP2)/9-activated hybridization chain reaction (HCR) and aptamer-mediated PD-L1 recognition (Figure 8A) [193]. Using PNA as a bridging scaffold, the system suppresses non-specific amplification in normal tissues and enhances localized signal amplification in tumor regions with high MMP expression. This design improves the discrimination between tumor and normal tissues, enabling accurate PD-L1 quantification and effective prediction of immunotherapy efficacy.

3.3.2. CD47

CD47 is a key innate immune checkpoint overexpressed in multiple malignancies. By binding signal regulatory protein alpha (SIRPα) on macrophages and dendritic cells, it transmits the “don’t eat me” signal to inhibit phagocytosis and antigen presentation, facilitating immune escape and TME immunosuppression [194,195]. Elevated CD47 expression is closely associated with tumor progression, metastasis and poor prognosis, especially in triple-negative breast cancer. Different from PD-L1

regulating adaptive immunity, CD47 imaging provides complementary information for innate immune status evaluation, enabling more comprehensive immune network profiling.

Traditional IHC is limited by sampling bias and cannot capture lesion heterogeneity or support intraoperative real-time navigation. Nanobodies, with small molecular size, excellent tissue penetration and rapid *in vivo* clearance, are ideal carriers for CD47-targeted imaging. Li *et al.* developed a dual-modal PET/second near-infrared window (NIR-II) imaging platform based on engineered anti-CD47 nanobodies [196]. High-affinity nanobody C2 and its albumin-binding derivative ABDC2 were conjugated with NIR-II fluorescent dye and radiolabeled tracer. The platform combines PET's advantage in whole-body tumor staging and NIR-II's strength in deep tissue penetration and intraoperative real-time navigation. In breast cancer models, the probe achieves high tumor-to-background contrast for primary tumor and lymph node metastasis detection, and accurately delineates tumor margins during surgery, showing great translational potential for precision imaging and image-guided oncologic surgery.

3.4. Adhesion and metastasis-associated targets

Most cancer-related deaths are caused by tumor metastasis, while conventional imaging only focuses on anatomical lesion identification rather than the biological mechanism of tumor dissemination [197–200]. Adhesion and metastasis-related membrane proteins fill this gap, enabling visualization of tumor invasive behavior, stromal interaction, vascular infiltration and pre-metastatic niche formation [201,202].

Different from proliferation-related receptors reflecting tumor growth rate, this type of target characterizes tumor cell plasticity and migratory potential, directly participating in EMT, ECM remodeling and organotropic metastasis. Imaging of these biomarkers can detect aggressive tumor phenotypes and micro-metastatic lesions that are invisible to conventional anatomical imaging, realizing the transformation from "tumor localization imaging" to "tumor behavioral imaging". Representative targets include EpCAM, integrin $\alpha_v\beta_3$, cluster of differentiation 44 (CD44) and MMP family proteins.

3.4.1. EpCAM

EpCAM is a transmembrane epithelial adhesion glycoprotein widely overexpressed in epithelial malignancies. In addition to cell adhesion function, it regulates tumor proliferation, stemness maintenance and epithelial phenotypic plasticity. High extracellular exposure and stable membrane localization make EpCAM an ideal target for tumor imaging and CTC enrichment [73,203,204]. EpCAM-targeted probes are widely used in fluorescence-guided surgery, radionuclide imaging and liquid biopsy platforms.

Bai *et al.* constructed an aptamer-conjoined polydiacetylene nanoliposome (APN) self-accelerated responsive fluorescent sensor [197]. Relying on multiple non-covalent interactions between EpCAM, aptamer and cationic nanoliposomes, the platform achieves rapid response, high sensitivity and excellent target selectivity. With near-infrared fluorescence turn-on mode, it realizes *in situ* imaging of living tumor cells and sustained tumor imaging in xenograft models, and effectively identifies cancer lesions in clinical pathological sections, providing a universal strategy for EpCAM sensing and targeted tumor imaging.

3.4.2. Integrin $\alpha_v\beta_3$

Integrin $\alpha_v\beta_3$ is a classic target associated with tumor metastasis and angiogenesis, highly expressed on invasive tumor cells and angiogenic endothelial cells [205]. It mediates tumor adhesion, migration and

ECM interaction via recognizing arginine-glycine-aspartic acid (RGD)-containing ligands [206]. RGD peptide has high binding affinity and easy chemical modification, becoming an ideal scaffold for PET, fluorescence and multimodal imaging. Radiolabeled RGD tracers visualize angiogenic activity and metastatic aggressiveness, while fluorescent RGD probes assist intraoperative tumor margin delineation. To overcome rapid *in vivo* diffusion and insufficient tumor retention of small-molecule probes, Wang *et al.* designed a nitroreductase (NTR)-responsive dual-modal fluorescence/MRI probe with cRGD targeting, hypoxic activation and *in situ* protein anchoring functions (Figure 8B) [198]. The probe specifically recognizes tumor cells via cRGD peptide, and is triggered to generate reactive intermediates under tumor hypoxic microenvironment, realizing covalent anchoring with intracellular proteins. This *in situ* locking strategy significantly prolongs tumor retention time and improves imaging signal-to-noise ratio. Validated in subcutaneous and orthotopic lung cancer models, the probe achieves high-contrast dual-modal imaging and clear tumor boundary delineation.

It is worth noting that integrin expression is highly dependent on tissue microenvironment. Highly vascularized lesions show strong probe uptake, while hypoxic and necrotic regions present weak signals. Inflammatory angiogenesis and wound healing tissues also cause non-specific uptake, limiting diagnostic specificity. Single angiogenesis-related imaging is insufficient to fully evaluate tumor metastatic potential, and needs to be combined with immune and metabolic biomarkers.

3.4.3. CD44

CD44 is a multifunctional adhesion receptor and typical biomarker of cancer stem cell characteristics. By binding hyaluronic acid and ECM components, it regulates tumor stemness maintenance, EMT progression, drug resistance and distant metastasis colonization. Abnormal CD44 elevation is closely correlated with tumor recurrence and chemotherapy insensitivity. Different from conventional proliferation biomarkers, CD44 imaging preferentially labels stem-like and drug-resistant tumor subpopulations.

Traditional antibody or HA-based recognition strategies suffer from large steric hindrance, poor stability and batch difference, limiting sensing performance. Jia *et al.* constructed an aggregation-induced electrochemiluminescence (AIECL) platform based on mesoporous silica nanosphere-confined tetraphenylethene (TPE) derivatives (Figure 8C) [205]. Spatial confinement restricts intramolecular rotation to enhance ECL emission. Artificially designed WC-7 heptapeptide replaces traditional recognition molecules to reduce steric hindrance. Combined with DNA strand displacement reaction, the platform realizes sensitive detection of CD44 antigen and CD44-overexpressed tumor cells, with excellent stability and anti-interference capability.

3.4.4. MMP

Different from secreted MMPs described in extracellular targets, membrane-anchored and pericellular MMP-2 acts as a TME-responsive enzymatic target for tumor invasion imaging. Such probes remain inert under normal physiological conditions and only undergo structural assembly or functional activation after specific cleavage by overexpressed pericellular MMP-2, achieving precise TME-activated targeting.

Lou *et al.* designed a peptide-conjugated transformable probe (DMFA) with MMP-2 cleavage-induced morphological switching (Figure 8D) [206]. The probe initially self-assembles into nanoparticles for stable membrane anchoring. After cleavage by pericellular MMP-2, it disassembles into α-helix and

β-sheet fragments: the former destroys cell membrane integrity to induce Ca^{2+} influx, while the latter self-assembles into nanofibers to inhibit ion pump activity. The two modules synergistically suppress PI3K-AKT signaling pathway and inhibit tumor growth, migration and invasion, providing an innovative paradigm for MMP-2 responsive imaging and targeted intervention.

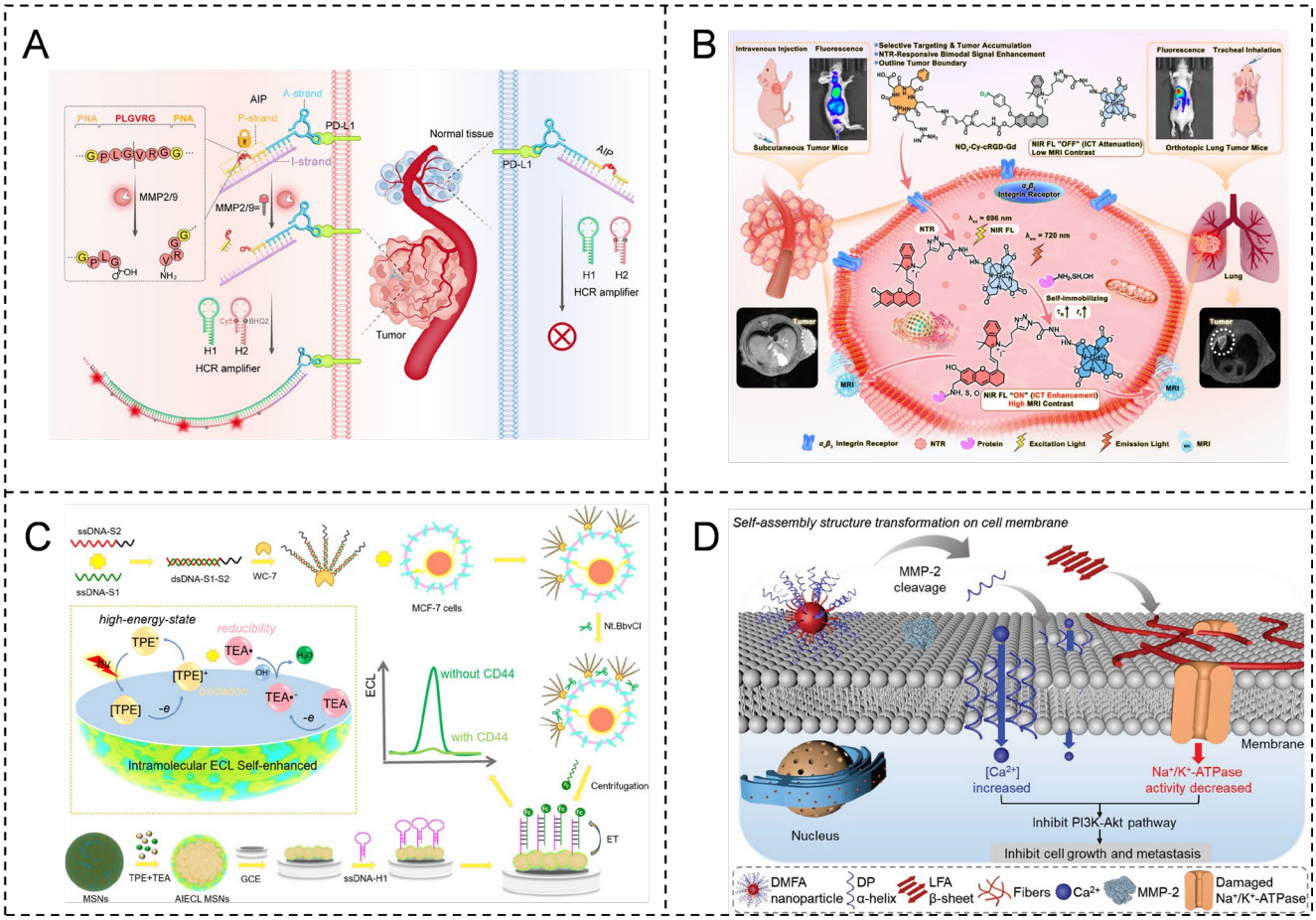

Figure 8. Strategies for imaging immune checkpoints and adhesion/metastasis-associated targets on cell membrane. **(A)** The orthogonal nucleic acid-peptide amplification circuit for PD-L1 imaging. Reprinted with permission [193]. Copyright 2026 Wiley-VCH; **(B)** The multistage tumor-targeted probe for dual-mode imaging of lung tumor. Reprinted with permission [198]. Copyright 2026 American Chemical Society; **(C)** The intracellular ECL self-enhanced biosensor for CD44 detection. Reprinted with permission [205]. Copyright 2023 American Chemical Society; **(D)** The MMP-2-responsive self-assembly transformation probe for tumor therapy. Reprinted with permission [206]. Copyright 2023 Wiley-VCH.

3.5. Tumor-specific membrane antigens

Tumor-specific membrane antigens integrate three core advantages of molecular imaging: high extracellular accessibility, low expression in normal tissues and definite pathological relevance [24]. Compared with widely expressed growth factor receptors and inflammation-related biomarkers, they provide higher tumor-to-background imaging contrast and support highly selective lesion visualization. Meanwhile, high surface density, prolonged membrane retention and efficient ligand internalization endow them with good pharmacological properties, suitable for radionuclide imaging, fluorescence-guided surgery and integrated theranostic systems [37]. The development of membrane antigen imaging reflects

the evolution of tumor imaging from non-specific metabolic detection to biologically stratified precision imaging, supporting molecular classification, patient selection and longitudinal treatment monitoring. Many tumor-specific antigens have developed from simple diagnostic biomarkers into integrated theranostic platforms, realizing the integration of imaging diagnosis and targeted therapy.

3.5.1. Prostate-specific membrane antigen

PSMA is one of the most successful translational imaging targets, fundamentally changing the clinical management mode of prostate cancer. Its excellent clinical performance benefits from high membrane density, strong prostate cancer specificity, efficient ligand internalization and long tumor retention, generating high imaging contrast for metastatic lesion, biochemical recurrence and minimal residual disease detection [24,37,39].

PSMA represents a typical target-guided theranostic model: small-molecule ligands can be conjugated with diagnostic radionuclides for PET imaging or therapeutic isotopes for radioligand therapy, realizing patient stratification, treatment planning and efficacy monitoring in one molecular framework [207]. Traditional MRI-based PSMA imaging is limited by low intrinsic sensitivity and lack of high-performance targeted contrast agents. Meade *et al.* constructed GSH-responsive activatable Gd(III) MRI probes via a targeting-activation-retention strategy (Figure 9A) [208]. Optimized PCP-2 probe adopts hydrophilic modified ligand to inhibit non-specific aggregation and enhance water solubility and binding affinity. It maintains low baseline signal in normal tissues, and is activated by intracellular GSH after tumor cell internalization. Aggregated probes enhance MRI relaxivity and turn on fluorescence signal, realizing dual-modal imaging and specific differentiation of PSMA-positive/negative tumors.

Notably, physiological PSMA expression in salivary glands, kidneys and lacrimal glands causes background interference, and neuroendocrine-differentiated prostate tumors often downregulate PSMA expression, leading to false-negative imaging results.

3.5.2. Glypican-3

Glypican-3 (GPC3) is a membrane heparan sulfate proteoglycan selectively overexpressed in hepatocellular carcinoma with negligible expression in normal adult tissues, possessing high tumor specificity for HCC precision imaging. Different from AFP with poor spatial localization, GPC3 imaging can directly visualize intratumoral heterogeneity and tissue distribution [209–211]. It participates in Wnt/β-catenin and other oncogenic signaling pathways, linking imaging signals with intrinsic tumor biological characteristics rather than simple biomarker accumulation. GPC3-targeted PET, MRI and fluorescence imaging show great potential for fluorescence-guided liver surgery and future theranostic integration.

Micro-hepatocellular carcinoma is difficult to detect due to low AFP sensitivity and insufficient performance of commercial MRI contrast agents. Zhang *et al.* established a dual-injection MRI platform based on *in vivo* membrane engineering and bioorthogonal chemistry (Figure 9B) [212]. Self-assembled peptide nanoparticles accumulate in HCC via enhanced permeability and retention (EPR) effect and bind membrane GPC3, exposing dibenzocyclooctyne (DBCO) click sites. Subsequent azide-modified gadolinium-DOTA (Gd-DOTA) realizes *in situ* immobilization via strain-promoted azide–alkyne cycloaddition (SPAAC) reaction, prolonging molecular rotation time and significantly improving MRI

relaxivity and tumor-to-liver contrast. This strategy achieves tumor-specific signal amplification with low systemic gadolinium deposition and good biosafety.

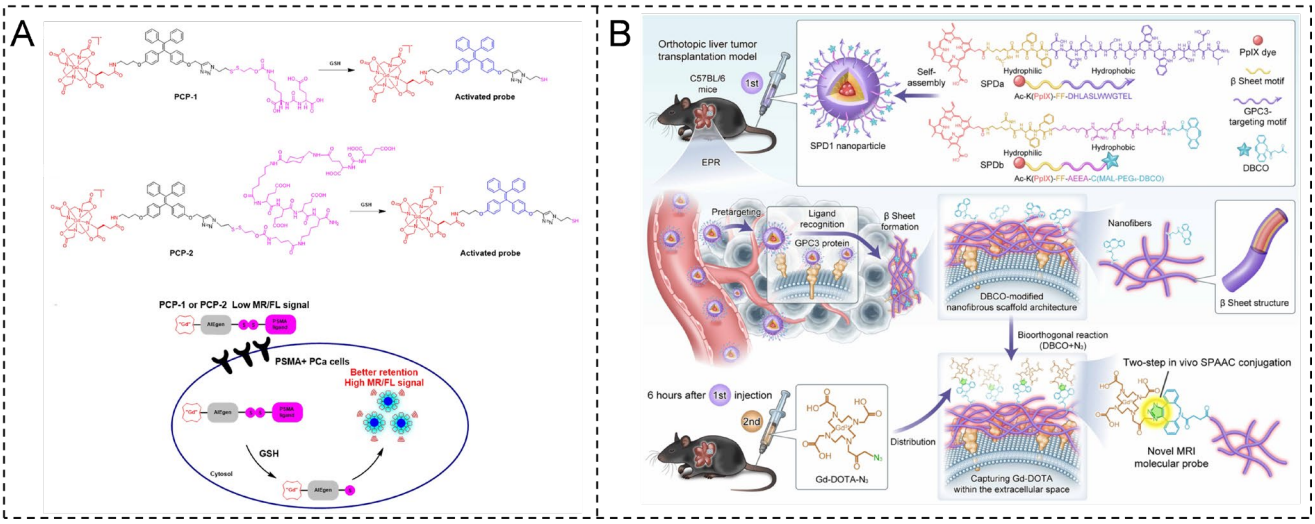

Figure 9. Strategies for imaging tumor-specific membrane antigens. **(A)** GSH-responsive activatable MRI/fluorescence dual-modal probes for PSMA-positive prostate cancer imaging. Reprinted with permission [208]. Copyright 2021 American Chemical Society; **(B)** The two-step *in vivo* bioorthogonal MRI platform for GPC3-targeted hepatocellular carcinoma imaging. Reprinted with permission [212]. Copyright 2026 American Association for the Advancement of Science.

3.6. Circulating tumor cell targets

CTCs are intact malignant cells shed from primary or metastatic lesions into peripheral blood, retaining complete genomic, transcriptomic and proteomic information at single-cell level. Different from cell-free biomarkers such as ctDNA and extracellular RNA, CTC detection provides unique insights into metastatic evolution and tumor heterogeneity [116,213–216]. CTC imaging realizes the transformation from molecular fragment detection to direct visualization of metastatic cellular behavior, playing an important role in evaluating tumor invasion, immune escape and therapeutic resistance.

Nevertheless, extremely low abundance and phenotypic plasticity bring great technical challenges. Most current enrichment strategies rely on membrane marker screening, which are prone to missing mesenchymal-like CTCs generated during EMT process.

3.6.1. EpCAM-positive CTCs

EpCAM is the most clinically validated target for CTC enrichment, and the FDA-approved CellSearch platform is based on EpCAM immunomagnetic separation [217]. Its epithelial specificity and membrane accessibility enable efficient capture of epithelial-derived CTCs. However, during EMT progression, aggressive tumor cells often downregulate EpCAM expression, leading to false-negative detection and underestimation of highly invasive metastatic subpopulations [218,219].

To compensate for the limitation of single-marker detection, a bioorthogonal click chemistry-based CTC detection platform was constructed (Figure 10A) [220]. Vertically aligned silicon nanowire chips modified with antifouling coating and tetrazine functional groups realize stable antibody immobilization via rapid covalent reaction with trans-cyclooctene (TCO)-modified ligands. Dual targeting of EpCAM

combined with trophoblast cell surface antigen 2 (TROP2) expands the recognition spectrum of heterogeneous CTCs, achieving twice the capture efficiency of traditional platforms. Integrated with enzyme-mediated chromogenic imaging, it avoids expensive fluorescence equipment and realizes accurate identification of low-abundance CTCs in peripheral blood.

Zuo *et al.* designed tetrahedral DNA framework-ensembled multivalent aptamers (TEA_n). Rigid DNA nanostructures serve as programmable scaffolds to anchor multiple EpCAM aptamers, realizing optimal spatial matching and cooperative binding with membrane EpCAM clusters (Figure 10B) [221]. The rigid framework enhances structural stability and anti-nuclease degradation ability in complex blood environment, maintaining high binding affinity under hydrodynamic shear force. Combined with magnetic bead separation, the platform exhibits excellent anti-interference performance in clinical samples and enables accurate CTC quantification and treatment response stratification in liver cancer patients.

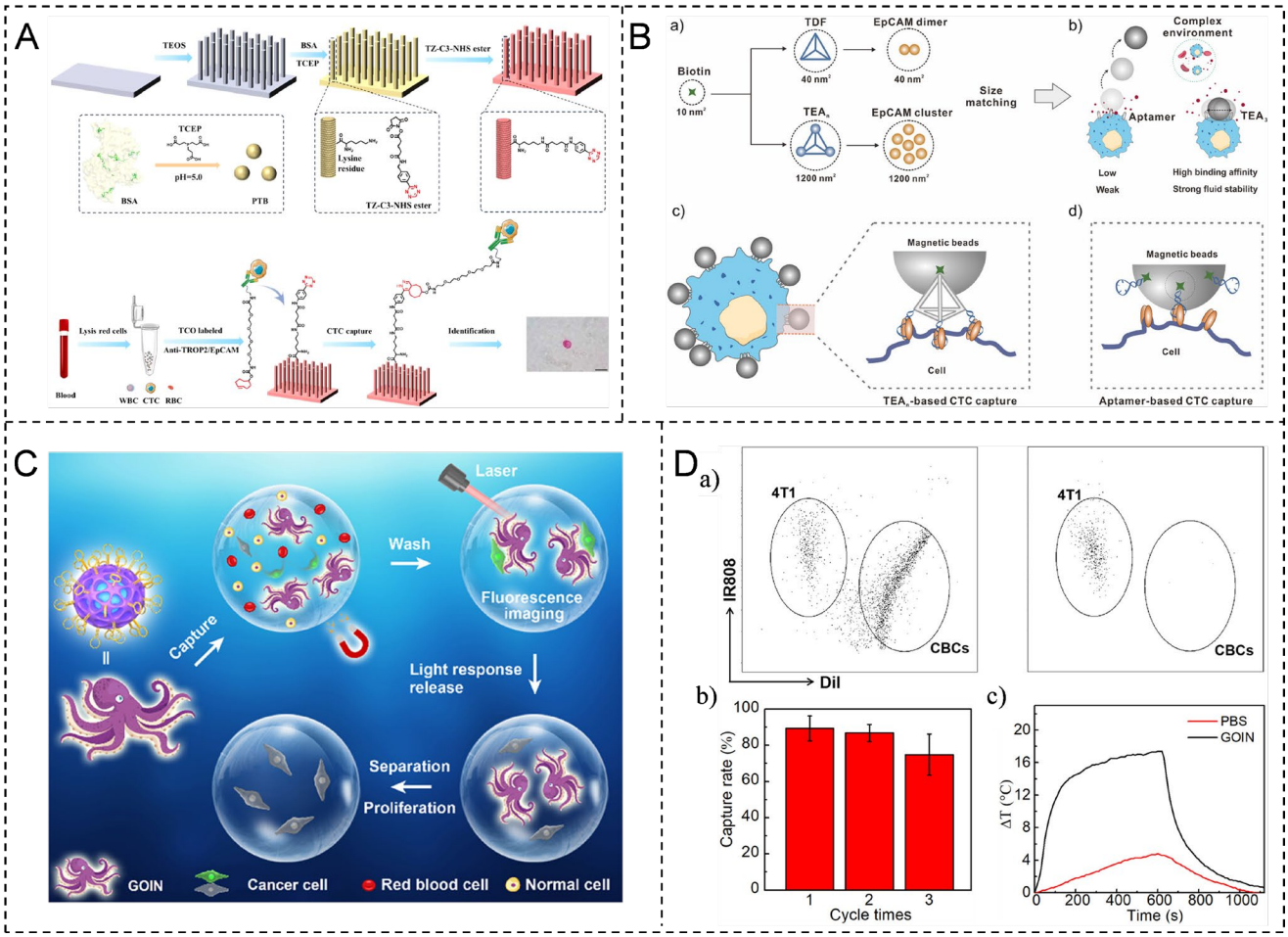

Figure 10. Strategies for imaging and analysis of CTCs. **(A)** The bioorthogonal click chemistry-based CTC detection platform for EpCAM/TROP2 dual-targeted capture. Reprinted with permission [220]. Copyright 2025 American Chemical Society; **(B)** The TEA_n platform for high-affinity EpCAM-positive CTC capture. Reprinted with permission [221]. Copyright 2025 Wiley-VCH; **(C, D)** The GOIN for nucleolin-positive CTC capture, imaging, and release. Reprinted with permission [222]. Copyright 2024 American Chemical Society; **(D) (a)** Flow cytometry analysis confirming specific capture of 4T1 cancer cells; **(b)** Capture rate over three capture-release cycles, demonstrating recyclability; **(c)** Photothermal heating curves showing efficient temperature elevation under NIR irradiation.

3.6.2. Nucleolin-positive CTCs

Nucleolin is highly overexpressed on various tumor-derived CTCs and stably maintains expression during EMT, becoming an ideal alternative biomarker independent of epithelial markers. Tang's group developed an octopus-inspired glowing nanomachine (GOIN) by modifying magnetic Fe3O4 nanoparticles with fluorescent covalent organic framework (COF) and AS1411 aptamers (Figure 10C,D) [222]. Densely arranged aptamers endow the platform with strong multivalent binding capacity for selective CTC capture. Intrinsic COF fluorescence enables label-free *in situ* visualization. Under NIR irradiation, mild photothermal effect reversibly weakens aptamer-cell binding by changing the secondary conformation of the aptamer, realizing gentle release of intact viable CTCs for subsequent biological analysis. The platform maintains stable performance for at least three capture-release cycles, integrating capture, imaging, separation and viable cell release into one recyclable system.

3.7. Current limitations and outlook

Most clinically mature membrane targets such as EGFR, HER2, PSMA and PD-L1 are evaluated based on static expression levels, which cannot fully reflect dynamic tumor biological states. Tumor spatial heterogeneity, temporal expression fluctuation and therapy-induced phenotype adaptation often reduce the reliability of single-target imaging.

A core contradiction exists between target accessibility and biological information depth: membrane targets have excellent clinical accessibility and translational feasibility, but mostly provide indirect phenotypic information; in contrast, intracellular targets can reflect core signaling and metabolic regulation, but are restricted by delivery barriers and unstable quantitative performance.

Driven by such limitations, research is gradually shifting from static biomarker quantification to dynamic functional imaging. Emerging targets related to ferroptosis, cuproptosis, immunometabolism and organelle stress can directly reflect tumor functional status and therapeutic vulnerability, breaking the limitation of traditional static markers. Meanwhile, imaging technology is evolving toward multi-target combination, activatable probe design, multimodal integration and AI-assisted quantitative analysis, which helps to comprehensively characterize tumor ecosystem and realize real-time monitoring of disease evolution.

The future development of membrane target imaging lies not only in exploring new biomarkers, but also in constructing adaptive imaging strategies to capture dynamic tumor characteristics at molecular, cellular and microenvironmental levels, supporting precise diagnosis and personalized therapeutic decision-making.

4. Intracellular targets for cancer imaging

4.1. Overview of intracellular targets

Intracellular targets refer to biomolecules and chemical substances located inside tumor cells, which directly dominate malignant progression [223], signaling activation [224], metabolic reprogramming [225,226] and cell fate regulation [227,228]. Different from extracellular markers reflecting tumor burden and membrane markers reflecting cell surface phenotype, intracellular targets reveal the real functional state of tumor cells, including signaling activity [229], metabolic flux [230,231], redox homeostasis [232] and stress adaptation [233,234].

Effective intracellular imaging requires probes to cross plasma membrane barriers and target specific subcellular compartments. According to molecular properties and biological functions, intracellular imaging targets are divided into four interrelated categories:

(1) Intracellular proteins: signaling proteins, molecular chaperones and apoptosis regulators controlling proliferation, stress adaptation and cell fate;

(2) Intracellular nucleic acids: oncogenic mRNAs and noncoding RNAs regulating transcriptional and post-transcriptional networks;

(3) Intracellular enzymes: proteases and metabolic enzymes whose catalytic activity can be monitored by activatable ratiometric probes;

(4) Intracellular small molecules and ions: ROS, GSH, adenosine triphosphate (ATP) and metal ions dynamically reflecting redox balance and metabolic stress.

4.2. Intracellular protein targets

Intracellular proteins carry the most functionally valuable information for tumor imaging, directly regulating core malignant hallmarks including uncontrolled proliferation, apoptotic resistance, proteotoxic stress adaptation and metabolic plasticity [210,235–237]. Compared with extracellular biomarkers mainly reflecting tumor existence, intracellular proteins provide mechanistic insights into tumor aggressiveness and treatment resistance [238]. Modern intracellular protein imaging has evolved from simple static expression detection to dynamic pathway state monitoring, focusing on pathway activation and cell fate determination rather than isolated molecular abundance.

4.2.1. Vimentin

Vimentin is a core intermediate filament protein and classic EMT biomarker, lowly expressed in normal epithelial tissues but significantly upregulated in malignant tumors. Its overexpression drives tumor migration, invasion and distant metastasis, closely correlated with poor clinical prognosis. Accurate *in situ* detection of intracellular vimentin is critical for early tumor screening and invasive risk assessment. Zou *et al.* developed a multifunctional DNA tetrahedron aptasensor integrating dual fluorescence modules for tumor identification and vimentin quantification [239]. The platform contains dual-target aptamers for EpCAM and protein tyrosine kinase 7 (PTK7) and AND-logic fluorescence reporting system, realizing highly specific tumor cell imaging. Meanwhile, cyanine 3 (Cy3)/black hole quencher 2 (BHQ2)-labeled hairpin aptamer enables specific recognition of intracellular vimentin, triggering hairpin opening and fluorescence recovery after target binding. The sensor achieves a detection limit of 1.1 nM and effectively distinguishes different EMT phenotypes in living cells.

4.2.2. Survivin

Survivin belongs to the inhibitor-of-apoptosis protein family, highly overexpressed in aggressive malignancies and rarely expressed in normal adult tissues [240]. It inhibits apoptotic signaling, promotes mitotic progression and enhances stress tolerance, leading to chemotherapy and radiotherapy resistance. Located at the intersection of proliferation and apoptosis regulation, survivin imaging can reflect tumor survival state and adaptive resistance pathway [241]. Fuchigami *et al.* designed a series of FRET-based survivin-sensitive fluorescent peptide probes (SSFPs) (Figure 11) [242]. The probe consists of high-affinity

targeting peptide, complementary protein segment and fluorophore-quencher pair. In the initial state, intramolecular interaction keeps fluorophore and quencher close to generate FRET quenching. After specific binding with survivin, probe conformation rearrangement breaks FRET effect and activates fluorescence. SSFP5 exhibits optimal performance with nanomolar affinity and negligible non-specific response, enabling specific labeling of survivin-positive tumor cells and providing a reliable tool for drug screening.

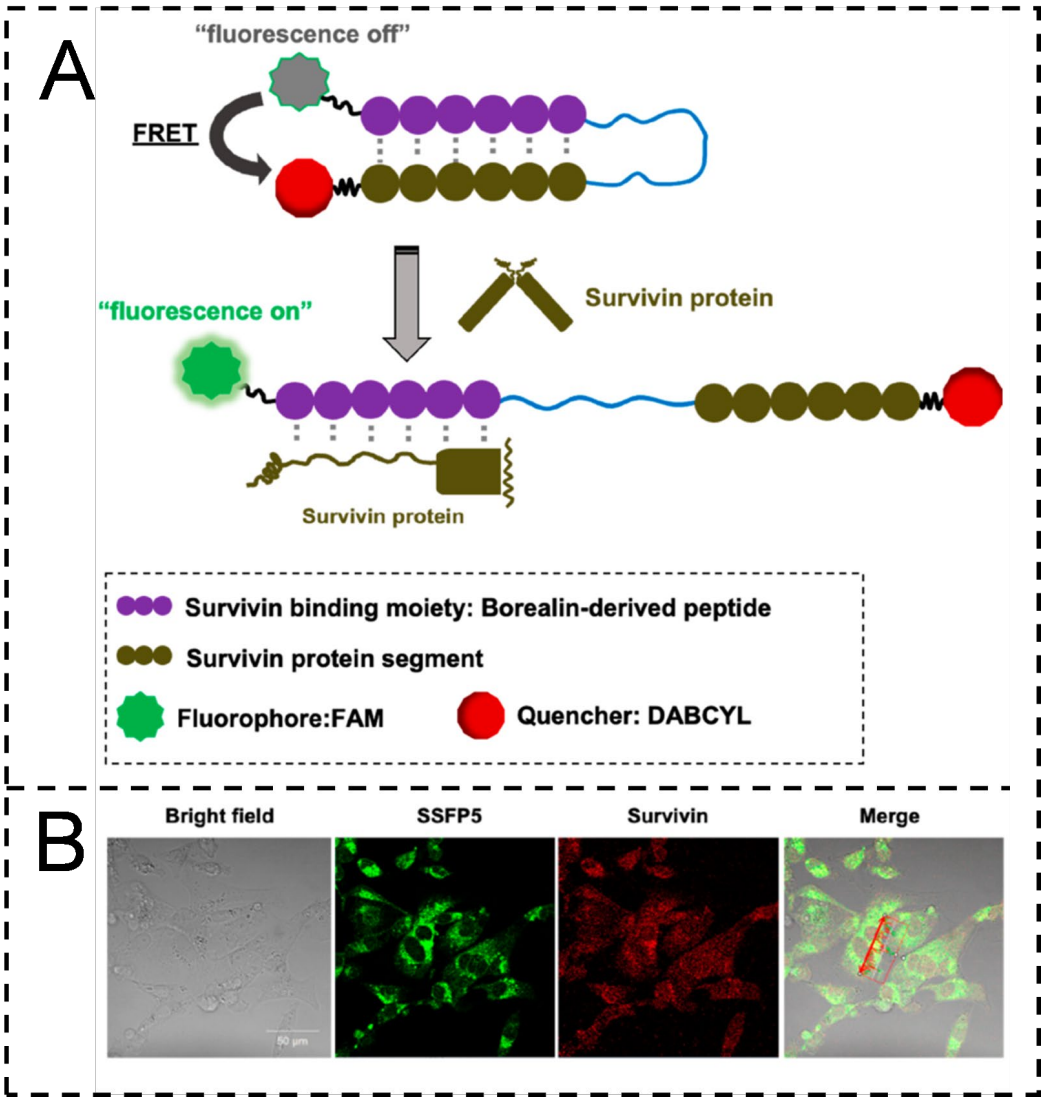

Figure 11. Strategy for intracellular protein imaging. **(A, B)** The FRET-based SSFP for intracellular survivin imaging. Reprinted with permission [242]. Copyright 2024 American Chemical Society.

4.2.3. Heat shock protein 90

Heat shock protein 90 (HSP90) is a key molecular chaperone abnormally overexpressed in tumors under proteotoxic stress, hypoxia and genomic instability. It acts as a global regulator of tumor stress adaptation and cell survival, making it a valuable target for functional oncology imaging. Different from proliferation biomarkers, HSP90 imaging mainly reflects tumor stress response and adaptive capacity. Li *et al.* constructed a dual-modal PET/near-infrared fluorescence probe ^{64}Cu-1,4,7-triazacyclononane-1,4,7-triacetic acid (NOTA)-San A-Cy7, using cyclopeptide San A as Hsp90α targeting ligand, conjugated with NOTA chelator and Cy7 fluorescent group [243]. The probe shows high targeting affinity and

physiological stability, enabling high-specificity tumor accumulation for PET whole-body imaging and precise tumor margin delineation for intraoperative fluorescence navigation. Blocking experiments confirm its excellent targeting specificity, integrating preoperative diagnosis and intraoperative guidance for esophageal cancer precision management.

4.3. Intracellular nucleic acid targets

Intracellular oncogenic mRNAs and noncoding RNAs are located upstream of tumor signaling networks, regulating transcription, epigenetics and post-transcriptional modification [42]. Their abnormal activation often precedes phenotypic changes, possessing unique advantages for early tumor detection and dynamic disease monitoring. Intracellular RNA imaging realizes real-time visualization of transcriptional activity, metabolic adaptation and cell plasticity at single-cell level, providing functional information that cannot be obtained by traditional histopathology and bulk omics.

4.3.1. MYC mRNA

MYC proto-oncogene is a central transcriptional regulator in cancer, driving cell proliferation, metabolic reprogramming, ribosome biogenesis and metastatic dissemination across multiple malignancies [244,245]. Its transcriptional activity better reflects tumor functional state than downstream protein biomarkers. MYC mRNA imaging represents a typical dynamic transcription-state detection mode, enabling real-time monitoring of transcriptional bursting, single-cell heterogeneity and adaptive response under microenvironmental stress [246–248].

A CHA-activated dual-modal Zn–Gd MOF-derived nanoplatform (ZGMD) nanoplatform was constructed for MYC mRNA imaging (Figure 12A) [248]. ZGO: Mn nanorods provide two-photon and afterglow luminescence, and CHA hairpin probes realize target-triggered cyclic signal amplification. In the presence of MYC mRNA, CHA assembly induces FRET and aggregation-enhanced resonance energy transfer (ARET) dual-signal response, achieving an ultra-low detection limit of 39 pM. The platform enables deep tissue two-photon imaging and ultra-high signal-to-background afterglow imaging, supporting longitudinal monitoring of tumor EMT status and chemotherapy efficacy.

To solve the limitation of sparse functional sites and non-specific adsorption of traditional nanocarriers, Tang's group proposed a bonding defect-amplified modification strategy to construct COF-based spherical nucleic acid probe (Figure 12B,C) [249]. Abundant carboxyl active sites are formed on COF surface for high-density grafting of hairpin DNA. Initial FRET quenching is eliminated after specific hybridization with MYC mRNA, turning on obvious fluorescence emission. The probe exhibits excellent specificity and nuclease resistance, enabling precise distinction of MYC-overexpressing tumor cells.

4.3.2. TK1 mRNA

Thymidine kinase 1 (TK1) mRNA is a key cell cycle biomarker abnormally upregulated in various malignancies, closely participating in DNA replication and cell proliferation regulation, with expression level correlated with tumor malignant progression and prognosis [250,251]. *In situ* visualization of TK1 mRNA can evaluate tumor proliferative activity in real time, while traditional single-function probes cannot integrate detection and targeted therapy.

Tang *et al.* constructed a nucleic acid-gated COF nanotheranostic platform (Figure 12D) [252]. Porphyrin COF nanoparticles serve as doxorubicin carriers, and Cy5-labeled TK1 recognition DNA acts as a molecular gate. In normal cells, adsorbed nucleic acid seals COF pores to avoid drug leakage and maintains FRET-induced fluorescence quenching. In tumor cells, TK1 mRNA hybridization disassembles the nucleic acid gate, restoring Cy5 fluorescence and triggering controlled drug release under tumor acidic microenvironment, realizing integrated imaging and targeted chemotherapy.

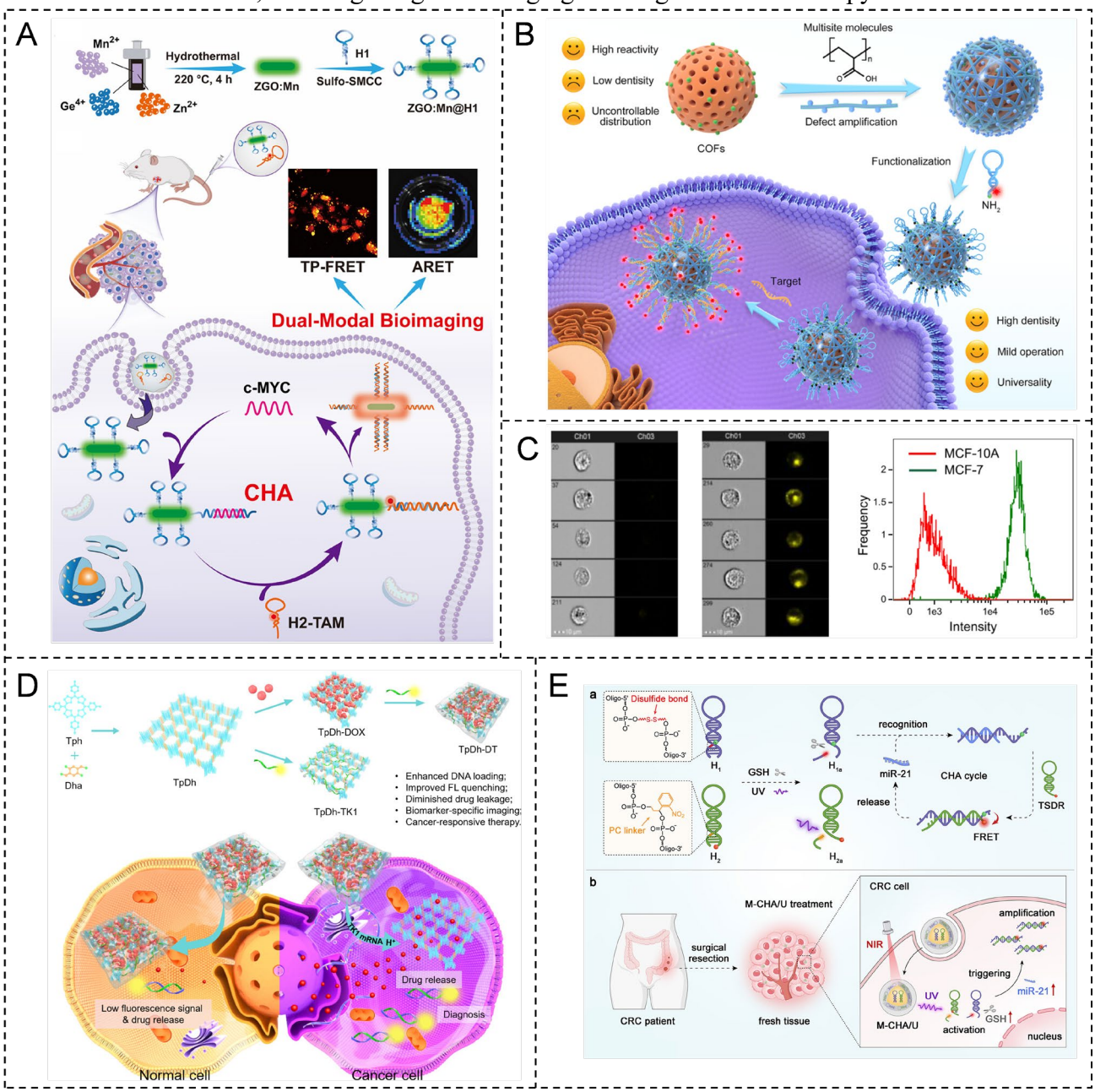

Figure 12. Strategies for intracellular nucleic acid imaging. **(A)** The CHA-activated dual-modal ZGMD nanoplatform for MYC mRNA imaging. Reprinted with permission [248]. Copyright 2026 American Chemical Society; **(B, C)** The bonding defect-amplified COF-based spherical nucleic acid probe for MYC mRNA detection. Reprinted with permission [249]. Copyright 2021 American Chemical Society; **(D)** Fluorescence microscopy images showing specific activation in TK1 mRNA -positive MCF-7 cells but not in MCF-10A cells. Reprinted with permission [252]. Copyright 2021 American Chemical Society; **(E)** The multivariate-gated CHA nanoplatform for miR-21 imaging in colorectal cancer. Reprinted with permission [253]. Copyright 2025 American Chemical Society.

4.3.3. miR-21

Intracellular microRNA-21 (miR-21) is a core post-transcriptional regulator, inhibiting multiple tumor suppressor pathways to promote proliferation, invasion, immune escape and drug resistance [122,225,235,254]. Different from relatively stable gene mutations, intracellular miR-21 expression dynamically fluctuates in response to chemotherapy, radiotherapy, oxidative stress and hypoxia, making it a sensitive indicator of tumor stress adaptation and treatment response.

Traditional CHA probes are prone to spontaneous signal leakage and reduce *in situ* imaging specificity. Yuan *et al.* constructed a multivariate-gated CHA nanoplatform based on upconversion nanoparticles (Figure 12E) [253]. Integrated with endogenous GSH-responsive disulfide bonds and exogenous NIR-photocleavable linkers, the platform locks CHA cascade in silent state under normal conditions. Only tumor sites with high GSH concentration and NIR irradiation can unlock dual gates to initiate miR-21-triggered cyclic amplification and FRET ratiometric fluorescence turn-on. This design effectively eliminates off-target activation and improves signal-to-background ratio, enabling correlation analysis of miR-21 expression and downstream DNA mismatch repair mechanism.

4.4. Intracellular enzyme targets

Intracellular enzyme activity directly reflects real-time biochemical flux and cellular functional state, rather than static protein abundance [255–258]. Enzyme-targeted imaging has inherent catalytic amplification advantage: a single enzyme molecule can continuously activate multiple probe substrates, significantly improving detection sensitivity for early tumors and micro-metastases. Enzyme activity is closely coupled with apoptosis, ECM remodeling, metabolic rewiring and autophagy, enabling imaging to capture dynamic tumor behavioral characteristics. Activatable probes remain optically silent under physiological conditions and are specifically activated in enzyme-rich tumor microenvironment, greatly improving imaging contrast. Apoptotic protease reflects treatment response, lysosomal protease indicates invasive potential, and metabolic enzyme mirrors tumor bioenergetic reprogramming. Representative targets include caspase-3 and cathepsin B.

4.4.1. Caspase-3

Caspase-3 is the core executioner protease in apoptotic cascade, located downstream of endogenous and exogenous death signaling pathways [259]. Activated caspase-3 cleaves multiple intracellular substrates to induce chromatin condensation, cytoskeletal collapse and irreversible cell apoptosis. Apoptosis response often appears earlier than anatomical tumor shrinkage after anti-tumor therapy, making caspase-3 imaging an important means for early evaluation of treatment efficacy.

Traditional MRI probes for caspase-3 imaging lack *in situ* self-assembly ability and suffer from insufficient low-field contrast. Liang *et al.* designed a caspase-3-responsive gadolinium probe based on 2-cyanobenzothiazole (CBT)-cysteine (Cys) bioorthogonal click chemistry (Figure 13A) [260]. After entering apoptotic cells, the probe is specifically cleaved by caspase-3, and endogenous GSH mediates disulfide bond reduction to trigger *in situ* self-assembly into gadolinium-rich nanoparticles, significantly enhancing T1-weighted MRI relaxivity at 0.5 T low magnetic field. The platform achieves high-specificity apoptotic imaging in cell and zebrafish models.

Peptide-functionalized AuNPs are promising for intracellular biomarker imaging due to good biocompatibility, fluorescence quenching performance and easy surface engineering. Conventional Au–S bonded peptide probes suffer from interference by intracellular thiols such as glutathione, causing non-specific fluorescence activation and false signals that hinder accurate *in situ* caspase-3 detection [40]. In contrast, Au–Se bonding delivers higher structural stability and anti-thiol resistance, enabling more reliable detection of apoptotic biomarkers [42]. However, traditional Au–Se probe synthesis requires 48 h room-temperature shaking and extra sodium dodecyl sulfate (SDS) surfactant, accompanied by residual contamination and low peptide loading efficiency.

To address these drawbacks, Tang *et al.* proposed a rapid freezing method for Au–Se-peptide nanoprobe fabrication (Figure 13B) [261]. Simply incubating AuNPs with selenol-modified peptides at −20 °C for 60 min yields surfactant-free nanoprobes. The freezing-induced molecular enrichment increases peptide loading by 20%–30% and ensures excellent serum stability and low cytotoxicity. By conjugating fluorescein isothiocyanate (FITC)-labeled caspase-3-cleavable peptide and tetramethylrhodamine (TAMRA)-tagged autophagy-related 4B (ATG4B)-targeted peptide onto AuNPs via Au–Se linkage, a dual-activatable nanoprobe was constructed based on enzyme cleavage-triggered fluorescence recovery. This platform exhibits high sensitivity, fast response and outstanding specificity toward caspase-3 and ATG4B. Cell experiments achieved real-time synchronous imaging of drug-regulated autophagy and apoptosis in HepG2 cells, distinguishing the differential effects of curcumin, SN-38 and rapamycin. This Au–Se nanoprobe provides a facile, biocompatible tool for dynamic caspase-3 monitoring and chemotherapeutic response evaluation.

4.4.2. Cathepsin B

Cathepsin B is a lysosomal cysteine protease, confined in lysosomes under physiological conditions but overexpressed and ectopically distributed in aggressive malignancies. It is secreted to extracellular and pericellular regions to promote ECM degradation, basement membrane destruction, tumor invasion and angiogenesis [262–264]. Different from caspase-3 reflecting therapeutic apoptosis, cathepsin B imaging focuses on tumor invasive and metastatic potential.

Xu *et al.* constructed a nucleolin-targeted ratiometric fluorescent nanoplatform with ultra-large emission displacement for cathepsin B imaging (Figure 13C) [265]. Amine-rich carbon quantum dots act as FRET donor, integrated with AS1411 aptamer and cathepsin B-cleavable peptide labeled with chlorin e6 acceptor. Efficient FRET quenching occurs in the initial assembly state. After targeted internalization into tumor cells, lysosomal cathepsin B specifically cleaves the peptide substrate, interrupting FRET process and realizing ratiometric fluorescence response with a 200 nm spectral shift. The sensor achieves ultrahigh sensitivity and enables precise distinction of tumor and normal cells.

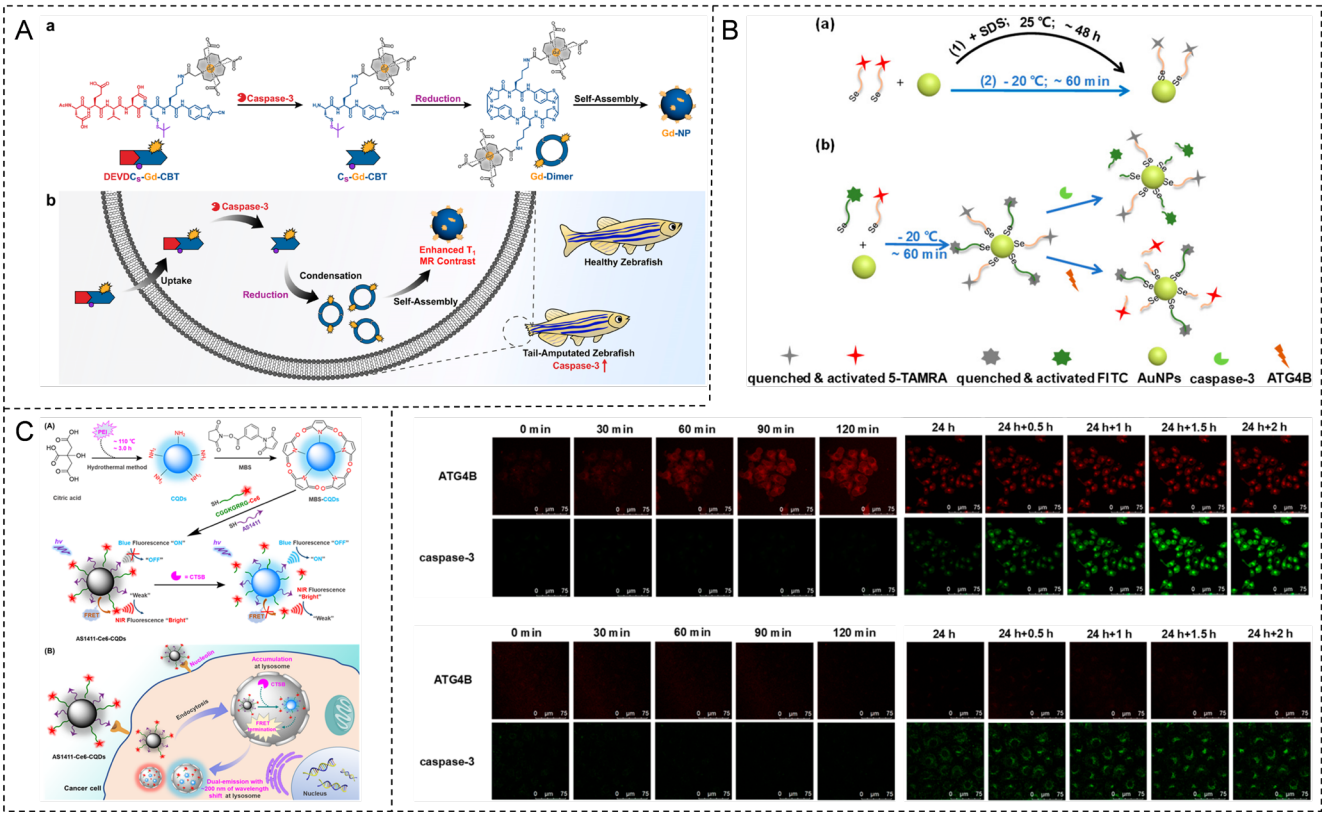

Figure 13. Strategies for intracellular enzyme imaging. **(A)** The caspase-3-responsive gadolinium probe based on CBT-Cys bioorthogonal click chemistry for MRI imaging of apoptosis. Reprinted with permission [260]. Copyright 2023 American Chemical Society; **(B)** The rapid freezing method for Au–Se-peptide nanoprobe fabrication and dual-activatable imaging of caspase-3 and ATG4B. Reprinted with permission [261]. Copyright 2019 American Chemical Society; **(C)** The nucleolin-targeted ratiometric fluorescent nanoplatform for cathepsin B imaging. Reprinted with permission [265]. Copyright 2021 American Chemical Society.

4.5. Intracellular small-molecule and ion targets

Intracellular small molecules, reactive species and metal ions represent a new generation of functional imaging targets. Different from static protein biomarkers reflecting tumor lineage characteristics, these chemical substances dynamically mirror metabolic reprogramming, redox homeostasis, stress adaptation and cell fate transition. Their spatiotemporal fluctuation is closely coupled with ferroptosis, cuproptosis, autophagy, hypoxic adaptation and therapy-induced stress response. Imaging of these substances realizes the upgrade from “structural biomarker detection” to “dynamic biochemical process visualization”.

4.5.1. Reactive oxygen species

ROS is a core regulator of intracellular redox homeostasis [266]. Oncogenic activation, mitochondrial dysfunction and metabolic reprogramming induce persistent ROS accumulation in tumor cells. Moderate ROS elevation promotes tumor proliferation, angiogenesis and drug resistance, while excessive ROS overload triggers oxidative damage and cell death [267]. ROS imaging can dynamically reflect tumor metabolic activity, stress adaptation and treatment-induced cell fate transition.

As the most stable and signaling-active ROS subtype, H_2O_2 elevation is closely associated with mitochondrial dysfunction, oncogenic signaling activation and therapeutic resistance. Yang *et al.* developed a microenvironment-tailored catalytic nanoprobe for ratiometric NIR-II fluorescence/photoacoustic imaging of H_2O_2 (Figure 14A) [268]. Liposome-confined nanoreactor constructs acidic GSH-shielded microenvironment to enhance H_2O_2 catalytic reaction. H_2O_2-triggered ABTS oxidation changes photoacoustic and NIR-II fluorescence signals, enabling accurate *in vivo* visualization of H_2O_2 in primary tumors and metastatic lymph nodes.

4.5.2. ATP

ATP is the universal intracellular energy currency, directly reflecting mitochondrial activity and metabolic flux. Tumor metabolic reprogramming reshapes ATP synthesis and distribution, supporting uncontrolled proliferation, stress adaptation and drug resistance [269–271]. Rapid ATP depletion is closely associated with apoptosis, ferroptosis and mitochondrial dysfunction, making ATP a key dynamic biomarker for monitoring cell fate transition.

Zhang *et al.* constructed a universal DNA nanohydrogel platform *via* RCA for ATP-responsive NIR-II imaging and synergistic therapy (Figure 14B) [272]. The nanohydrogel self-assembles from RCA skeleton and programmable staple strands, with fluorophores initially in aggregation-caused quenching state. Tumor-overexpressed ATP binds aptamer domain to disassemble nanohydrogel and turn on 1071 nm NIR-II fluorescence. The platform can replace aptamer for other biomarker detection and intercalate doxorubicin for ATP-triggered drug release, integrating diagnosis and targeted chemotherapy.

4.5.3. Glutathione

GSH is the dominant intracellular antioxidant maintaining redox homeostasis. Tumor cells upregulate GSH level to neutralize excessive ROS and enhance stress tolerance, which is also a key suppressor of ferroptosis by maintaining glutathione peroxidase 4 (GPX4) activity and preventing lipid peroxide accumulation. GSH depletion has become a hallmark event of ferroptosis induction and tumor metabolic vulnerability.

Zhu *et al.* fabricated 2D ZnO/MnO_2 nanosheet heterostructure for dual-modal GSH-responsive MRI imaging and granzyme B detection (Figure 14C) [273]. MnO_2 nanosheet is degraded by intracellular GSH to release Mn^{2+} and enhance T1 MRI signal; meanwhile, RGD targeting and FRET peptide motif enable simultaneous detection of immune effector granzyme B activity, realizing real-time monitoring of tumor redox status and immunotherapy efficacy.

Liu *et al.* designed a GSH/ATP dual-lock activatable DNA nanoprobe based on honeycomb MnO_2 nanovectors (Figure 14D) [274]. Split aptazyme assemblies remain quenched under normal conditions; only tumor cells with simultaneous GSH and ATP upregulation can trigger MnO_2 degradation, aptazyme assembly and cyclic signal amplification. This dual-logic design effectively eliminates false positives of single-biomarker probes and improves tumor recognition specificity.

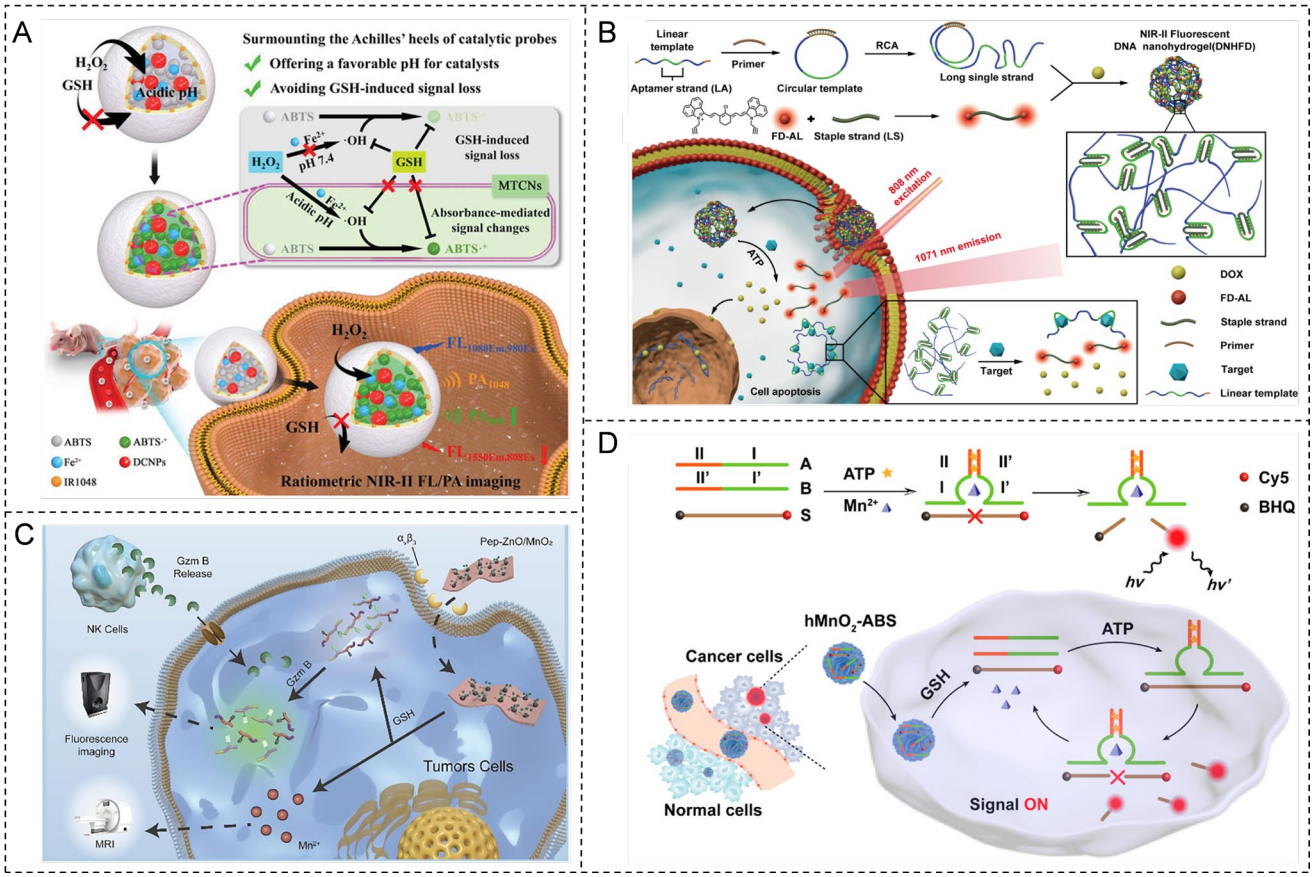

Figure 14. Strategies for intracellular small molecule and ion imaging. **(A)** The microenvironment-tailored catalytic nanoprobe (MTCNs) for ratiometric NIR-II fluorescence/photoacoustic imaging of H_2O_2. Reprinted with permission [268]. Copyright 2022 Wiley-VCH; **(B)** The RCA-derived DNA nanohydrogel (DNHFD) for ATP-responsive NIR-II imaging and synergistic therapy. Reprinted with permission [272]. Copyright 2025 American Chemical Society; **(C)** The 2D ZnO/MnO_2 nanosheet heterostructure for dual-modal GSH-responsive MRI imaging and granzyme B detection. Reprinted with permission [273]; **(D)** The GSH/ATP dual-lock activatable DNA nanoprobe based on honeycomb MnO_2 nanovectors. Reprinted with permission [274]. Copyright 2021 American Chemical Society.

4.6. Perspective on intracellular imaging targets

Among the three major target categories, intracellular biomarkers carry the deepest biological information, directly revealing oncogenic signaling, metabolic reprogramming, redox regulation and cell death pathway regulation. Different from extracellular and membrane markers only reflecting molecular expression abundance, intracellular targets support visualization of tumor dynamic functional states.

However, high biological information value is accompanied by greater technical challenges: probes need to overcome cell uptake, endosomal escape and subcellular targeting barriers; dynamic expression fluctuation of intracellular molecules also increases the difficulty of quantitative interpretation.

With the progress of probe engineering, nanotechnology and signal amplification strategy, intracellular imaging has become one of the most promising frontiers in precision oncology. Emerging targets related to ferroptosis, cuproptosis, immunometabolism and organelle stress expand the connotation of molecular imaging, shifting the research focus from "what tumors express" to "how

tumors function". Future technological advances will further promote the application of intracellular imaging in tumor functional characterization and personalized therapeutic guidance.

5. Challenges and future perspectives

Despite remarkable progress in molecular imaging probe design and biomarker exploration, multiple fundamental bottlenecks still restrict large-scale clinical translation, including tumor heterogeneity, insufficient early detection sensitivity, biological delivery barriers, non-specific background interference, biosafety risks and lack of unified quantitative standards [275]. These constraints interact and restrict each other, becoming the core obstacles limiting the transformation of preclinical research into routine clinical application. From a strategic perspective, resolving these bottlenecks requires a paradigm shift in molecular oncology: moving away from the reductionist approach of isolating individual targets, and moving toward a holistic, systems-biology view that treats the tumor, its microenvironment, and its dynamic evolution as an interconnected, living ecosystem.

5.1. Tumor heterogeneity and dynamic biomarker variability

Tumors exhibit obvious heterogeneity among patients, lesions and disease stages, leading to significant differences in biomarker expression, probe enrichment efficiency and therapeutic response. Many key imaging targets such as PD-L1, ROS and cell death-related molecules show dynamic temporal fluctuation during tumor progression and drug intervention. Single-target static imaging cannot adapt to such heterogeneous and dynamic characteristics. Future research needs to develop multi-target combined imaging and longitudinal dynamic monitoring strategies, combined with spatial omics, single-cell analysis and AI modeling to reconstruct tumor evolutionary characteristics and optimize patient stratification.

5.2. Sensitivity for early detection and minimal residual disease

Early-stage tumors, micro-metastases and minimal residual disease are difficult to detect due to low biomarker abundance and weak signal output. Moreover, most classic serum and membrane biomarkers are upregulated in the middle and late stages of tumorigenesis, lacking early warning value. Future research should focus on early functional abnormal events including oxidative stress, metabolic rewiring and DNA damage response. Activatable probes, DNA nanotechnology, CRISPR-assisted signal amplification and catalytic biocircuits are effective means to improve detection sensitivity for early tumor screening.

5.3. Biological barriers and probe delivery

Probe delivery is a major technical bottleneck, especially for intracellular and organelle-targeted imaging. Dense tumor extracellular matrix, abnormal tumor vasculature, endosomal trapping and inefficient intracellular trafficking jointly hinder probe penetration and target accessibility. Future probe design should integrate target recognition and delivery optimization, adopting biomimetic carriers, exosome-inspired nanoplatforms and organelle-targeting ligands to break biological barriers and improve intracellular localization efficiency.

5.4. Background interference and imaging specificity

Most tumor imaging biomarkers are not completely cancer-specific, and their abnormal expression also exists in inflammation, fibrosis and tissue regeneration lesions, easily generating false-positive signals. To improve specificity, imaging systems are evolving from constitutive always-on probes to microenvironment-responsive, logic-gated and multi-condition activatable platforms, which require multiple tumor-specific stimulation signals to trigger fluorescence or MRI activation, effectively reducing off-target background interference. Dynamic functional characteristics such as metabolic flux and immune state transition are more reliable for tumor identification than static molecular expression.

5.5. Biosafety and clinical translation

A large number of imaging probes have achieved excellent performance in preclinical experiments, but few have entered routine clinical application. The main barriers include long-term *in vivo* toxicity, poor biodegradability, complex synthetic routes, difficult large-scale production and strict regulatory approval procedures. Future translational research should prioritize biodegradable and clinically approved raw materials, simplify probe structure, balance imaging performance, biosafety and manufacturing feasibility, and accelerate the standardization of production and clinical verification.

5.6. Quantitative imaging and standardization

Precise quantitative molecular imaging underpins reliable clinical decision-making. However, quantification accuracy is susceptible to multiple confounding factors, including variable probe pharmacokinetics, heterogeneous tissue penetration, divergent instrument hardware parameters and inconsistent experimental operating protocols. Notably, dynamic functional targets, such as ROS, intracellular metabolites and enzymatic activity, present far greater barriers to robust quantitative imaging owing to their inherent temporal and spatial fluctuations. Against this backdrop, it is particularly critical to develop dedicated dynamic calibration standards and universal reference systems. Concurrently, unified probe calibration workflows, standardized imaging acquisition protocols need to be established.

5.7. Artificial intelligence and computational imaging

AI technology is transforming cancer imaging from qualitative visual observation to data-driven biological inference. Integrating imaging data with multi-omics and clinical records, AI enables automated lesion identification, tumor heterogeneity analysis, therapeutic response forecasting and novel biomarker discovery. Representative cutting-edge applications include multimodal image fusion and intelligent automated probe design. Limited medical datasets and weak generalization hinder clinical translation; future multimodal foundation models and interpretable AI will reconstruct tumor biological features and guide precision oncology decisions.

6. Conclusions

Cancer diagnostic imaging has completed the evolution from simple morphological observation to biology-driven functional profiling of tumor behavior. The core driving force of this evolution lies in the renewal of imaging targets: research focus has shifted from static anatomical markers to

dynamic biomarkers reflecting signaling activation, metabolic remodeling, immune interaction and cell fate transition.

Extracellular, membrane and intracellular targets form a hierarchical and complementary research system for cancer imaging. Extracellular biomarkers support non-invasive liquid biopsy and longitudinal systemic monitoring; membrane targets, as the most clinically mature subtype, are compatible with multiple mainstream imaging modalities and image-guided surgery; intracellular targets reveal core oncogenic signaling, metabolic reprogramming and cell death regulation mechanisms, linking imaging phenotypes with intrinsic tumor molecular logic.

Advances in probe engineering, nanotechnology and multimodal imaging greatly improve the sensitivity, specificity and quantitative capability of molecular imaging, promoting the transformation of imaging technology from passive lesion visualization to active interrogation of tumor biological characteristics. Future cancer imaging will break through the limitation of single-target and single-modality detection, developing integrated platforms combining multi-target recognition, functional metabolic imaging, spatial resolved analysis and AI-driven data interpretation. Emerging targets related to ferroptosis, cuproptosis, immunometabolism and organelle stress further expand the research boundary of molecular imaging.

At present, tumor heterogeneity, insufficient early detection sensitivity, biological delivery barriers, non-specific interference, biosafety risks and lack of quantitative standardization still restrict clinical translation. Solving these problems requires interdisciplinary integration of chemistry, materials science, molecular biology, imaging physics and clinical oncology.

In summary, the integration of intelligent molecular probes, multimodal imaging technology, systems biology and artificial intelligence is reshaping cancer imaging into a predictive, quantitative and decision-guiding precision medical platform, which is expected to realize real-time whole-process monitoring and precise management of tumors in the whole biological lifecycle.

Declaration of generative AI and AI-assisted technologies

During the preparation of this manuscript, the authors used generative AI tools only to improve language and readability. Specifically, the authors used Grammarly for language polishing only in limited sections. The authors take full responsibility for the content of the manuscript.

Acknowledgments

This work was supported by the National Natural Science Foundation of China (22374092, 22504078), Natural Science Foundation of Shandong Province (Major Basic Research Project) (ZR2023ZD44), the Project of Shandong Provincial Center for Fundamental Science Research (YDZX2024150), and Postdoctoral Fellowship Program of China Postdoctoral Science Foundation (GZC20250640).

Authors' contribution

Conceptualization, Peng Gao; writing—original draft preparation, Peng Gao; writing—review and editing, Wei Pan and Na Li; supervision, Na Li and Bo Tang; project administration, Na Li and Bo Tang; funding acquisition, Peng Gao, Wei Pan and Na Li. All authors have read and agreed to the published version of the manuscript.

Conflicts of interest

Na Li, who serves as Associate Editor-in-Chief of *Life Analysis*, and Bo Tang, who serves as Editor-in-Chief of *Life Analysis*, have not participated in the peer review process or made any editorial decisions for this manuscript. The other authors declare no conflicts of interest.

References

[1] Pan T, Zhang J, Wang X, Song Y. Global burden and trends of hematologic malignancies based on Global Cancer Observatory 2022 and Global Burden of Disease 2021. *Exp. Hematol. Oncol.* 2025, 14(1):98.

[2] Bray F, Laversanne M, Sung H, Ferlay J, Siegel RL, *et al.* Global cancer statistics 2022: GLOBOCAN estimates of incidence and mortality worldwide for 36 cancers in 185 countries. *CA Cancer J. Clin.* 2024, 74(3):229–263.

[3] Gao P, Chen Y, Pan W, Li N, Liu Z, *et al.* Antitumor agents based on metal-organic frameworks. *Angew. Chem., Int. Ed.* 2021, 133(31):16901–16914.

[4] Budach V, Tinhofer I. Novel prognostic clinical factors and biomarkers for outcome prediction in head and neck cancer: a systematic review. *Lancet Oncol.* 2019, 20(6):e313–e326.

[5] Blumen H, Fitch K, Polkus V. Comparison of treatment costs for breast cancer, by tumor stage and type of service. *Am. Health Drug Benefits* 2016, 9(1):23.

[6] Hestetun KE, Rosenlund NB, Stanisavljević L, Dahl O, Myklebust MP. Stage-dependent prognostic shift in mismatch repair-deficient tumors: assessing patient outcomes in stage II and III colon cancer. *Front. Oncol.* 2022, 12:853545.

[7] Cerdas MG, Farhat J, Elshafie SI, Mariyam F, James L, *et al.* Exploring the evolution of breast cancer imaging: a review of conventional and emerging modalities. *Cureus* 2025, 17(4):e82762.

[8] Hussain S, Mubeen I, Ullah N, Shah SSUD, Khan BA, *et al.* Modern diagnostic imaging technique applications and risk factors in the medical field: a review. *BioMed Res. Int.* 2022, (1):5164970.

[9] Wang T, Ni Y, Liu L. Innovative imaging techniques for advancing cancer diagnosis and treatment. *Cancers* 2024, 16(14):2607.

[10] Lu Z, Laney V, Li Y. Targeted contrast agents for magnetic resonance molecular imaging of cancer. *Acc. Chem. Res.* 2022, 55(19):2833–2847.

[11] Gagliardi T, Adejolu M, DeSouza NM. Diffusion-weighted magnetic resonance imaging in ovarian cancer: exploiting strengths and understanding limitations. *J. Clin. Med.* 2022, 11(6):1524.

[12] Schwenck J, Sonanini D, Cotton JM, Rammensee HG, la Fougère C, *et al.* Advances in PET imaging of cancer. *Nat. Rev. Cancer* 2023, 23(7):474–490.

[13] Connolly M, Srinivasan A. Diffusion-weighted imaging in head and neck cancer: technique, limitations, and applications. *Magn. Reson. Imaging Clin. N. Am.* 2018, 26(1):121–133.

[14] Pulumati A, Pulumati A, Dwarakanath BS, Verma A, Papineni RV. Technological advancements in cancer diagnostics: improvements and limitations. *Cancer Rep.* 2023, 6(2):e1764.

[15] Li Y, Wang Y, Jing Y, Zhu Y, Huang X, *et al.* Visualization analysis of breast cancer-related ubiquitination modifications over the past two decades. *Discover Oncol.* 2025, 16(1):431.

[16] de Souza N, Zhao S, Bodenmiller B. Multiplex protein imaging in tumour biology. *Nat. Rev. Cancer* 2024, 24(3):171–191.

[17] Zhou Z, Lu Z. Molecular imaging of the tumor microenvironment. *Adv. Drug Delivery Rev.* 2017, 113:24–48.
[18] Li Y, Bao Q, Yang S, Yang M, Mao C. Bionanoparticles in cancer imaging, diagnosis, and treatment. *View* 2022, 3(4):20200027.
[19] Wang K, Lin X, Lv X, Xie M, Wu J, *et al.* Nanozyme-based aptasensors for the detection of tumor biomarkers. *J. Biol. Eng.* 2025, 19(1):13.
[20] Han Z, Ke M, Liu X, Wang J, Guan Z, *et al.* Molecular imaging, how close to clinical precision medicine in lung, brain, prostate and breast cancers. *Mol. Imaging Biol.* 2022, 24(1):8.
[21] Rowe SP, Pomper MG. Molecular imaging in oncology: current impact and future directions. *CA Cancer J. Clin.* 2022, 72(4):333–352.
[22] Bai J, Qiu S, Zhang G. Molecular and functional imaging in cancer-targeted therapy: current applications and future directions. *Signal Transduct. Target. Ther.* 2023, 8(1):89.
[23] Kamali H, Golmohammadzadeh S, Zare H, Nosrati R, Fereidouni M, *et al.* The recent advancements in the early detection of cancer biomarkers by DNAzyme-assisted aptasensors. *J. Nanobiotechnol.* 2022, 20(1):438.
[24] Bakht MK, Beltran H. Biological determinants of PSMA expression, regulation and heterogeneity in prostate cancer. *Nat. Rev. Urol.* 2025, 22(1):26–45.
[25] Seferbekova Z, Lomakin A, Yates LR, Gerstung M. Spatial biology of cancer evolution. *Nat. Rev. Genet*. 2023, 24(5):295–313.
[26] Lin Z, Li M, Pan Z, Hu W, Feng Y, *et al.* Glypican-3–targeted PET imaging for precise diagnosis of hepatocellular carcinoma: from bench to bedside. *Clin. Cancer Res.* 2026, 32(3):550–561.
[27] Sadeghpour S, Aghaee A, Sadeghpour S, Rizzo A, Pizzuto DA, *et al.* Predicting the unpredictable: prognostic and predictive power of FAPI-PET imaging in oncology: a systematic review and meta-analysis. *Eur. J. Nucl. Med. Mol. Imaging* 2026, 53:2927–2938.
[28] Mieog JSD, Achterberg FB, Zlitni A, Hutteman M, Burggraaf J, *et al.* Fundamentals and developments in fluorescence-guided cancer surgery. *Nat. Rev. Clin. Oncol.* 2022, 19(1):9–22.
[29] Klocker EV, Hasenleithner S, Bartsch R, Gampenrieder SP, Egle D, *et al.* Clinical applications of next-generation sequencing-based ctDNA analyses in breast cancer: defining treatment targets and dynamic changes during disease progression. *Mol. Oncol.* 2025, 19(7):1897–1917.
[30] Sleeboom JJ, van Tienderen GS, Schenke-Layland K, van der Laan LJ, Khalil AA, *et al.* The extracellular matrix as hallmark of cancer and metastasis: from biomechanics to therapeutic targets. *Sci. Transl. Med.* 2024, 16(728):eadg3840.
[31] Kumar MA, Baba SK, Sadida HQ, Marzooqi SA, Jerobin J, *et al.* Extracellular vesicles as tools and targets in therapy for diseases. *Signal Transduct. Target. Ther.* 2024, 9(1):27.
[32] Ernst SM, Aldea M, von der Thüsen JH, de Langen AJ, Smit EF, *et al.* Utilizing ctDNA to discover mechanisms of resistance to targeted therapies in patients with metastatic NSCLC: towards more informative trials. *Nat. Rev. Clin. Oncol.* 2025, 22(5):371–378.
[33] Zhao T, Huang Y, Zhu J, Qin Y, Wu H, *et al.* Extracellular matrix signaling cues: biological functions, diseases, and therapeutic targets. *MedComm* 2025, 6(8):e70281.
[34] Gao P, Wei R, Chen Y, Liu X, Zhang J, *et al.* Multicolor covalent organic framework-DNA nanoprobe for fluorescence imaging of biomarkers with different locations in living cells. *Anal. Chem.* 2021, 93(40):13734–13741.

[35] Swain SM, Shastry M, Hamilton E. Targeting HER2-positive breast cancer: advances and future directions. *Nat. Rev. Drug Discovery*23, 22(2):101–126.

[36] Lee D, Cho M, Kim E, Seo Y, Cha JH. PD-L1: from cancer immunotherapy to therapeutic implications in multiple disorders. *Mol. Ther.* 2024, 32(12):4235–4255.

[37] Huang S, Ong S, McKenzie D, Mirabelli A, Chen DC, *et al.* Comparison of 18F-based PSMA radiotracers with [68Ga] Ga-PSMA-11 in PET/CT imaging of prostate cancer—a systematic review and meta-analysis. *Prostate Cancer Prostatic Dis.* 2024, 27(4):654–664.

[38] Levantini E, Maroni G, Del Re M, Tenen DG. EGFR signaling pathway as therapeutic target in human cancers. *Semin. Cancer Biol.* 2022, 85:253–275.

[39] Sallam M, Nguyen NT, Sainsbury F, Kimizuka N, Muyldermans S, *et al.* PSMA-targeted radiotheranostics in modern nuclear medicine: then, now, and what of the future? *Theranostics* 2024, 14(8):3043.

[40] Gao P, Chen Y, Pan W, Li N, Tang B. Biosensors based on the Au–Se bond. *Anal. Chem.* 2020, 92(14):9441–9448.

[41] Gao P, Shen X, Liu X, Cui B, Wang M, *et al.* Covalent organic framework-derived carbonous nanoprobes for cancer cell imaging. *ACS Appl. Mater. Interfaces* 2021, 13(35):41498–41506.

[42] Gao P, Liu B, Pan W, Li N, Tang B. A spherical nucleic acid probe based on the Au-Se bond. *Anal. Chem.* 2020, 92(12):8459–8463.

[43] Claps G, Faouzi S, Quidville V, Chehade F, Shen S, *et al.* The multiple roles of LDH in cancer. *Nat. Rev. Clin. Oncol.* 2022, 19(12):749–762.

[44] Li H, Wen X, Ren Y, Fan Z, Zhang J, *et al.* Targeting PI3K family with small-molecule inhibitors in cancer therapy: current clinical status and future directions. *Mol. Cancer* 2024, 23(1):164.

[45] Chagri S, Ng DY, Weil T. Designing bioresponsive nanomaterials for intracellular self-assembly. *Nat. Rev. Chem.* 2022, 6(5):320–338.

[46] Zhulai G, Oleinik E, Shibaev M, Ignatev K. Adenosine-metabolizing enzymes, adenosine kinase and adenosine deaminase, in cancer. *Biomolecules* 2022, 12(3):418.

[47] Wang R, Liang L, Matsumoto M, Iwata K, Umemura A, *et al.* Reactive oxygen species and NRF2 signaling, friends or foes in cancer? *Biomolecules* 2023, 13(2):353.

[48] Gao P, Yin J, Wang M, Wei R, Pan W, *et al.* COF-DNA bicolor nanoprobes for imaging tumor-associated mRNAs in living cells. *Anal. Chem.* 2022, 94(38):13293–13299.

[49] Gao P, Lou R, Liu X, Cui B, Pan W, *et al.* Rational design of a dual-layered metal-organic framework nanostructure for enhancing the cell imaging of molecular beacons. *Anal. Chem.* 2021, 93(13):5437–5441.

[50] Liu Y, Wang H. Biomarkers and targeted therapy for cancer stem cells. *Trends Pharmacol. Sci.* 2024, 45(1):56–66.

[51] Liu Y, Wu Z, Armstrong DW, Wolosker H, Zheng Y. Detection and analysis of chiral molecules as disease biomarkers. *Nat. Rev. Chem.* 2023, 7(5):355–373.

[52] Son MH, Park SW, Sagong HY, Jung YK. Recent advances in electrochemical and optical biosensors for cancer biomarker detection. *BioChip J.* 2023, 17(1):44–67.

[53] Blau R, Shelef O, Shabat D, Satchi-Fainaro R. Chemiluminescent probes in cancer biology. *Nat. Rev. Bioeng.* 2023, 1(9):648–664.

[54] Diao J, Jia Y, Dai E, Liu J, Kang R, *et al.* Ferroptotic therapy in cancer: benefits, side effects, and risks. *Mol. Cancer* 2024, 23(1):89.
[55] Conway JR, Joshi O, Kaivola J, Follain G, Gounis M, *et al.* Dynamic regulation of integrin β1 phosphorylation supports invasion of breast cancer cells. *Nat. Cell Biol.* 2025, 27(6):1021–1034.
[56] Zhang Z, Wang J, Wuethrich A, Trau M. Conventional techniques and emerging nanotechnologies for early detection of cancer metastasis via epithelial-mesenchymal transition monitoring. *Natl. Sci. Rev.* 2025, 12(3):nwae452.
[57] Najdian A, Beiki D, Abbasi M, Gholamrezanezhad A, Ahmadzadehfar H, *et al.* Exploring innovative strides in radiolabeled nanoparticle progress for multimodality cancer imaging and theranostic applications. *Cancer Imaging* 2024, 24(1):127.
[58] Biswas S, Chohan DP, Wankhede M, Rodrigues J, Bhat G, *et al.* Photoacoustic-integrated multimodal approach for colorectal cancer diagnosis. *ACS Biomater. Sci. Eng.* 2025, 11(7):4033–4049.
[59] Wu L, Tanwar S, Kaur G, Date S, Goel L, *et al.* DNA origami-engineered plasmonic nanoprobes for targeted cancer imaging. *Adv. Funct. Mater.* 2024, 34(30):2309929.
[60] Kong S, Liu H, Zhang Y, Fan J, Huang W. Clinical applications of nanoprobes of high-resolution *in vivo* imaging. *Iscience* 2025, 28(1):111459.
[61] Li S, Wei J, Yao Q, Song X, Xie J, *et al.* Emerging ultrasmall luminescent nanoprobes for *in vivo* bioimaging. *Chem. Soc. Rev.* 2023, 52(5):1672–1696.
[62] Song W, Song Y, Li Q, Fan C, Lan X, *et al.* Advances in aptamer-based nuclear imaging. *Eur. J. Nucl. Med. Mol. Imaging* 2022, 49(8):2544–2559.
[63] Kou X, Zhang X, Shao X, Jiang C, Ning L. Recent advances in optical aptasensor technology for amplification strategies in cancer diagnostics. *Anal. Bioanal. Chem.* 2020, 412(25):6691–6705.
[64] Fitzgerald RC, Antoniou AC, Fruk L, Rosenfeld N. The future of early cancer detection. *Nat. Med.* 2022, 28(4):666–677.
[65] Liu Z, Wang Q, Qiu W, Lyu Y, Zhu Z, *et al.* AIE-active luminogens as highly efficient free-radical ROS photogenerator for image-guided photodynamic therapy. *Chem. Sci.* 2022, 13(12):3599–3608.
[66] Wang K, Du Y, Zhang Z, He K, Cheng Z, *et al.* Fluorescence image-guided tumour surgery. *Nat. Rev. Bioeng.* 2023, 1(3):161–179.
[67] Fujita K, Urano Y. Activity-based fluorescence diagnostics for cancer. *Chem. Rev.* 2024, 124(7):4021–4078.
[68] Perez-Lopez R, Ghaffari Laleh N, Mahmood F, Kather JN. A guide to artificial intelligence for cancer researchers. *Nat. Rev. Cancer* 2024, 24(6):427–441.
[69] Li Z, Li J, Bai X, Huang X, Wang Q. Tumor microenvironment as a complex milieu driving cancer progression: a mini review. *Clin. Transl. Oncol.* 2025, 27(5):1943–1952.
[70] Siminzar P, Tohidkia MR, Eppard E, Vahidfar N, Tarighatnia A, *et al.* Recent trends in diagnostic biomarkers of tumor microenvironment. *Mol. Imaging Biol.* 2023, 25(3):464–482.
[71] de Visser KE, Joyce JA. The evolving tumor microenvironment: from cancer initiation to metastatic outgrowth. *Cancer Cell* 2023, 41(3):374–403.
[72] Ignatiadis M, Sledge GW, Jeffrey SS. Liquid biopsy enters the clinic—implementation issues and future challenges. *Nat. Rev. Clin. Oncol.* 2021, 18(5):297–312.
[73] Heitzer E, Haque IS, Roberts CE, Speicher MR. Current and future perspectives of liquid biopsies in genomics-driven oncology. *Nat. Rev. Genet.* 2019, 20(2):71–88.

[74] Liang C, Xu L, Song G, Liu Z. Emerging nanomedicine approaches fighting tumor metastasis: animal models, metastasis-targeted drug delivery, phototherapy, and immunotherapy. *Chem. Soc. Rev.* 2016, 45(22):6250–6269.

[75] Topalian SL, Taube JM, Anders RA, Pardoll DM. Mechanism-driven biomarkers to guide immune checkpoint blockade in cancer therapy. *Nat. Rev. Cancer* 2016, 16(5):275–287.

[76] Rao L, Bu L, Cai B, Xu J, Li A, *et al.* Cancer cell membrane-coated upconversion nanoprobes for highly specific tumor imaging. *Adv. Mater.* 2016, 28(18):3460–3466.

[77] Guo Z, Park S, Yoon J, Shin I. Recent progress in the development of near-infrared fluorescent probes for bioimaging applications. *Chem. Soc. Rev.* 2013, 43(1):16–29.

[78] Huang X, Song J, Yung BC, Huang X, Xiong Y, *et al.* Ratiometric optical nanoprobes enable accurate molecular detection and imaging. *Chem. Soc. Rev.* 2018, 47(8):2873–2920.

[79] Koker T, Tang N, Tian C, Zhang W, Wang X, *et al.* Cellular imaging by targeted assembly of hot-spot SERS and photoacoustic nanoprobes using split-fluorescent protein scaffolds. *Nat. Commun.* 2018, 9(1):607.

[80] Xiong H, Li F, Zeng L, Lei Q. Recent and emerging trends of DNA/RNA hybridized COF nanoprobes for analytes detection and biomarkers imaging in clinical biomedicines. *TrAC Trends Anal. Chem.* 2024, 170:117414.

[81] Flitcroft JG, Verheyen J, Vemulkar T, Welbourne EN, Rossi SH, *et al.* Early detection of kidney cancer using urinary proteins: a truly non-invasive strategy. *BJU Int.* 2022, 129(3):290–303.

[82] Sypabekova M, Amantayeva A, Vangelista L, González-Vila Á, Caucheteur C, *et al.* Ultralow limit detection of soluble HER2 biomarker in serum with a fiber-optic ball-tip resonator assisted by a tilted FBG. *ACS Meas. Sci. Au* 2022, 2(4):309–316.

[83] Boyd LN, Ali M, Leeflang MM, Treglia G, de Vries R, *et al.* Diagnostic accuracy and added value of blood-based protein biomarkers for pancreatic cancer: a meta-analysis of aggregate and individual participant data. *EClinicalMedicine* 2023, 55:101747.

[84] Johdi NA, Mazlan L, Sagap I, Jamal R. Profiling of cytokines, chemokines and other soluble proteins as a potential biomarker in colorectal cancer and polyps. *Cytokine* 2017, 99:35–42.

[85] Li J, Wang J, Grewal YS, Howard CB, Raftery LJ, *et al.* Multiplexed SERS detection of soluble cancer protein biomarkers with gold–silver alloy nanoboxes and nanoyeast single-chain variable fragments. *Anal. Chem.* 2018, 90(17):10377–10384.

[86] Luo P, Wu S, Yu Y, Ming X, Li S, *et al.* Current status and perspective biomarkers in AFP negative HCC: towards screening for and diagnosing hepatocellular carcinoma at an earlier stage. *Pathol. Oncol. Res.* 2020, 26(2):599–603.

[87] Zhang Z, Wang B, Wu P, Jarnda KV, Tian Y, *et al.* Advances in optical and electrochemical aptasensors for tumor biomarker alpha-fetoprotein. *Microchim. Acta* 2026, 193(2):107.

[88] Zhang G, Zhao L, Song X, Ding C. A dual-functional signal “on-off-on” biosensor based on coordination-induced enhancement and interface antifouling for trace analysis of alpha-fetoprotein in serum. *Anal. Chem.* 2025, 97(42):23488–23495.

[89] Van Poppel H, Albreht T, Basu P, Hogenhout R, Collen S, *et al.* Serum PSA-based early detection of prostate cancer in Europe and globally: past, present and future. *Nat. Rev. Urol.* 2022, 19(9):562–572.

[90] Rivas L, de la Escosura-Muñiz A, Serrano L, Altet L, Francino O, *et al.* Triple lines gold nanoparticle-based lateral flow assay for enhanced and simultaneous detection of Leishmania DNA and endogenous control. *Nano Res.* 2015, 8(11):3704–3714.

[91] Huang Y, Feng L, Wu M, Gao X, Ji Y, *et al.* Wettability-enhanced photothermal vertical flow biosensor on a syringe for PSA detection using TaTe(2) nanosheets. *Anal. Chem.* 2026, 98(3):2203–2213.

[92] Wang X, Che Y, Liu S, Ma B, Liu Y, *et al.* Single-molecule liquid biopsy detects low- and high-abundance protein markers simultaneously for pancreatic cancer diagnosis. *Anal. Chem.* 2025, 97(15):8385–8393.

[93] Qi Q, Xu Z, Yu Y, Guan P, Lin J, *et al.* Exogenous-label-free colorimetric/SERS dual-mode immunosensing platform driven by Au NCs@Pt nanozyme for ultrasensitive and rapid detection of the pancreatic cancer biomarker CA19-9. *Anal. Chem.* 2026, 98(7):5715–5724.

[94] Gu L, Xu X, Zhang R, Xing Y, Kou B, *et al.* Antifouling cyclic peptide nanotubes combined with Rh-Ti(3)C(2)T(X) multifunctional nanozyme for the sensitive detection of CA125 in complex biological samples. *Anal. Chem.* 2025, 97(32):17562–17569.

[95] Forster JC, Harriss-Phillips WM, Douglass MJ, Bezak E. A review of the development of tumor vasculature and its effects on the tumor microenvironment. *Hypoxia* 2017, 5:21–32.

[96] Ahmad A, Nawaz MI. Molecular mechanism of VEGF and its role in pathological angiogenesis. *J. Cell. Biochem.* 2022, 123(12):1938–1965.

[97] Patel SA, Nilsson MB, Le X, Cascone T, Jain RK, *et al.* Molecular mechanisms and future implications of VEGF/VEGFR in cancer therapy. *Clin. Cancer Res.* 2023, 29(1):30–39.

[98] Liu Z, Chen H, Zheng L, Sun L, Shi L. Angiogenic signaling pathways and anti-angiogenic therapy for cancer. *Signal Transduct. Target. Ther.* 2023, 8(1):198.

[99] Zhou S, Zhou J, Ran J, Man S, Zhuo Y, *et al.* Retractable DNA nanoprobes for ultrasensitive sers detection and imaging of the VEGF. *Anal. Chem.* 2025, 97(45):25138–25147.

[100] Yuan G, Xia X, Zhang J, Huang J, Xie F, *et al.* A novel “signal on-off-super on” sandwich-type aptamer sensor of CRISPR-Cas12a coupled voltage enrichment assay for VEGF detection. *Biosens. Bioelectron.* 2023, 221:114424.

[101] Gao J, Zhu X, Long Y, Liu M, Li H, *et al.* Boronic acid-decorated carbon dot-based semiselective multichannel sensor array for cytokine discrimination and oral cancer diagnosis. *Anal. Chem.* 2024, 96(4):1795–1802.

[102] Shi H, Zeng T, Liang Q, Yang J, Chen R, *et al.* Multiplex assay of cytokines with tunable detection ranges for the precise diagnosis of breast cancer. *Anal. Chem.* 2024, 96(8):3662–3671.

[103] Wu Y, Jin R, Lei T, Liu J, Chang Y, *et al.* Aptamer-coupled droplet CRISPR/Cas12a enables ultrasensitive sPD-L1 detection. *Anal. Chem.* 2026, 98(22):16296–16305.

[104] Li Y, Wang S, Zhao Y, Li Y, Wang P, *et al.* Design of a double-photoelectrode sensing system with a metal-organic framework-based antenna-like strategy for highly sensitive detection of PD-L1. *Anal. Chem.* 2023, 95(22):8720–8727.

[105] Tong F, Wang Y, Xu Y, Zhou Y, He S, *et al.* MMP-2-triggered, mitochondria-targeted PROTAC-PDT therapy of breast cancer and brain metastases inhibition. *Nat. Commun.* 2024, 15(1):10382.

[106] Chen C, Zhang Y, Hou Z, Cui X, Zhao Y, *et al.* Rational design of short peptide-based hydrogels with MMP-2 responsiveness for controlled anticancer peptide delivery. *Biomacromolecules* 2017, 18(11):3563–3571.

[107] He X, Hu X, James TD, Yoon J, Tian H. Multiplexed photoluminescent sensors: towards improved disease diagnostics. *Chem. Soc. Rev.* 2017, 46(22):6687–6696.
[108] Gao X, Jiang L, Hu B, Kong F, Liu X, *et al.* Au-Se-bond-based nanoprobe for imaging MMP-2 in tumor cells under a high-thiol environment. *Anal. Chem.* 2018, 90(7):4719–4724.
[109] Luan M, Li N, Pan W, Yang L, Yu Z, *et al.* Simultaneous detection of multiple targets involved in the PI3K/AKT pathway for investigating cellular migration and invasion with a multicolor fluorescent nanoprobe. *Chem. Commun.* 2016, 53(2):356–359.
[110] Zhong Z, Ashraf G, Chen W, Liu B, Wang G, *et al.* Detection of matrix metalloproteinase-1 in human saliva based on a pregnancy test strip platform. *Anal. Chem.* 2022, 94(47):16384–16392.
[111] Ji T, Ding Y, Zhao Y, Wang J, Qin H, *et al.* Peptide assembly integration of fibroblast-targeting and cell-penetration features for enhanced antitumor drug delivery. *Adv. Mater.* 2015, 27(11):1865–1873.
[112] Zhen Z, Tang W, Wang M, Zhou S, Wang H, *et al.* Protein nanocage mediated fibroblast-activation protein targeted photoimmunotherapy to enhance cytotoxic T cell infiltration and tumor control. *Nano Lett.* 2017, 17(2):862–869.
[113] Feng Y, Xie C, Ren T, Xu S, Huang S, *et al.* A general strategy to develop highly sensitive FAPalpha fluorescent probes for invasive cancer detection. *Angew. Chem., Int. Ed.* 2025, 64(41):e202512588.
[114] Pantel K, Alix-Panabieres C. Liquid biopsy and minimal residual disease—latest advances and implications for cure. *Nat. Rev. Clin. Oncol.* 2019, 16(7):409–424.
[115] Siravegna G, Marsoni S, Siena S, Bardelli A. Integrating liquid biopsies into the management of cancer. *Nat. Rev. Clin. Oncol.* 2017, 14(9):531–548.
[116] Ring A, Nguyen-Strauli BD, Wicki A, Aceto N. Biology, vulnerabilities and clinical applications of circulating tumour cells. *Nat. Rev. Cancer* 2023, 23(2):95–111.
[117] Mirlohi MS, Yousefi T, Razaviyan J, Nomiri S, Pishbin E, *et al.* Advances and challenges in KRAS mutation detection and clinical implications. *Cancers* 2025, 18(1):31.
[118] Bhaskar S, Umrao S, Lee HK, Tibbs J, Bacon A, *et al.* Critical review: point of care molecular cancer diagnostics. *Lab Chip* 2026, 26:2948–3001.
[119] Pan Y, Wang D, Wei R, Wang S, Li Y, *et al.* Lateral flow platform for lung cancer diagnosis through simultaneous detection of ctDNA and microRNA. *Anal. Chem.* 2025, 97(13):7063–7070.
[120] Desai A, Vázquez TA, Arce KM, Corassa M, Mack PC, *et al.* ctDNA for the evaluation and management of EGFR-mutant non-small cell lung cancer. *Cancers* 2024, 16(5):940.
[121] Chen D, Wu Y, Hoque S, Tilley RD, Gooding JJ. Rapid and ultrasensitive electrochemical detection of circulating tumor DNA by hybridization on the network of gold-coated magnetic nanoparticles. *Chem. Sci.* 2021, 12(14):5196–5201.
[122] Tao X, Li X, Lv Q, Tian G, Jia H, *et al.* Machine learning-enhanced analysis of miRNA biomarkers for accurate breast cancer diagnosis using DNA seagrass. *Anal. Chem.* 2025, 97(41):22582–22594.
[123] Mirzaei S, Paskeh MDA, Okina E, Gholami MH, Hushmandi K, *et al.* Molecular landscape of lncRNAs in prostate cancer: a focus on pathways and therapeutic targets for intervention. *J. Exp. Clin. Cancer Res.* 2022, 41(1):214.
[124] Mallela VR, Rajtmajerová M, Trailin A, Liška V, Hemminki K, *et al.* miRNA and lncRNA as potential tissue biomarkers in hepatocellular carcinoma. *Noncoding RNA Res.* 2024, 9(1):24–32.

[125] Zhang H, Huang X, Liu J, Liu B. Simultaneous and ultrasensitive detection of multiple microRNAs by single-molecule fluorescence imaging. *Chem. Sci.* 2020, 11(15):3812–3819.
[126] Yang L, Ren Y, Pan W, Yu Z, Tong L, *et al.* Fluorescent nanocomposite for visualizing cross-talk between microRNA-21 and hydrogen peroxide in ischemia-reperfusion injury in live cells and *in vivo*. *Anal. Chem.* 2016, 88(23):11886–11891.
[127] Bhattacharjee R, Prabhakar N, Kumar L, Bhattacharjee A, Kar S, *et al.* Crosstalk between long noncoding RNA and microRNA in Cancer. *Cell. Oncol.* 2023, 46(4):885–908.
[128] Ma C, Cao Y, Gou X, Zhu J. Recent progress in electrochemiluminescence sensing and imaging. *Anal. Chem.* 2019, 92(1):431–454.
[129] Wang D, Wang J, Cui Y, Wang Y, Tang A, *et al.* Nanolantern-based DNA probe and signal amplifier for tumor-related biomarker detection in living cells. *Anal. Chem.* 2019, 91(20):13165–13173.
[130] Wang S, Wei S, Wang S, Zhu X, Lei C, *et al.* Chimeric DNA-functionalized titanium carbide MXenes for simultaneous mapping of dual cancer biomarkers in living cells. *Anal. Chem.* 2018, 91(2):1651–1658.
[131] Peng H, Newbigging AM, Reid MS, Uppal JS, Xu J, *et al.* Signal amplification in living cells: a review of microRNA detection and imaging. *Anal. Chem.* 2019, 92(1):292–308.
[132] Yang Z, Tian T, Kong J, Chen H. ChatExosome: an Artificial Intelligence (AI) agent based on deep learning of exosomes spectroscopy for hepatocellular carcinoma (HCC) diagnosis. *Anal. Chem.* 2025, 97(8):4643–4652.
[133] Lu J, Wang M, Han Y, Deng Y, Zeng Y, *et al.* Functionalization of covalent organic frameworks with DNA via covalent modification and the application to exosomes detection. *Anal. Chem.* 2022, 94(12):5055–5061.
[134] Zhang X, Liu C, Pei Y, Song W, Zhang S. Preparation of a novel raman probe and its application in the detection of circulating tumor cells and exosomes. *ACS Appl. Mater. Interfaces* 2019, 11(32):28671–28680.
[135] Liu Q, Fan T, Zheng Y, Yang S, Yu Z, *et al.* Immunogenic exosome-encapsulated black phosphorus nanoparticles as an effective anticancer photo-nanovaccine. *Nanoscale* 2020, 12(38):19939–19952.
[136] Wu J, Zhou Y, Jiang Y, Xu W, Yan T, *et al.* Dual roles of exosomes in tumor progression and their bioengineering as targeted drug carriers. *Anal. Chem.* 2026, 98(14):10217–10247.
[137] Poggio M, Hu T, Pai CC, Chu B, Belair CD, *et al.* Suppression of exosomal PD-L1 induces systemic anti-tumor immunity and memory. *Cell* 2019, 177(2):414–427.
[138] Morrissey SM, Yan J. Exosomal PD-L1: roles in tumor progression and immunotherapy. *Trends Cancer* 2020, 6(7):550–558.
[139] Haderk F, Schulz R, Iskar M, Cid LL, Worst T, *et al.* Tumor-derived exosomes modulate PD-L1 expression in monocytes. *Sci. Immunol.* 2017, 2(13):eaah5509.
[140] Zhang Y, Wu Q, Huang Y, Wang W, Lu Y, *et al.* Reliable detection of extracellular PD-L1 by DNA computation-mediated microfluidics. *Anal. Chem.* 2023, 95(24):9373–9379.
[141] Kuang J, Fu Z, Sun X, Lin C, Yang S, *et al.* A colorimetric aptasensor based on a hemin/EpCAM aptamer DNAzyme for sensitive exosome detection. *Analyst* 2022, 147(22):5054–5061.
[142] Yu W, Lou F, Chen L, Zhao S, Wei F, *et al.* Selective recognition of tumor-derived EVs by EpCAM-imprinted polymers for proteomic biomarker discovery. *Anal. Chem.* 2026, 98(20):15241–15249.

[143] Yan S, Zheng H, Zhao J, Gao M, Zhang X. Quantification of GPC1(+) exosomes based on MALDI-TOF MS *in situ* signal amplification for pancreatic cancer discrimination and evaluation. *Anal. Chem.* 2023, 95(27):10196–10203.

[144] Deng J, Zhao S, Xie K, Liu C, Sheng C, *et al.* Spherical DNA nanomotors enable ultrasensitive detection of active enzymes in extracellular vesicles for cancer diagnosis. *Angew. Chem., Int. Ed.* 2025, 64(5):e202417165.

[145] Xie M, Wang F, Yang J, Guo Y, Ding F, *et al.* DNA zipper mediated membrane fusion for rapid exosomal miRNA detection. *Anal. Chem.* 2022, 94:13043–13051.

[146] Li J, Li B, Ren C, Chen Y, Guo X, *et al.* The clinical significance of circulating GPC1 positive exosomes and its regulative miRNAs in colon cancer patients. *Oncotarget* 2017, 8(60):101189.

[147] Hsu CC, Yang Y, Kannisto E, Zeng X, Yu G, *et al.* Simultaneous detection of tumor derived exosomal protein–MicroRNA pairs with an exo-PROS biosensor for cancer diagnosis. *ACS Nano* 2023, 17(9):8108–8122.

[148] Hsu MT, Wang Y, Tseng YJ. Exosomal proteins and lipids as potential biomarkers for lung cancer diagnosis, prognosis, and treatment. *Cancers* 2022, 14(3):732.

[149] Wang J, Yue B, Huang Y, Lan X, Liu W, *et al.* Exosomal RNAs: novel potential biomarkers for diseases—a review. *Int. J. Mol. Sci.* 2022, 23(5):2461.

[150] Wang F, Wang C, Chen S, Wei C, Ji J, *et al.* Identification of blood-derived exosomal tumor RNA signatures as noninvasive diagnostic biomarkers for multi-cancer: a multi-phase, multi-center study. *Mol. Cancer* 2025, 24(1):60.

[151] Tiong T, Chan M, Wang C, Yadav VK, Pikatan NW, *et al.* Exosomal miR-21 determines lung-to-brain metastasis specificity through the DGKB/ERK axis within the tumor microenvironment. *Life Sci.* 2023, 329:121945.

[152] Wang M, Wang Y, Tian X, Wang Q, Huang H, *et al.* Diagnostic and predictive value of liquid biopsy-derived exosome miR-21 for breast cancer: a systematic review and meta-analysis. *Expert Rev. Mol. Diagn.* 2023, 23(4):315–324.

[153] Chen Y, Morihiro K, Nemoto Y, Ichimura A, Ueki R, *et al.* Selective inhibition of cancer cell migration using a pH-responsive nucleobase-modified DNA aptamer. *Chem. Sci.* 2024, 15(41):17097–17102.

[154] Jia H, Zhu Y, Duan Q, Wu F. Cell surface-localized imaging and sensing. *Chem. Soc. Rev.* 2021, 50(10):6240–6277.

[155] Li Y, Shao T, Kuang J, Yi H, Zhu L, *et al.* Aptamers as a new frontier in molecular cancer imaging technologies. *Chem. Biomed. Imaging* 2025, 3(5):267–279.

[156] Meng H, Liu H, Kuai H, Peng R, Mo L, *et al.* Aptamer-integrated DNA nanostructures for biosensing, bioimaging and cancer therapy. *Chem. Soc. Rev.* 2016, 45(9):2583–2602.

[157] Neha, Nikita, Sharma T, Gupta T, Narang U. Aza-BODIPY-derived fluorescent probe for cancer cell imaging and combined PDT/PTT applications. *Chem. Biodivers.* 2026, 23(3):e03508.

[158] Lau AN, Vander Heiden MG. Metabolism in the tumor microenvironment. *Annu. Rev. Cancer Biol.* 2020, 4(1):17–40.

[159] Steuer CE, Griffith CC, Nannapaneni S, Patel MR, Liu Y, *et al.* A correlative analysis of PD-L1, PD-1, PD-L2, EGFR, HER2, and HER3 expression in oropharyngeal squamous cell carcinoma. *Mol. Cancer Ther.* 2018, 17(3):710–716.

[160] Maron SB, Chatila W, Walch H, Chou JF, Ceglia N, *et al.* Determinants of survival with combined HER2 and PD-1 blockade in metastatic esophagogastric cancer. *Clin. Cancer Res.* 2023, 29(18):3633–3640.

[161] Bai X, Sun P, Wang X, Long C, Liao S, *et al.* Structure and dynamics of the EGFR/HER2 heterodimer. *Cell Discovery* 2023, 9(1):18.

[162] Chen H, Liang K, Lai J, Lan C, Liao M, *et al.* EpCAM signaling promotes tumor progression and protein stability of PD-L1 through the EGFR pathway. *Cancer Res.* 2020, 80(22):5035–5050.

[163] Wollman AJ, Fournier C, Llorente-Garcia I, Harriman O, Payne-Dwyer AL, *et al.* Critical roles for EGFR and EGFR–HER2 clusters in EGF binding of SW620 human carcinoma cells. *J. R. Soc. Interface* 2022, 19(190):20220088.

[164] Butti R, Das S, Gunasekaran VP, Yadav AS, Kumar D, *et al.* Receptor tyrosine kinases (RTKs) in breast cancer: signaling, therapeutic implications and challenges. *Mol. Cancer* 2018, 17(1):34.

[165] Yang W, Nan H, Xu Z, Huang Z, Chen S, *et al.* DNA-templated glycan labeling for monitoring receptor spatial distribution in living cells. *Anal. Chem.* 2021, 93(36):12265–12272.

[166] Qiao S, Wang Y, Lin Y, An H, Ma Y, *et al.* Thermo-controlled *in situ* phase transition of polymer-peptides on cell surfaces for high-performance proliferative inhibition. *ACS Appl. Mater. Interfaces* 2016, 8(27):17016–17022.

[167] Chernov KG, Redchuk TA, Omelina ES, Verkhusha VV. Near-infrared fluorescent proteins, biosensors, and optogenetic tools engineered from phytochromes. *Chem. Rev.* 2017, 117(9):6423–6446.

[168] Li B, Xie X, Chen Z, Zhan C, Zeng F, *et al.* Tumor inhibition achieved by targeting and regulating multiple key elements in EGFR signaling pathway using a self-assembled nanoprodrug. *Adv. Funct. Mater.* 2018:1800692.

[169] Zhu J, Li Y, Wu X, Li Y, Wang L, *et al. In vivo* PET imaging of EGFR expression: an overview of radiolabeled EGFR TKIs. *Curr. Top. Med. Chem.* 2022, 22(28):2329–2342.

[170] Chiu FY, Yen Y. Imaging biomarkers for clinical applications in neuro-oncology: current status and future perspectives. *Biomark. Res.* 2023, 11(1):35.

[171] Li H, Kim Y, Jung H, Hyun JY, Shin I. Near-infrared (NIR) fluorescence-emitting small organic molecules for cancer imaging and therapy. *Chem. Soc. Rev.* 2022, 51(21):8957–9008.

[172] Zhang L, Chu M, Ji C, Wei J, Yang Y, *et al. In situ* visualization of epidermal growth factor receptor nuclear translocation with circular bivalent aptamer. *Anal. Chem.* 2022, 94(50):17413–17421.

[173] Li W, Wang H, Zhao Z, Gao H, Liu C, *et al.* Emerging nanotechnologies for liquid biopsy: the detection of circulating tumor cells and extracellular vesicles. *Adv. Mater.* 2019, 31(45):1805344.

[174] Vajhadin F, Mazloum-Ardakani M, Shahidi M, Moshtaghioun SM, Haghiralsadat F, *et al.* MXene-based cytosensor for the detection of HER2-positive cancer cells using CoFe(2)O(4)@Ag magnetic nanohybrids conjugated to the HB5 aptamer. *Biosens. Bioelectron.* 2022, 195:113626.

[175] Guo X, Xu C, Zhu X, Wang X, Hao Y, *et al.* In silico design and evaluation of novel peptide-based PET probe for noninvasive imaging of HER2 expression in breast cancer. *J. Med. Chem.* 2025, 68(10):10461–10472.

[176] Lan L, Xue G, Song Q, Wu R, Li X, *et al.* A proximity-driven, spatially matched 3D aptasensor for precise HER2 diagnostics in living cells and clinical specimens. *Anal. Chem.* 2026, 98(18):13576–13586.

[177] Wang X, Tang Y, Xiao M, Huang J, Dai Y, *et al.* Preclinical evaluation of rationally designed peptide-NIRF probe for c-Met positive liver cancer imaging-guided surgery. *Anal. Chem.* 2026, 98(5):4179–4190.

[178] Floresta G, Abbate V. Recent progress in the imaging of c-Met aberrant cancers with positron emission tomography. *Med. Res. Rev.* 2022, 42(4):1588–1606.

[179] Sun B, Xu F, Zhang Y, Hu Y, Chen Y. Dual-probe approach for mass spectrometric quantification of MUC1-specific terminal Gal/GalNAc *in situ*. *Anal. Chem.* 2020, 92(12):8340–8349.

[180] Liu X, Mao D, Deng G, Song Y, Zhang F, *et al.* Nondestructive analysis of tumor-associated membrane protein MUC1 in living cells based on dual-terminal amplification of a DNA ternary complex. *Theranostics* 2020, 10(10):4410–4421.

[181] Chen X, Sandrine IK, Yang M, Tu J, Yuan X. MUC1 and MUC16: critical for immune modulation in cancer therapeutics. *Front. Immunol.* 2024, 15:1356913.

[182] Song Z, Zhou Y, Shen M, Zhao D, Hu H, *et al.* MUC1 detection and *in situ* imaging method based on aptamer conformational switch and hybridization chain reaction. *Talanta* 2022, 239:123129.

[183] Qing L, Li Q, Dong Z. MUC1: an emerging target in cancer treatment and diagnosis. *Bull. Cancer* 2022, 109(11):1202–1216.

[184] Li L, Xue Y, Li X, Li J, Fu Y, *et al.* Copper nanosheet-based wash-free fluorescence imaging of cancer cells. *Anal. Chem.* 2024, 96(5):2052–2058.

[185] He Q, Guo S, Qian Z, Chen X. Development of individualized anti-metastasis strategies by engineering nanomedicines. *Chem. Soc. Rev.* 2015, 44(17):6258–6286.

[186] Chen Q, Chen M, Liu Z. Local biomaterials-assisted cancer immunotherapy to trigger systemic antitumor responses. *Chem. Soc. Rev.* 2019, 48(22):5506–5526.

[187] Gao Y, Qi F, Zhou W, Jiang P, Hu M, *et al.* Liquid biopsy using plasma proteomics in predicting efficacy and tolerance of PD-1/PD-L1 blockades in NSCLC: a prospective exploratory study. *Mol. Biomed.* 2025, 6(1):51.

[188] Zhang R, Peng W, Wang Y, Jiang Y, Wang J, *et al.* MRI radiomics model for predicting tumor immune microenvironment types and efficacy of anti-PD-1/PD-L1 therapy in hepatocellular carcinoma. *BMC Med. Imaging* 2025, 25(1):211.

[189] Wang L, Yang Z, Guo F, Chen Y, Wei J, *et al.* Research progress of biomarkers in the prediction of anti-PD-1/PD-L1 immunotherapeutic efficiency in lung cancer. *Front. Immunol.* 2023, 14:1227797.

[190] Zhou X, Yan S, Ma X, Zhu H, Liu B, *et al.* Efficacy of radiolabelled PD-L1-targeted nanobody in predicting and evaluating the combined immunotherapy and chemotherapy for resectable non-small cell lung cancer. *Eur. J. Nucl. Med. Mol. Imaging* 2025, 52(7):2343–2354.

[191] Smit J, Borm FJ, Niemeijer ALN, Huisman MC, Hoekstra OS, *et al.* PD-L1 PET/CT imaging with radiolabeled durvalumab in patients with Advanced-Stage Non–Small cell lung cancer. *J. Nucl. Med.* 2022, 63(5):686–693.

[192] Zhou X, Jiang J, Yang X, Liu T, Ding J, *et al.* First-in-humans evaluation of a PD-L1–binding peptide PET radiotracer in non–small cell lung cancer patients. *J. Nucl. Med.* 2022, 63(4):536–542.

[193] Wu B, Yi X, Zhao J, Li L. An orthogonal nucleic acid/peptide amplification circuit enables protease-triggered, cancer cell-selective PD-L1 imaging. *Angew. Chem., Int. Ed.* 2026, 65(4):e20284.

[194] Liu M, O'onnor RS, Trefely S, Graham K, Snyder NW, *et al.* Metabolic rewiring of macrophages by CpG potentiates clearance of cancer cells and overcomes tumor-expressed CD47-mediated 'don't-eat-me' signal. *Nat. Immunol.* 2019, 20(3):265–275.

[195] Li Y, Zhang M, Wang X, Liu W, Wang H, *et al.* Vaccination with CD47 deficient tumor cells elicits an antitumor immune response in mice. *Nat. Commun.* 2020, 11(1):581.

[196] Li J, Zhao R, Zhang J, Huang Z, Wang X, *et al.* PET/NIR-II fluorescence imaging and image-guided surgery of breast cancer using a CD47-specific nanobody. *View* 2025, 6(6):20250091.

[197] Wolf I, Schultze-Seemann S, Gratzke C, Wolf P. Targeting CD44 and EpCAM with Antibody dye conjugates for the photoimmunotherapy of prostate cancer. *Antibodies* 2025, 14(1):5.

[198] Wang J, Li S, Qiu M, Xiao L, Liu Y, *et al.* Enzyme-anchored signal amplification: a dual-modal probe for precise imaging of orthotopic lung cancer via nitroreductase activation. *Anal. Chem.* 2026, 98(19):14250–14259.

[199] Boya M, Ozkaya-Ahmadov T, Swain BE, Chu CH, Asmare N, *et al.* High throughput, label-free isolation of circulating tumor cell clusters in meshed microwells. *Nat. Commun.* 2022, 13(1):3385.

[200] Vandghanooni S, Sanaat Z, Barar J, Adibkia K, Eskandani M, *et al.* Recent advances in aptamer-based nanosystems and microfluidics devices for the detection of ovarian cancer biomarkers. *TrAC, Trends Anal. Chem.* 2021, 143:116343.

[201] Bai S, Yang J, He L, Abduwahap A, Dou X, *et al.* A self-accelerated responsive fluorescent sensor for rapid and specific cancer biomarker EpCAM detection and cancer imaging *in vivo*. *Sens. Actuators B Chem.* 2025, 443:138230.

[202] Yameen B, Choi WI, Vilos C, Swami A, Shi J, *et al.* Insight into nanoparticle cellular uptake and intracellular targeting. *J. Controlled Release* 2014, 190:485–499.

[203] Zhang Y, Zhu J, Qiu L, Lv Z, Zhao Z, *et al.* Stimulus-activated ribonuclease targeting chimeras for tumor microenvironment activated cancer therapy. *Nat. Commun.* 2025, 16(1):1288.

[204] Li N, Xiao L, Li S, Zhang L, Chen S. β-galactosidase-activated near-infrared fluorescence and (1)H/(19)F MRI trimodal probe for real-time *in vivo* imaging of ovarian cancer. *Anal. Chem.* 2026, 98(7):5261–5270.

[205] Jia Y, Du Y, Ru Z, Fan D, Yang L, *et al.* Aggregation-induced electrochemiluminescence frame of silica-confined tetraphenylethylene derivative matrixes for CD44 detection via peptide recognition. *Anal. Chem.* 2023, 95(16):6725–6731.

[206] Zhang W, Hu J, Liu R, Dai J, Yuan L, *et al.* A peptide-conjugated probe with cleavage-induced morphological change for treatment on tumor cell membrane. *Adv. Sci.* 2023, 10(11):e2207228.

[207] Luo Y, Gong X, Peng K, Yang Y, Chen M, *et al.* PSMA-targeting chimeras for cell-type-specific degradation of surface immune checkpoint protein PD-L1. *JACS Au* 2026, 6(1):279–289.

[208] Li H, Luo D, Yuan C, Wang X, Wang J, *et al.* Magnetic resonance imaging of PSMA-positive prostate cancer by a targeted and activatable Gd(III) MR contrast agent. *J. Am. Chem. Soc.* 2021, 143(41):17097–17108.

[209] Wu L, Wang Y, Zhu L, Liu Y, Wang T, *et al.* Aptamer-based liquid biopsy. *ACS Appl. Bio Mater.* 2020, 3(5):2743–2764.

[210] Wu L, Wang Y, Xu X, Liu Y, Lin B, *et al.* Aptamer-based detection of circulating targets for precision medicine. *Chem. Rev.* 2021, 121:12035–12105.

[211] Kievit FM, Zhang M. Cancer nanotheranostics: improving imaging and therapy by targeted delivery across biological barriers. *Adv. Mater.* 2011, 23(36):H217–H247.
[212] Mao C, Yi J, Deng F, Zhu W, Zhao J, *et al. In vivo* membrane engineering traps Gd-based MRI contrast agents for detecting microhepatocellular carcinoma. *Sci. Adv.* 2026, 12(18):eaec9913.
[213] Pramani KA, Jones S, Gao Y, Sweet C, Vangara A, *et al.* Multifunctional hybrid graphene oxide for circulating tumor cell isolation and analysis. *Adv. Drug Delivery Rev.* 2018, 125:21–35.
[214] Guo X, Lin F, Yi C, Song J, Sun D, *et al.* Deep transfer learning enables lesion tracing of circulating tumor cells. *Nat. Commun.* 2022, 13(1):7687.
[215] Gandara DR, Paul SM, Kowanetz M, Schleifman E, Zou W, *et al.* Blood-based tumor mutational burden as a predictor of clinical benefit in non-small-cell lung cancer patients treated with atezolizumab. *Nat. Med.* 2018, 24(9):1441–1448.
[216] Myung JH, Tam KA, Park SJ, Cha A, Hong S. Recent advances in nanotechnology-based detection and separation of circulating tumor cells. *WIREs Nanomed. Nanobiotechnol.* 2016, 8(2):223–239.
[217] Franken A, Kraemer A, Sicking A, Watolla M, Rivandi M, *et al.* Comparative analysis of EpCAM high-expressing and low-expressing circulating tumour cells with regard to their clonal relationship and clinical value. *Br. J. Cancer* 2023, 128(9):1742–1752
[218] Perelmuter VM, Grigoryeva ES, Alifanov VV, Kalinchuk AY, Andryuhova ES, *et al.* Characterization of EpCAM-positive and EpCAM-negative tumor cells in early-stage breast cancer. *Int. J. Mol. Sci.* 2024, 25(20):11109.
[219] Xiao D, Xiong M, Wang X, Lyu M, Sun H, *et al.* Regulation of the function and expression of EpCAM. *Biomedicines* 2024, 12(5):1129.
[220] Chen Y, Luo Z, Li X, Yan H, Xia C, *et al.* A covalent click chemistry chip for highly efficient capture and brightfield identification of circulating tumor cells. *Anal. Chem.* 2025, 97(46):25612–25622.
[221] Chen Y, Li F, Zhang S, Liu F, Mao C, *et al.* DNA framework-ensembled aptamers enhance fluid stability in circulating tumor cells capture for tumor treatment evaluation. *Angew. Chem., Int. Ed.* 2025, 137(24):e202425252.
[222] Gao P, Li X, Wei R, Pan W, Li N, *et al.* Glowing octopus-inspired nanomachine: a versatile aptasensor for efficient capture, imaging, separation, and NIR-triggered release of cancer cells. *Anal. Chem.* 2023, 96(1):309–316.
[223] Bai M, Chen F, Cao X, Zhao Y, Xue J, *et al.* Intracellular entropy-driven multi-bit DNA Computing for tumor progression discrimination. *Angew. Chem., Int. Ed.* 2020, 59(32):13267–13272.
[224] Hwang K, Wu P, Kim T, Lei L, Tian S, *et al.* Photocaged DNAzymes as a general method for sensing metal ions in living cells. *Angew. Chem., Int. Ed.* 2014, 53(50):13798–13802.
[225] Cui M, Li X, Chen H, Xu J. Smart engineering of a self-powered and integrated nanocomposite for intracellular microRNA imaging. *CCS Chem.* 20213(8):2063–2073.
[226] Tan W, Donovan MJ, Jiang J. Aptamers from cell-based selection for bioanalytical applications. *Chem. Rev.* 2013, 113(4):2842–2862.
[227] Zhao Y, Chen F, Li Q, Wang L, Fan C. Isothermal amplification of nucleic acids. *Chem. Rev.* 2015, 115(22):12491–12545.

[228] Torabi SF, Wu P, McGhee CE, Chen L, Hwang K, *et al. In vitro* selection of a sodium-specific DNAzyme and its application in intracellular sensing. *Proc. Natl. Acad. Sci. U. S. A.* 2015, 112(19):5903–5908.

[229] Li B, Liu Y, Liu Y, Tian T, Yang B, *et al.* Construction of dual-color probes with target-triggered signal amplification for *in situ* single-molecule imaging of microRNA. *ACS Nano* 2020, 14(7):8116–8125.

[230] Chai S, Lv W, He J, Li C, Li Y, *et al.* Dual energy transfer-based fluorescent nanoprobe for imaging miR-21 in nonalcoholic fatty liver cells with low background. *Anal. Chem.* 2019, 91(10):6761–6768.

[231] Su J, Wang D, Norbel L, Shen J, Zhao Z, *et al.* Multicolor gold-silver nano-mushrooms as ready-to-use SERS probes for ultrasensitive and multiplex DNA/miRNA detection. *Anal. Chem.* 2017, 89(4):2531–2538.

[232] Qing Z, Luo G, Xing S, Zou Z, Lei Y, *et al.* Pt-S bond-mediated nanoflares for high-fidelity intracellular applications by avoiding thiol cleavage. *Angew. Chem., Int. Ed.* 2020, 59(33):14044–14048.

[233] Wang W, Satyavolu NSR, Wu Z, Zhang J, Zhu J, *et al.* Near-infrared photothermally activated DNAzyme-gold nanoshells for imaging metal ions in living cells. *Angew. Chem., Int. Ed.* 2017, 129(24):6902–6906.

[234] Wang Z, Luo Y, Xie X, Hu X, Song H, *et al. In situ* spatial complementation of aptamer-mediated recognition enables live-cell imaging of native RNA transcripts in real time. *Angew. Chem., Int. Ed.* 2018, 57(4):972–976.

[235] Zhao Y, Zuo X, Li Q, Chen F, Chen Y, *et al.* Nucleic acids analysis. *Sci. China Chem.* 2020, 64(2):171–203.

[236] Chen B, Liu M, Huang C. Recent advances of carbon dots in imaging-guided theranostics. *TrAC Trends Anal. Chem.* 2021, 134:116116.

[237] Li C, Lv W, Yan Y, Yang F, Zhen S, *et al.* Nucleolin-targeted DNA nanotube for precise cancer therapy through forster resonance energy transfer-indicated telomerase responsiveness. *Anal. Chem.* 2021, 93(7):3526–3534.

[238] Gao P, Wei R, Chen Y, Li X, Pan W, *et al.* Pt nanozyme-bridged covalent organic framework-aptamer nanoplatform for tumor targeted self-strengthening photocatalytic therapy. *Biomaterials* 2023, 297:122109.

[239] Zou Z, Hu K, Li H. Aptamer-integrated DNA tetrahedral sensors for cancer cell imaging and invasiveness assessment. *Talanta* 2026, 305:129606.

[240] Gao P, Wang M, Chen Y, Pan W, Zhou P, *et al.* A COF-based nanoplatform for highly efficient cancer diagnosis, photodynamic therapy and prognosis. *Chem. Sci.* 2020, 11(26):6882–6888.

[241] Yu S, Zhou Y, Sun Y, Wu S, Xu T, *et al.* Endogenous mRNA triggered DNA-Au nanomachine for *in situ* imaging and targeted multimodal synergistic cancer therapy. *Angew. Chem., Int. Ed.* 2021, 133(11):6013–6023.

[242] Fuchigami T, Nakayama T, Miyanari Y, Nozaki I, Ishikawa N, *et al.* Peptide-based turn-on fluorescent probes for highly specific detection of survivin protein in the cancer cells. *Chem. Biomed. Imaging* 2024, 2(5):374–383.

[243] Li Z, Peng T, Yang M, Qiu Y, Ye P, *et al.* Dual functionality of [(64)Cu]Cu-NOTA-San A-Cy7 for diagnostic imaging and surgical guidance in Hsp90alpha-positive tumors. *Mol. Pharm.* 2025, 22(6):3231–3241.

[244] Dhanasekaran R, Deutzmann A, Mahauad-Fernandez WD, Hansen AS, Gouw AM, *et al.* The MYC oncogene—the grand orchestrator of cancer growth and immune evasion. *Nat. Rev. Clin. Oncol.* 2022, 19(1):23–36.

[245] Whitfield JR, Soucek L. MYC in cancer: from undruggable target to clinical trials. *Nat. Rev. Drug Discovery* 2025, 24(6):445–457.

[246] Cheng C, Su T, Morselli M, Kurdistani SK. Coordinated histone methylation loss and MYC activation promote translational capacity under amino acid restriction. *Cancer Metab.* 2025, 13(1):29.

[247] Li X, Zhang Z, Gao F, Ma Y, Wei D, *et al.* c-Myc-targeting PROTAC based on a TNA-DNA bivalent binder for combination therapy of triple-negative breast cancer. *J. Am. Chem. Soc.* 2023, 145(16):9334–9342.

[248] Wu X, Yu S, Zhang T, Feng R, Liu Z, *et al.* Unlocking spatiotemporal dynamics: precise dual-modal bioimaging of endogenous c-MYC mRNA in tumors via a CHA-activated ratiometric nanoplatform. *Anal. Chem.* 2026, 98(17):13091–13104.

[249] Gao P, Tang K, Lou R, Liu X, Wei R, *et al.* Covalent organic framework-based spherical nucleic acid probe with a bonding defect-amplified modification strategy. *Anal. Chem.* 2021, 93(35):12096–12102.

[250] He M, He M, Nie C, Yi J, Zhang J, *et al.* mRNA-activated multifunctional DNAzyme nanotweezer for intracellular mRNA sensing and gene therapy. *ACS Appl. Mater. Interfaces* 2021, 13(7):8015–8025.

[251] Zhong L, Cai S, Huang Y, Yin L, Yang Y, *et al.* DNA octahedron-based fluorescence nanoprobe for dual tumor-related mRNAs detection and imaging. *Anal. Chem.* 2018, 90(20):12059–12066.

[252] Gao P, Shen X, Liu X, Chen Y, Pan W, *et al.* Nucleic acid-gated covalent organic frameworks for cancer-specific imaging and drug release. *Anal. Chem.* 2021, 93:11751–11757.

[253] Zhang X, Chen W, Wan S, Qu B, Liao F, *et al.* Spatially selective microRNA imaging in human colorectal cancer tissues using a multivariate-gated signal amplification nanosensor. *J. Am. Chem. Soc.* 2025, 147(8):6679–6687.

[254] Zhu X, Qu B, Ying Z, Liu J, Wu Z, *et al.* Cascade circuits on self-assembled DNA polymers for targeted RNA imaging *in vivo*. *Anal. Chem.* 2020, 92(24):15953–15958.

[255] Shi H, Wang Y, Zheng J, Ning L, Huang Y, *et al.* Dual-responsive DNA nanodevice for the available imaging of an apoptotic signaling pathway *in situ*. *ACS Nano* 2019, 13(11):12840–12850.

[256] Huang Z, Lin M, Zhang C, Wu Z, Yu R, *et al.* Recombinant fusion streptavidin as a scaffold for DNA nanotetrads for nucleic acid delivery and telomerase activity imaging in living cells. *Anal. Chem.* 2019, 91(15):9361–9365.

[257] Liu W, Liu S, Kuang Y, Luo F, Jiang J. Developing activity localization fluorescence peptide probe using thiol-ene click reaction for spatially resolved imaging of caspase-8 in live cells. *Anal. Chem.* 2016, 88(15):7867–7872.

[258] Tang J, Huang C, Shu J, Zheng J, Ma D, *et al.* Azoreductase and target simultaneously activated fluorescent monitoring for cytochrome c release under hypoxia. *Anal. Chem.* 2018, 90(9):5865–5872.

[259] Liu X, Sun X, Ma Y, Jiang Q, Yin Y, *et al.* Apoptosis-amplified intracellular paclitaxel nanoparticle formation enhances microtubule aggregation and PANoptosis. *Angew. Chem., Int. Ed.* 2026, 138(6):e17035.

[260] Xu H, Cheng X, Sun X, Chen P, Zhan W, *et al.* Caspase-3-triggered intracellular gadolinium nanoparticle formation for T(1)-weighted magnetic resonance imaging of apoptosis *in vivo*. *Nano Lett.* 2023, 23(13):6178–6183.

[261] Pan W, Liu X, Wan X, Li J, Li Y, *et al.* Rapid preparation of Au-Se-peptide nanoprobe based on a freezing method for bioimaging. *Anal. Chem.* 2019, 91(24):15982–15987.

[262] Peng Y, Li T, Liu D, Li W, Zhang Y, *et al.* Development of cathepsin B-responsive GalNAc-PROTACs for hepatocyte-targeting protein degradation. *J. Med. Chem.* 2025, 69(1):517–532.

[263] Roth-Konforti ME, Bauer CR, Shabat D. Unprecedented sensitivity in a probe for monitoring cathepsin B: chemiluminescence microscopy cell-imaging of a natively expressed enzyme. *Angew. Chem., Int. Ed.* 2017, 56(49):15633–15638.

[264] Wang Y, Li J, Feng L, Yu J, Zhang Y, *et al.* Lysosome-targeting fluorogenic probe for cathepsin B imaging in living cells. *Anal. Chem.* 2016, 88(24):12403–12410.

[265] Shen Y, Wu T, Wang Y, Zhang S, Zhao X, *et al.* Nucleolin-targeted ratiometric fluorescent carbon dots with a remarkably large emission wavelength shift for precise imaging of cathepsin B in living cancer cells. *Anal. Chem.* 2021, 93(8):4042–4050.

[266] Gao P, Pan W, Li N, Tang B. Fluorescent probes for organelle-targeted bioactive species imaging. *Chem. Sci.* 2019, 10(24):6035–6071.

[267] Giorgio M, Trinei M, Migliaccio E, Pelicci PG. Hydrogen peroxide: a metabolic by-product or a common mediator of ageing signals? *Nat. Rev. Mol. Cell Biol.* 2007, 8(9):722–728.

[268] Chen T, Chen Z, Zhou Q, Ding H, Gong P, *et al.* Microenvironment-tailored catalytic nanoprobe for ratiometric NIR-II fluorescence/photoacoustic imaging of H2O2 in tumor and lymphatic metastasis. *Adv. Funct. Mater.* 2022, 32(47):2208720.

[269] Li N, Xiang M, Liu J, Tang H, Jiang J. DNA polymer nanoparticles programmed via supersandwich hybridization for imaging and therapy of cancer cells. *Anal. Chem.* 2018, 90(21):12951–12958.

[270] Liu Z, Chen S, Liu B, Wu J, Zhou Y, *et al.* Intracellular detection of ATP using an aptamer beacon covalently linked to graphene oxide resisting nonspecific probe displacement. *Anal. Chem.* 2014, 86(24):12229–12235.

[271] Liu J, Li R, Yuan B, Wang J, Li Y, *et al.* Mitochondria-targeting single-layered graphene quantum dots with dual recognition sites for ATP imaging in living cells. *Nanoscale* 2018, 10(36):17402–17408.

[272] Gao F, Guo L, Lin W, Zhang X, Zhan Q, *et al.* Simply designed and universal DNA nanohydrogel for stimuli-responsive NIR-II fluorescence imaging of early-stage tumor. *Anal. Chem.* 2025, 97(20):10699–10708.

[273] Xiang J, Liu Z, Liu M, Zhang Y, Zhu X. Fluorogenic peptide-modulated 2D ZnO/MnO(2) nanosheet heterostructure enables monitoring of tumor early response to immunotherapy. *Anal. Chem.* 2026, 98(5):3577–3587.

[274] Zhou Y, Zou L, Li G, Shi T, Yu S, *et al.* A cooperatively activatable DNA nanoprobe for cancer cell-selective imaging of ATP. *Anal. Chem.* 2021, 93(41):13960–13966.

[275] Shi Y, Yu Q, Tan L, Wang Q, Zhu W. Tumor microenvironment-responsive polymer delivery platforms for cancer therapy. *Angew. Chem., Int. Ed.* 2025, 137(26):e202503776.